Rend. Sem. Mat. Univ. Pol. Torino - Vol. 65, 2 (2007)
ISASUT Intensive Seminar

J. Engelbrecht - J. Janno*

MICROSTRUCTURED SOLIDS AND INVERSE PROBLEMS

Abstract. Microstructured solids are characterized by their dispersive properties and dispersive effects can be used for solving the inverse problems, i.e. for Nondestructive Testing. In this paper the Mindlin-type one-dimensional model is derived for longitudinal wave motion in such solids. In case of linear approximation, the inverse problems based on harmonic waves and localized boundary conditions are posed and solved, using the measurements of phase and group velocities and phase shifts. The full nonlinear model leads to solitary waves due to the balance of dispersive and nonlinear effects resulting in an asymmetric solitary wave. In this case the characteristics of wave profiles are used for solving an inverse problem.

1. Introduction

Contemporary materials are often characterized by their complex structure at various scales. For short, such materials are refered to as "microstructured materials". The microstructural properties influence strongly the macro-behaviour of compound materials and/or structures, that is why stress analysis should be based on proper modelling of possible physical effects caused by the microstructure. Two possible classes of problems must be distinguished: (i) given the properties of the material and its constituencies, and external disturbance, determine the global behaviour; (ii) given the external disturbance and the global behaviour, determine the properties of the material. The first class is identified as direct problems, the second – as inverse problems. In technical terms, the second class (inverse problems) is the Nondestructive Testing (NDT) with the aim to determine the physical and/or geometrical properties of materials (specimens) by measuring the wave fields at given excitations. By using ultrasound, NDT has found wide range of applications not only in engineering but also in medicine.

The ideas of using ultrasound in NDT have been developed since the discovery of the piezoelectric effect in quartz in 1880 (see [1]). The ideas were developed further for detecting objects in water (or air) and for detecting flaws in solids. Overviews on later applications are given in [2] - [5], for example.

Quite often in engineering applications of NDT, simplified mathematical models are used and the origin of these models, based on continuum mechanics, is forgotten. In [6], a simple straight-forward idea is advocated: for theoretical background of NDT, the conservation and constitutive laws should be stated first in the full correspondence to the axioms of continuum mechanics. The outcome could be rather complicated but all the possible simplifications (approximations) of the basic model should be based on clear procedures retaining the effects of the same order of accuracy. Only then the solutions of the inverse problems reflect reality.

*The support from the Estonian Science Foundation, and European Science Foundation programme NATEMIS is gratefully acknowledged.

In most general terms, microstructured materials mean polycrystalline solids, ceramic composites, functionally graded materials, granular materials, etc. The existence of grains, inclusions, layers, block walls, etc. – all that refers to microstructure. There are powerful methods in continuum mechanics in order to describe such materials or the existence of irregularities in materials starting from early studies of Cosserats and Voigt up to contemporary formulations [7]. The straight-forward modelling of microstructured solids leads to assigning concrete physical properties to every irregularity or to every volume element in a solid. This means introducing direct dependencies of all the physical properties on material coordinates and consequently leads to an extremely complex system. Another approach is to separate macro- and microstructure in continua. Then the conservation laws for both structures should be separately formulated [7, 11] or the microstructural quantities are separately taken into account in one set of conservation laws [8].

In this paper, we present a mathematical model for microstructured solids following the ideas of separating macro- and microstructure [11]. The details of modelling are described in [12, 13]. Based on that model, inverse problems in one-dimensional (1D) setting are posed and solved by making use of wave field characteristics. Presented are the main ideas whereas the uniqueness and stability theorems are published elsewhere [14, 15].

In Section 2 the basic assumptions are presented and the mathematical model is derived. The physical effects described by such a model are listed in Section 3. The focal point of this paper is Section 4 where three inverse problems are posed and their solutions briefly envisaged. In Section 5, results are summed up.

2. Mathematical model

We start from the Mindlin model [11] for microstructured solids. This model has a clear physical background interpreting the microstructure as deformable cells which can be "a molecule of a polymer, a crystallite of a polycrystal or a grain of a granular material". The displacement **u** of a material particle in terms of macrostructure is defined as usual by its components $u_i \equiv x_i - X_i$, where $x_i, X_i (i = 1, 2, 3)$ are the components of the spatial and material position vectors, respectively. Within each material volume there is a microvolume (microstructure) and the microdisplacement $\mathbf{u}'$ is defined by $u_i' \equiv x_i' - X_i'$, where the origin of the coordinates x_i' moves with the displacement **u**. The displacement gradient is assumed to be small and that permits to use the basic assumption of the Mindlin model

$$u_j' = x_k' \varphi_{kj}(x_i, t) \tag{1}$$

and consequently

$$\frac{\partial u_j'}{\partial x_i'} = \partial_i' u_j' = \varphi_{ij}. \tag{2}$$

Further we limit ourselves to the 1D case (see discussion in Section 5) and

denote $u_1 = u$, $\varphi_{11} = \varphi$. The fundamental balance laws are formulated separately for macroscopic and microscopic scales.

We assume that free energy function W has the form $W = W_2 + W_3$, where W_2 is the simplest quadratic function

$$W_2 = \frac{1}{2}\left(\alpha u_x^2 + B\varphi^2 + C\varphi_x^2 + 2A\varphi u_x\right) \tag{3}$$

and W_3 includes nonlinearities on both the macro- and microlevel

$$W_3 = \frac{1}{6}\left(N u_x^3 + M\varphi_x^3\right). \tag{4}$$

Here α, A, B, C, N and M are constants and indices here and below denote differentiation. The non-quadratic potential W_3 is the first approximation towards nonlinear theory. Then the governing equations (for details, see [12, 13] are the following:

$$\rho u_{tt} = \alpha u_{xx} + N u_x u_{xx} + A\varphi_x, \tag{5}$$

$$I\varphi_{tt} = C\varphi_{xx} + M\varphi_x\varphi_{xx} - Au_x - B\varphi, \tag{6}$$

where ρ is the macrodensity, and I is the microinertia. It can be shown that this system can also be interpreted as a balance of pseudomomentum [14] - for that see [16].

Let us rewrite this system (5), (6) in dimensionless variables $X = x/L$, $T = tc_0/L$, $U = u/U_0$, where U_0 is the amplitude of an excitation, and L - the wavelength of an excitation, and $c_0^2 = \alpha/\rho$. Note that φ is already dimensionless. We introduce also the geometric parameters $\delta = l^2/L^2$, $\epsilon = U_o/L$, where l is the scale of the microstructure. System (5), (6) yields then

$$U_{TT} = U_{XX} + \frac{N\epsilon}{\rho c_0^2} U_X U_{XX} + \frac{A}{\rho c_0^2 \epsilon}\varphi_X, \tag{7}$$

$$\delta\alpha I^* \varphi_{TT} = \delta C^* \varphi_{XX} + \delta^{3/2} M^* \varphi_X \varphi_{XX} - A\epsilon U_X - B\varphi, \tag{8}$$

where $I = I^*\rho l^2$, $C = C^* l^2$ and $M = M^* l^3$.

For further analysis we eliminate microdeformation φ from (7), (8) by making use of the slaving principle [16, 17]. This results in the following hierarchical governing equation for U

$$\begin{aligned} U_{TT} &= (1-b)\, U_{XX} + \frac{\mu}{2}(U_X^2)_X + \delta(\beta U_{TT} - \gamma\, U_{XX})_{XX} - \\ &- \delta^{3/2}\frac{\lambda}{2}(U_{XX}^2)_{XX}, \end{aligned} \tag{9}$$

where

$$b = \frac{A^2}{\alpha\, B}, \quad \mu = \frac{N\varepsilon}{\alpha}, \quad \beta = \frac{A^2 I^*}{B^2}, \quad \gamma = \frac{A^2\, C^*}{\alpha\, B^2}, \quad \lambda = \frac{A^3\, M^*\, \varepsilon}{\alpha\, B^3}.$$

This is the sought model equation for longitudinal waves in 1D setting.

3. Direct problem: physical effects

Equation (9) is a comparatively simple model but surprisingly rich. For the sake of further analysis we separate linear ($N = M = 0$) and nonlinear ($N \neq 0, \quad M \neq 0$) cases. In the linear case

$$U_{TT} = (1-b)\, U_{XX} + \delta(\beta U_{TT} - \gamma\, U_{XX})_{XX} \tag{10}$$

the hierarchical structure is explicitly seen. Indeed, Eq. (10) includes two wave operators - one for macrostructure ($\mathcal{L}_{macro} = U_{TT} - (1-b)\, U_{XX}$), another for microstructure ($\mathcal{L}_{micro} = \beta U_{TT} - \gamma\, U_{XX}$). If the scale parameter δ is small then $\mathcal{L}_{micro}$ can be neglected; if δ is large then on contrary the influence of macrostructure is weaker and $\mathcal{L}_{macro}$ can be neglected; clearly the intermediate case includes both effects. The wave speed in the compound material is affected by the microstructure (1 *versus* b) and clearly only $A = 0$ excludes this dependence. The influence of the microstructure on wave motion is, as expected, characterized by dispersive terms. However, the double dispersion occurs due to the different higher order terms (U_{TTXX} and U_{XXXX}) – cf. [16, 18].

The dispersion analysis [12, 13] shows that the phase velocity depends strongly on the wave number, i.e. on frequency of the excitation. Consequently, this effect could be used for solving the inverse problem in the linear setting.

In nonlinear case of Eq. (9) with ($N \neq 0, M \neq 0$), dispersive and nonlinear terms act together. From the theory of nonlinear waves it is known that if dispersive and nonlinear effects are balanced, then solitary waves may emerge. It would be of interest to analyse this case separately from the viewpoint of an inverse problem – can the form of a solitary wave (if it exists) give information about the properties of microstructure?

In what follows, we present the main ideas of solving the inverse problems in linear (Eq. (10)) and nonlinear (Eq. (9)) cases. In other words, we are going to determine the coefficients of these equations related to physical parameters in (3), (4), (5), (6).

4. Inverse problems

4.1. Linear case, harmonic waves

For sake of simplicity, we rewrite Eq. (10) with lower case letters

$$u_{tt} = (1-b)\, u_{xx} + \delta(\beta\, u_{ttxx} - \gamma\, u_{xxxx}). \tag{11}$$

Obviously (see Eq. (3)) b, δ, β, γ are positive and $b < 1$. If we consider the scale parameter δ to be known, then the number of parameters to be determined for the inverse problem is three.

Assume that Eq. (11) has a solution in the form of harmonic waves

$$u(x,t) = exp[i(kx - \omega t)], \tag{12}$$

where k and ω are the wave number and frequency, respectively. Then the phase velocity c_{ph} is determined by

$$c_{ph}(k) = \left(\frac{\delta\gamma k^2 + 1 - b}{\delta\beta k^2 + 1} \right)^{1/2}. \tag{13}$$

The inverse problem is the following: given three phase velocities $c_{ph}(k_1)$, $c_{ph}(k_2)$, and $c_{ph}(k_3)$ which correspond to wave numbers k_1, k_2, k_3 such that $k_1^2 \neq k_2^2$, $k_1^2 \neq k_3^2$, $k_2^2 \neq k_3^2$, determine the parameters b, β, and γ. The qualitative behaviour of phase velocities is shown in Fig. 1. This means solving the system of nonlinear equations with three unknowns

$$c_{ph}(k_j) = \left(\frac{\delta\gamma k_j^2 + 1 - b}{\delta\beta k_j^2 + 1} \right)^{1/2}, \qquad j = 1, 2, 3, \tag{14}$$

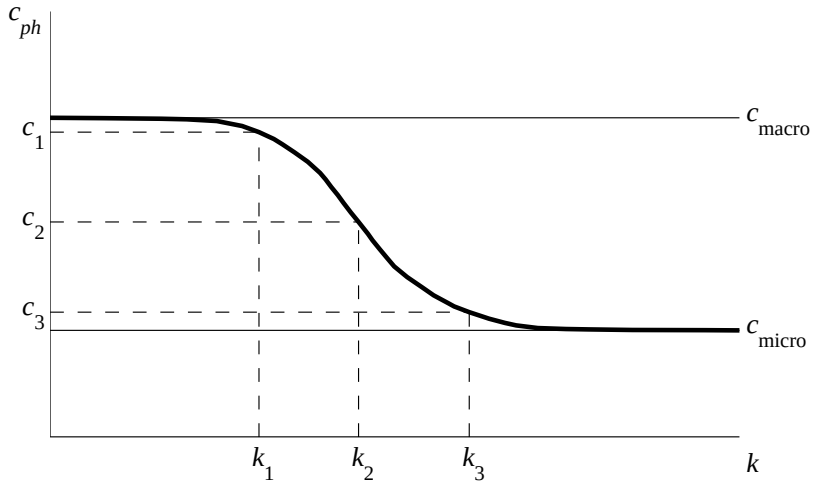

Figure 1: Qualitative behaviour of phase velocities. Here c_{macro} and c_{micro} denote the velocities in pure macro- and microstructure, respectively; c_j, $j = 1, 2, 3$ are phase velocities $c_{ph}(k_j)$.

Actually it is possible to transform Eq. (14) to a more suitable form for practical solution

$$b + \delta k_j^2 c_{ph}^2(k_j)\beta - \delta k_j^2 \gamma = 1 - c_{ph}^2(k_j), \qquad j = 1, 2, 3. \tag{15}$$

The detailed analysis of uniqueness of solution to Eq. (15) is given in [14].

4.2. Linear case, localized boundary condition

In practice of NDT, the excitations (boundary conditions) are usually localized. The general solution to Eq. (11) satisfying the boundary condition $u(0,t) = g(t)$ is the following:

$$u(x,t) = \frac{1}{2\pi}\int_{-\infty}^{\infty} G(\omega)\exp\left[i\,(k(\omega)x - \omega t)\right]d\omega, \tag{16}$$

$$G(\omega) = \int_{-\infty}^{\infty} g(t)\exp(i\omega t)dt. \tag{17}$$

We assume now

$$g(t) = A\exp\left(-\frac{t^2}{4\nu^2}\right)\exp(-i\eta t), \tag{18}$$

where A, ν are given and η is the fixed frequency.

Then expression (16) yields (for details see [17])

$$u(x,t) = \frac{A\nu}{\sqrt{\pi}}\int_{-\infty}^{\infty}\exp\left[-\nu^2(\omega-\eta)^2\right]\exp\left[i\,(k(\omega)x - \omega t)\right]\,d\omega. \tag{19}$$

Further on, we use an approximation and derive $k(\omega)$ into the Taylor series around $\omega = \eta$. Keeping three first terms, we have

$$k(\omega) \approx k(\eta) + k'(\eta)(\omega-\eta) + \frac{1}{2}k''(\eta)(\omega-\eta)^2, \tag{20}$$

where prime denotes differentiation. From the definition of phase and group velocities we determine

$$k\,(\eta) = \frac{\eta}{c_{ph}}, \quad k'(\eta) = \frac{1}{c_g} \tag{21}$$

and denote $d = \frac{1}{2}k''(\eta)$.

The real part of the integral (19) can now be evaluated [14] ($\tilde{u}$ denotes the approximation):

$$Re\tilde{u}(x,t) = A_1(x)\exp\left[-\nu^2 f_1(x,t)\right]\cos\left[\eta\left(\frac{x}{c_{ph}} - t\right) + \Phi(x) - \right. \\ \left. - xdf_1(x,t)\right], \tag{22}$$

$$A_1 = A\nu(\nu^4 + x^2d^2)^{-\frac{1}{4}}, \tag{23}$$

$$f_1(x,t) = \frac{1}{4}\left(\frac{x}{c_g} - t\right)^2(\nu^4 + x^2d^2)^{-1}, \tag{24}$$

$$\Phi(x) = \frac{\arctan \frac{1}{2} x d}{\nu^2}. \tag{25}$$

From (22) - (25) it follows that the amplitude of the wave is decreasing with increasing x and the dispersion of the normal distribution in $g(t)$ is increasing. So it is possible to determine the number d from the measurement.

The inverse problem stated now is the following: given the phase and group velocities c_{ph}, c_g and the number d, determine the parameters b, β, γ. This problem has the unique solution provided $c_{ph} \neq c_g$:

$$\beta = \frac{1}{\delta m^2}(4F(m) - 1), \tag{26}$$

$$\gamma = \frac{c_{ph}}{\delta m^2}(4c_g F(m) - c_{ph}), \tag{27}$$

$$b = 1 + c_{ph}\left[4(c_g - c_{ph})F(m) - c_{ph}\right] \tag{28}$$

with

$$F(m) = \left[\frac{c_g}{c_{ph}} - \frac{2dmc_g^3}{c_g - c_{ph}}\right]^{-1}, \tag{29}$$

where m is the wave number corresponding to the frequency η and the condition $0 < F^{-1}(m) < 4$ must be satisfied in order to get positive β.

4.3. Nonlinear case, solitary wave

As in Section 4.1, we rewrite the basic equation – Eq. (9) with lower case letters. As far as here is no need to distinguish the wave speed components for microstructure, we denote by $b_1 = 1 - b$. Equation (9) reads then in terms of $v = u_x$

$$v_{tt} = b_1\, v_{xx} + \frac{\mu}{2}(v^2)_{xx} + \delta(\beta v_{tt} - \gamma v_{xx})_{xx} - \delta^{3/2}\frac{\lambda}{2}(v_x^2)_{xxx}. \tag{30}$$

First we establish a solution to the direct problem and then analyse the possibilities to solve the inverse problem. We seek the travelling waves

$$v(xt) = w(x - ct) = w(\xi) \tag{31}$$

where c is a free parameter (velocity of the wave) and $w(\xi)$ satisfies the equation

$$(c^2 - b_1)w'' - \frac{\mu}{2}(w^2)'' - \delta(\beta c^2 - \gamma)w^{IV} + \delta^{3/2}\frac{\lambda}{2}\left[(w')^2\right]''' = 0. \tag{32}$$

When looking for solitary waves, the conditions $\omega(\xi)$, $\omega'(\xi)$, $\omega''(\xi) \to 0$ as $|\xi| \to \infty$ should be satisfied. After integrating Eq. (32) three times (before the last integration multiplying by ω'), we obtain

$$\frac{1}{2}\delta\left(\beta c^2 - \gamma\right)\left(w'\right)^2 - \frac{1}{3}\delta^{3/2}\lambda\left(w'\right)^3 = \frac{1}{2}\left(c^2 - b_1\right)w^2 - \frac{1}{6}\mu w^3. \tag{33}$$

It can be proved [18] that for the existence of the solitary wave solution the following in equalities should be satisfied

$$\beta c^2 - \gamma \neq 0, \quad c^2 - b_1 \neq 0, \quad \mu \neq 0. \tag{34}$$

In addition, the necessary solvability condition is

$$\left(c^2 - b_1\right) / \left(\beta c^2 - \gamma\right) > 0. \tag{35}$$

Now we introduce the following three parameters which have certain physical or geometrical meaning:

$$\kappa = \sqrt{\frac{c^2 - b_1}{\delta(\beta c^2 - \gamma)}}, \quad A = \frac{3(c^2 - b_1)}{\mu}, \quad \theta = 2\left[\frac{c^2 - b_1}{\beta c^2 - \gamma}\right]^{3/2} \frac{\lambda}{\mu}. \tag{36}$$

In terms of these parameters, Eq. (33) has the form

$$(w')^2 - \frac{\theta}{\kappa A}(w')^3 = \kappa^2 w^2 \left(1 - \frac{w}{A}\right). \tag{37}$$

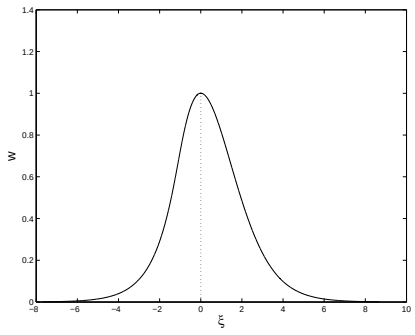

Figure 2: Solitary wave in case $\theta = 0.9$

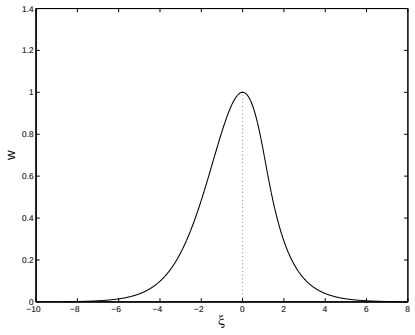

Figure 3: Solitary wave in case $\theta = -0.9$

The parameter κ is the exponential decay rate of the solution as $|\xi| \to \infty$. The inverse of decay rate $1/\kappa$ is usually referred to as the width of the wave. Parameter A is actually the amplitude of the wave and parameter θ is related to the asymmetry of the wave. We remind now that in our model two nonlinearities are taken into account: on the macrolevel ($\mu \neq 0$) and on the microlevel ($\lambda \neq 0$) – cf. Eq. (9). If $\lambda = 0$, i.e. nonlinearity on the microlevel is neglected then a symmetric bell-shaped solitary wave can be found [16, 18]

$$w(\xi) = A \cosh^2\left(\frac{\kappa\xi}{2}\right). \tag{38}$$

In case $\mu \neq 0$, $\lambda \neq 0$, the situation is more complicated and we have used numerical integration for finding the solitary wave. Two examples of solitary waves, computed by means of the second-order Adams-Bashforth method, are depicted in Figs 2, 3, where $\zeta = \kappa\xi$, $y = \omega/A$. The results are clearly asymmetric. Let us fix same relative level $y \in (0, 1)$ and consider the front and rear half-lengths of the wave at this level – namely the quantities $|\xi^-(yA)|$ and $|\xi^+(yA)|$. The asymmetry at this level is the ratio of those quantities which depends on [18]:

$$\frac{|\xi^+(yA)|}{|\xi^-(yA)|} = F_y(\theta), \tag{39}$$

where $F_y(\theta)$ is an increasing function of θ in the interval (-1,1) and $F_y(0) = 1$. The details on complicated function F_y are presented in [15].

In the model equation (30) there are 5 material parameters: $b_1, \mu, \beta, \gamma, \lambda$ which need to be determined in the NDT. Measuring just a single solitary wave, one could recover maximally κ, A, and θ, i.e. only 3 parameters. That is why for solving the full problem, one should use the measurements of two independent solitary waves [19]. The full procedure is formed by two stages. As before, we assume δ to be known.

The first stage is to determine the parameters of macrostructure, b_1 and μ. Let be given two solitary waves ω_1 and ω_2 with the velocities c_1 and c_2, and amplitudes A_1 and A_2.

We expect that the conditions $c_1^2 \neq c_2^2$ and hence $A_1 \neq A_2$ are satisfied. Then from expressions (36) we have the system

$$3b_1 + A_j\mu = 3c_j^2, \quad j = 1, 2, \tag{40}$$

which determine uniquely b_1 and μ.

The second stage is to find other unknowns β, γ, λ. For that not only the amplitudes A_j and c_j should be known but also some additional information. We fix two numbers w_{11}, w_{12} which lie between 0 and A_1 for the first solitary wave at both sides of the maximum amplitude A_1, respectively and a number w_{21} which lies between 0 and A_2 for the second solitary wave. We need also to registrer time when the first wave reaches w_{11}, $w = A_1$, and w_{12} and the second – w_{21} and $w = A_2$. Then knowing c_1 and c_2, the corresponding coordinates ξ_{11}, ξ_{12} and ξ_{21} can be calculated. Note that $\xi = 0$ for both A_1 and A_2. Now the inverse problem posed is the following: given b_1, μ, the points (ξ_{11}, w_{11}), (ξ_{12}, w_{12}) with $\xi_{11} > 0$, $\xi_{12} < 0$ on the graph of the first wave and the point (ξ_{21}, w_{21}) with $\xi_{21} \neq 0$ on the graph of the second wave, determine β, γ, λ. The details of solving this inverse problem with the proof of the uniqueness and a stability estimate are given in [19].

5. Summary

It has been demonstrated how to solve the inverse problem of determining the material parameters from wave characteristics in microstructured materials. The following physical effects have been used: (i) the dependencies of phase and group velocities on

wave numbers and (ii) the asymmetric structure of solitary waves. The measurements of velocities are easily carried on, the measurements of wave profiles need higher accuracy. However, the experimental studies of strain waves in microstructured materials [20] have demonstrated the asymmetry of solitary waves. In this case tungsten-epoxy composites were used with reference samples made of aluminium.

In practical realizations the ultrasonic transducers are used for generating waves in samples. In principle, the generated wave beams are not one-dimensional but the diffractional expansion in the transverse direction is rather weak. On the axis of the wave beam, the 1D approximation is possible [21].

References

[1] BHARDWAJ M.C., *Fundamental developments in ultrasonics for advanced NDT*, in: "Nondestructive Testing of High-Performance Ceramics, Proceedings of the conference, Boston 1997", Conf. MA. American Ceramic Society, Ohio, 472–527.

[2] BENSON R.W. AND RAELSON V.J., *Acoustoelasticity*, Product Engineering **20** (1959), 56–59.

[3] MCCONNAGIE W.J., *Nondestructive testing*, McGraw-Hill, New York 1961.

[4] TRUELL R., ELBAUM C., AND CHICK B.B., *Ultrasonic methods in solid state physics*, Academic Press, New York 1969.

[5] THOMPSON D.O. AND CHIMENTI D.E. (Eds), *Review of progress in quantitative nondestructive evaluation*, Plenum, New York 1986.

[6] ENGELBRECHT J. AND RAVASOO A., *From continuum mechanics to applications in the nondestructive testing*, Bull. Tech. Univ. Istanbul **47** (1994), 83–103.

[7] ERINGEN A.C., *Microcontinuum field theories. Foundations and solids*, Springer-Verlag, New York 1999.

[8] MAUGIN G.A., *Material inhomogeneities in elasticity*, Chapman and Hall, London 1993.

[9] SUQUET P. (Ed.), *Continuum micromechanics*, Springer, Vienna 1997.

[10] CAPRIZ G., *Continua with microstructure*, Springer-Verlag, New York 1989.

[11] MINDLIN R.D., *Micro-structure in linear elasticity*, Arch. Rat. Mech. Anal. **16** (1964), 51–78.

[12] ENGELBRECHT J., BEREZOVSKI A., PASTRONE F., AND BRAUN M., *Waves in microstructured materials and dispersion*, Phil. Mag. **85** (2005), 4127–4141.

[13] ENGELBRECHT J., PASTRONE F., BRAUN M., AND BEREZOVSKI A., *Hierarchies of waves in nonclassical materials*, in: "The universality of nonclassical elasticity with applications to NDE and ultrasonics", (Ed. Delsanto P.-P.), Springer, New York 2007, 29–48.

[14] JANNO J. AND ENGELBRECHT J., *Waves in microstructured solids: inverse problems*, Wave Motion **43** (2005), 1–11.

[15] JANNO J. AND ENGELBRECHT J., *Solitary waves in nonlinear microstructured materials*, J. Phys. A: Math. Gen. **38** (2005), 5159–5172.

[16] PORUBOV A.V., *Amplification of nonlinear strain waves in solids*, World Scientific, Singapore 2003.

[17] ENGELBRECHT J. AND PASTRONE F., *Waves in microstructured solids with strong nonlinearities in microscale*, Proc. Estonian Acad. Sci. Phys. Math., **52** (2003), 12–20.

[18] SAMSONOV A.M., *Strain solitons in solids and how to construct them*, Chapman and Hall, London 2001.

[19] JANNO J. AND ENGELBRECHT J., *An inverse solitary wave problem related to microstructured materials*, Inverse Problems **21** (2005), 2019–2034.

[20] POTAPOV A.I. AND RODYUSHKIN V.M., *Experimental study of of strain waves in materials with microstructure*, Acoust. Phys. **47** (2001), 347–352.

[21] ENGELBRECHT J., *Nonlinear wave dynamics. Complexity and simplicity*, Kluwer, Dordrecht 1997.

AMS Subject Classification: 74A30, 74J25, 74J30, 74J25.

Jüri ENGELBRECHT, Jaan JANNO, Centre for Nonlinear Studies, Institute of Cybernetics at Tallinn University of Technology, Akadeemia tee 21, 12618 Tallinn, ESTONIA
e-mail: je@ioc.ee, janno@ioc.ee

Rend. Sem. Mat. Univ. Pol. Torino - Vol. 65, 2 (2007)
ISASUT Intensive Seminar

J. F. Ganghoffer

DIFFERENTIAL GEOMETRY, LEAST ACTION PRINCIPLES AND IRREVERSIBLE PROCESSES

"*Les phénomènes irréversibles et le théorême de Clausius ne sont pas explicables au moyen des équations de Lagrange*". Poincaré, 1908.

Abstract. This contribution is intended as both a course on differential geometry and an illustration of the involvement of differential geometry in the calculus of variations, in articulation with the occurrence of irreversibility. Potential applications in terms of the continuous symmetries of the constitutive laws of dissipative materials shall be mentionned, leading potentially to a systematic and predictive approach of the construction of the so-called master curves.

1. Introduction

The contribution of differential forms to mathematics and physics is considerable, due to fact that they allow the unification, generalization and conception of notions encountered in a wide range of disciplines: mention amongst others elementary geometry, analysis, thermodynamics, continuum mechanics, electromagnetism, and analytical mechanics, (see [1, 2, 9, 11, 12, 16, 26, 28, 29, 30, 31]). The first part of the contribution gives the essentials of differential geometry in a synthetic manner. The proofs shall most of the time be omitted (the reader shall refer to one of the references related to differential geometry).
The following notations shall be used in the sequel: the partial derivative of a quantity a with respect to the variable x shall be noted a_x, or $a_{,x}$, or $\partial_x a$. The transpose of a vector or a tensor A is noted with a superscript A^t. The convention of summation of the repeated index in monomials is implicitly used (unless explicitly stated). The following abbreviations shall be used: w.r. for with respect to; s.t. for such that; r.h.s. for right-hand side; iff for iff and only if; notation := stands for the definition (expressed on the r.h.s.) of the quantity placed on the left hand-side.

2. Differential geometry: a reminder of the essential notions

2.1. Differentiable manifolds (submanifolds)

Consider M a set of points endowed with a topology and E_n a finite dimensional vector space (dimension n). A local chart on M is the pair (U_i, ϕ) consisting of an open set U_i of M and an homeomorphism ϕ: $U_i \longrightarrow \phi(U_i) \subset E_n$: one says that U_i is the domain of the chart (fig1).

Since a point in M can belong to 2 distinct open sets U_j, U_k, with the charts $\left(U_j, \phi_j\right)$ and (U_k, ϕ_k), a C^q-compatibility condition between the 2 charts is defined

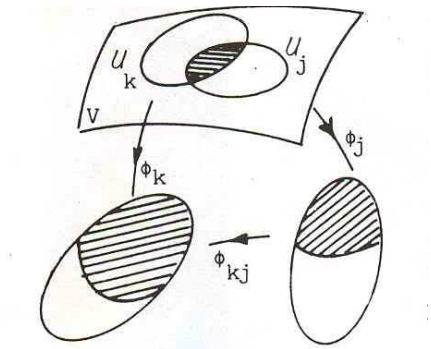

Figure 1: Chart of a manifold.

as $U_j \cap U_k \neq \emptyset \Rightarrow \phi_k \circ \phi_j^{-1}\Big|_{U_j \cap U_k}$ is a diffeomorphism of class C^q between the open sets $\phi_j\left(U_j \cap U_k\right)$ and $\phi_k\left(U_j \cap U_k\right)$. Points p on M are conveniently labeled by local coordinates x^i, which are the coordinates in $\mathbb{R}^n$ of the point $\phi(p)$. An atlas of class C^q on M is a set of charts $(U_i, \phi_i)_i$, s.t. the domains of the charts cover M; all charts of the atlas are C^q-compatible.

EXAMPLE 1. Consider the sphere of radius unity in $3D$ space, defined by

$$S^2 = \left((x_1, x_2, x_3) \in \mathbb{R}^3 / \sum_{i=1}^{3} x_i^2 = 1 \right)$$

the stereographic projection of the North pole n onto the plane defined by $x_3 = 0$ is a bijection between $S^2 \setminus \{n\}$ and this plane. A similar projection of the South Pole can be defined.

In the following, the base of the topology of M is supposed countable, thus the manifold M is supposed separable. Submanifolds of $\mathbb{R}^{n+k}$ can be defined from the notions of submersion and immersion. For U open in $\mathbb{R}^n$, a C^∞ map $\psi : U \to \mathbb{R}^{n+k}$ is an immersion if its differential $d\psi(u) \in L\left(T_u\mathbb{R}^n \to T_{\psi(u)}\mathbb{R}^{n+k}\right)$ is a one-to-one map at every $u \in U$. The linear algebra characterization of an immersion is that the differential $d\psi(u)$ induces a one to one linear map from $\mathbb{R}^n$ to $\mathbb{R}^{n+k}$ (equivalently, the differential map $d\psi(u)$ has rank n). The dual notion of submersion is defined in the following manner: for V open in $\mathbb{R}^{n+k}$, and $f :\to \mathbb{R}^k$ a smooth map, f is a *submersion* if its differential $Df(x) \in L\left(T_x\mathbb{R}^{n+k} \to T_{f(x)}\mathbb{R}^k\right)$ in an onto map, thus when the matrix $Df(x)$ has rank k.

EXAMPLE 2. Consider the case $n = 2$ and $k = 1$; for $h \in C^\infty(\mathbb{R})$ a strictly positive function, the map which rotates the curve $x = h(z)$ around the z axis, namely

$\psi(u,\theta) = (h(u)\cos(\theta), h(u)\sin\theta, u)$ gives a parameterized surface of revolution. The differential is

$$D\psi\ (u,\ \theta) = \begin{pmatrix} h'(u)\cos\theta & -h(u)\sin\theta \\ h'(u)\sin\theta & h(u)\cos\theta \\ 1 & 0 \end{pmatrix},$$

the column of which being independent, thus ψ is an immersion. As an example of an submersion, let consider $V = \left\{(x_1, x_2, x_3)\, x_1^2 + x_2^2 + x_3^2 > 0\right\}$, and the function $f\ (x_1, x_2, x_3) = x_1^2 + x_2^2 + x_3^2$. Its differential is $Df\ (x_1, x_2, x_3) = 2\,(x_1, x_2, x_3)$, which is not zero on V, thus f is a submersion.

Manifolds can be parametrized as curves and surfaces traditionally; consider M as a subset of $\mathbb{R}^{n+k}$; an n-dimensional parametrization of M is given by a one-to-one immersion $\psi : W \to U \subset \mathbb{R}^{n+k}$, with U an open subset of $\mathbb{R}^{n+k}$ with $U \cap M \neq \emptyset$, and $\psi(W) = U \cap M$. The image of a $1D$ parametrization is a parametrized curve, and that of a $2D$ parametrization is a parametrized surface. For instance, the application

$$\begin{array}{rcl} \theta : (0, 2\pi) & \to & U = \mathbb{R}^2(1, 0) \\ \theta & \mapsto & (\cos\theta, \sin\theta) \end{array}$$

gives a $1D$ parametrization of the unit circle in $\mathbb{R}^2$.

The implicit function theorem gives a convenient *implicit function parametrization*, i.e. one having the special form $\psi\ (x_1, \ldots, x_n, h_1(x), \ldots, h_n(x))$, with h an implicit function.

For example, a $2D$ implicit function parametrization at the point $(0, 0, 1)$ of the sphere S^2 in $\mathbb{R}^3$ is given by $\psi(x, y) = \left(x, y, \sqrt{1 - x^2 - y^2}\right)$, with domain

$$W = \left\{(x, y) \in \mathbb{R}^2 / x^2 + y^2 < 1\right\}$$

and range $W \times (0, +\infty)$.

2.2. Transformations, Lie groups and Lie derivatives

Generally speaking, transformations map a set into itself, and a mathematical structure cam be characterized by those transformations that leaves it invariant (for instance, Euclidean geometry is invariant under orthogonal transformations, whereas special relativity has a structure compatible with invariance w.r. to the Lorentz group). Very often, transformations establish as a group, and the prime tool there is the infinitesimal transformation, which is described by a vector field (an infinitesimal generator of the group).

To each point of the manifold can be attached an n-dimensional vector space, called the tangent space (local notion). At a point $p_0 \in M$, let define the *germ* of a differentiable function g as the equivalence class of differentiable functions that coincide in an open neighborhood of p_0. Furthermore, a *tangent vector* is an equivalence class of curves having the same tangency at p_0; the curves $c : I \subset \mathbb{R} \to M$ are tangent

at a point p_0, if, in a given chart $(U\phi)$, they give the same value $\frac{d}{dt}(\phi \circ c)(0)$, with $p_0 = c(0)$. Using further the composition of functions theorem gives the rate of variation of the function g along the curve c (i.e. the composite map $g \circ \phi^{-1} : \mathbb{R}^n \to \mathbb{R}$), as $\frac{d}{dt}(g \circ c)(0) = \sum_{I=1}^{n} \left(\frac{\partial g}{\partial xi}\right)_{x_0} \frac{dx_i}{dt}(0)$. Thereby, the notion of tangent vector receives a second definition: the tangent vector also is derivation acting on the set of germs of functions defined in an open neighborhood of p_0, i.e. a linear application $X_{p_0} : g \mapsto X_{p_0}(g) = \frac{d}{dt}(g \circ c)(0)$. Thus, the vector field X_{p_0} has the coordinates $\frac{dx_i}{dt}(0)$ (in the local basis $(x_i)_i$), and is given intrinsically by $X_{p_0} = \left(\frac{dx_i}{dt}\right)_{x_0} \frac{\partial}{\partial x_i}$. It is easy to see that the value of the action of X_{p_0} on any function is the same for any representant in the class of curves having he same tangent at p_0.

DEFINITION 1. *The tangent space to M at the point p_0 is the set of equivalence classes of tangent curves to M at p_0; it is also the set of tangent vectors to M at p_0. It is noted $T_{p_0}M$, and its dimension is n. The notion of tangent space to a manifold allows an intrinsic definition of the differential (independent from the local coordinates).*

For V_n, W_m differentiable manifolds, $f : V_n \to W_m$ differentiable, X_0 a tangent vector to V_n at point x_0, with $z_0 = f(x_0) \in W \in W_m$, the differential of f at x_0 is the linear application $df_{x_0} : T_{x_0}V_n \to T_{z_0}W_m$; $X_0 \mapsto df_{x_0}X_0$, s.t. $\forall h$, $df_{x_0}X_0(f^*h)$, see fig 2. The application f^* therein is the reciprocal image

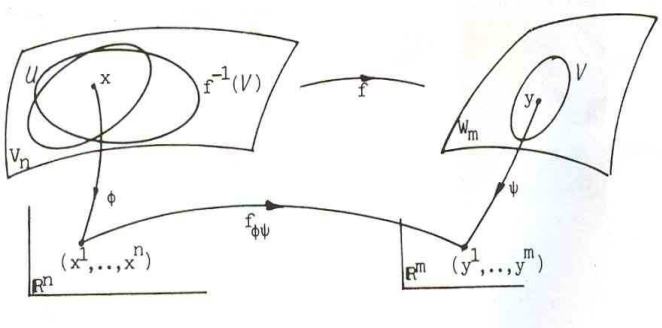

Figure 2: Differentiable functions and tangent mappings between manifolds.

The vector $Z_0 := df_{x_0}X_0$ is tangent to W_m at z_0. In local coordinates, one simply has

$$Z^j = \frac{\partial f^j}{\partial x_i}(x_0)\, X^i$$

and the matrix of elements $\left\{\dfrac{\partial f^i}{\partial x_i}(x_0)\right\}_{i,j}$ therein is the Jacobean matrix. This notion obviously reminds the transformation gradient in continuum mechanics.

DEFINITION 2 (Derivation). *A derivation is a first-order differential operator, which is sensitive only to linear terms, thus a derivation X shall operate on products of functions according to the rule $X(fg) = fX(g) + gX(f)$. This defines the Leibniz rule for derivatives that warrants X being insensitive to quadratic and higher-order terms (as shown earlier, vector fields act as derivations).*

For two vector fields X, Y acting on functions, the double operation XY also maps functions to functions, but is not a derivation. As an example, any derivation at the point $(0, 0)$ acting on the function $f(x, y) = x^2 + y^2$ must give zero (use Leibniz rule). But, composing ∂_x with itself gives $\partial_x \partial_x f(x, y) = 2$, thus $\partial_x \circ \partial_x$ is not a derivation (and the composition of derivations does not give a derivation in general). However, the operation of *Lie bracket* restores the property of being a derivation: it is defined by $[XY - YX]$, which in 3-vector notation would read $[X, Y] = (X \cdot \nabla) Y - (Y \cdot \nabla) X$. The Lie bracket receives an important geometric interpretation, in connection to **Frobenius Theorem**: if at every point, the Lie bracket of tangent vectors to two families of curves are a linear combination of the two vectors, the curves then fit together to define a 2-surface. This can easily be generalized to higher dimension.

DEFINITION 3. *A Lie group G is a set that both has the structure of a group and of a manifold. Thus, it is a differentiable manifold of class C^∞, and the group structure is characterized by the following operations (product and inversion)*

$$G \times G \to G; (x, y) \mapsto xy; \qquad G \to G; x \mapsto x^{-1}.$$

Every neighborhood of e is then sent by L_y to a neighborhood of y by the left translation; the differential application $dL_y : T_eG \to T_yG$ allows the definition of left invariant vector fields: $\forall y \in G,\ dL_y X(e) = X(y)$.

It can easily be shown that the left invariant vector fields on G have a vectorial structure (same dimension as G), and that this vectorial space is isomorphic to the tangent space T_eG. Furthermore, the bracket of two left invariant vector fields is itself a left invariant vector field, namely one has $dL_y[X, Y](e) = \left[dL_y X, dL_y Y\right](e) = [X, Y](y)$. The left invariant vector fields on the Lie group G thus have the structure of *Lie algebra*.

DEFINITION 4. *The Lie algebra of the Lie group G is the Lie algebra of the left invariant vector fields. A Lie group action on a manifold M is given by a map $\mu : G \times M \to M; (a, q) \mapsto \mu_a(q)$, satisfying $\mu_e(q) = q$ and the composition rule $\mu_a \circ \mu_b = \mu_{ab}$. Lie groups and Lie algebra are most of the case discussed in terms of their matrix representations.*

EXAMPLE 3. The Lorentz group action in ED space-time can be represented

by the one-parameter family of matrices

$$\begin{bmatrix} ch\psi & sh\psi, \\ sh\psi & ch\psi, \end{bmatrix}$$

which defines a one-dimensional group (identity element is given by $\psi = 0$), with group manifold $\mathbb{R}$. The group action on $\mathbb{R}^2$ is defined by the application

$$(t, x) \mapsto (t, ch\psi + x\, sh\psi, t\, sh\psi + x\, ch\psi)$$

The Lie algebra is endowed with the bracket operation (of vector fields); it satisfies the properties of linearity, anticommutativity ($[X, Y] = -[Y, X]$), and the Jacobi identity ($[X, [Y, Z]] + [Y, [Z, X]] + [Z, [X, Y]] = 0$).
Once the action of a transformation on points is defined, the action on tangent vectors (or more generally on elements of the tangent bundle), on tensors and differential forms (on elements of the cotangent bundle) are determined. The change operated on those objects is called the *Lie derivative*. Recall that any differentiable vector field X on a manifold M generates a 1-parameter local group of diffeomorphisms ϕ_t relating neighborhoods of M, viz $\phi_t : M \to M\ x \mapsto \phi_t x$, that satisfies the differential equation

$$\frac{d\phi_t}{dt} = X\,(\phi_t x)$$

with the initial condition $\phi_0(x) = x$. The orbit of the group passing through point $x_0 = \phi(x_0)$ is the integral curve $\mathbb{R} \to M; \mapsto x(t) = \phi_t x_0$ tangent to the vectors $X\,(\phi_t x_0)$ of the field at each point $\phi_t x_0$. Since the manifolds (contrary to the Euclidean spaces) do not allow an easy comparison of vector fields attached at different points (thus leaving in different vectorial spaces), a novel derivative needs to be introduced. Consider g a differentiable function on M; the tangent vector to the group ϕ_t at the point x_0 is $X_0 = \left(\frac{d}{dt}x(t)\right)_{t=0} = \left(\frac{d}{dt}\phi_t x_0\right)_{t=0}$. The derivative of (the germ of) g in the direction of X at the point x_0 is the real $X_0\, g = \left(\frac{d}{dt}\,(f \circ \phi_t)\,(x_0)\right)_{t=0} = X^I \left(\frac{\partial}{\partial x_i} g\right)_{x_0^I} \left(\frac{dx^i}{dt}\right)_0$.

- The Lie derivative of the function g in the direction of X at point x_0, is defined as the directional derivative $L_{x_0} g = X_0 g = \lim_{t\to 0} \frac{g\,(\phi_t x_0) - g\,(x_0)}{t}$. The operation achieved therein means a pull-back along the orbit to the point x_0, comparing the value $g\,(\phi_t x_0)$ to the value $g\,(x_0)$ at the same point. In a set of local coordinates, one writes
$$L_x g = X^I \partial_i\, g$$
- The Lie derivative of the vector field Y in the direction of the vector field X at point x_0 is $L_X Y = \lim_{t\to 0} \frac{1}{t}\left(d\phi_t^{-1} Y_{\phi_t x_0} - Y_{x_0}\right) = \left(\frac{d}{dt} d\phi t^{-1} Y\right) t = 0$. It can be

proven that the Lie derivative coincides with the Lie bracket $L_X Y = [X, Y]$. In a set of local coordinates, one writes

$$L_X Y = \left(X^j \partial_j Y^I - Y^j \partial_j X^i \right) \partial i.$$

- The Lie derivative of a $\begin{pmatrix} q \\ 0 \end{pmatrix}$ tensor field is similarly defined as

$$L_X T := \lim_{t \to 0} \frac{1}{t} \left(d\phi_t^{-1} T_{\phi_t x_0} - Y_{x_0} \right)$$

- Noting $\phi_t^* T_{\phi_t x_0}$ the pull-back at point x_0 of the tensor $T_{\phi_t x_0}$, the Lie derivative of a $\begin{pmatrix} 0 \\ p \end{pmatrix}$ tensor field is elaborated as

$$L_X T := \lim_{t \to 0} \frac{1}{t} \left(\phi_t^* T_{\phi_t x_0} - Y_{x_0} \right) = \left(\frac{d}{dt} \phi_t^* T \right)_{t=0}$$

- Similarly, for completely antisymmetrical tensors of the previous type, i.e. for differential forms ω, the Lie derivative is defined as

$$(L_X \omega)_{x_0} = \lim_{t \to 0} \frac{1}{t} \left(\phi_t^* \omega_{\phi_t x_0 - \omega_{x_0}} \right) = \left(\frac{d}{dt} \phi_t^* \omega \right)_{t=0}$$

  In a set of local coordinates, one writes for the Lie derivative of a 1-form $(L_X \omega)_I = X^j \partial_j \omega i + \omega_j \partial_i X^j$.

Properties

Only the essential properties of the differential operations so far introduced are listed in the sequel. A vector field v s.t. $L_w v = 0$ is said to be **Lie-transported** or dragged along the vector field w. Since the Lie derivative is a local approximation, it shall satisfy Leibniz rule, thus

$$L_w (a \otimes b) = L_w a \otimes b + a \otimes L_w b.$$

Using the same rule gives the Lie derivative of a 1-form α: differentiating the function $f = \alpha.v$ renders $(L_w \alpha).v = d(\alpha.v) w - \alpha[w, v]$, thus in terms of a set of coordinates $L_w \alpha = \left(\alpha \mu, \theta w v + \alpha \theta w^{\nu}_{,} v \right) dx^{\nu}$. Lie derivatives inform about symmetries of geometrical objects; so for instance, the infinitesimal symmetries of the 1-form field dx are given by those vector fields $w = X \dfrac{\partial}{\partial x} + Y \dfrac{\partial}{\partial y} + Z \dfrac{\partial}{\partial z}$, that satisfies $L_w dx = 0$, thus X has to be constant.

2.3. Calculus on differential forms

Differential forms find their origin in 1889 in the work of Elie Cartan (1869 – 1951), and in the third volume of *Les Methodes Nouvelles de la Mecanique Celeste* by Henri Poincaré (1854 – 1912). The program of writing the laws of physics in an invariant form (using differential forms), was started by g. Ricci-Curbastro (1853 – 1925) and his student T. Levi-Civita (1873 – 1941); it provided the useful framework for A. Einstein (1879 – 1955) to develop the theory of relativity.
Consider M an n-dimensional manifold and $(x_1, x_2, \ldots, x_n)$ a coordinate system on this manifold.

DEFINITION 5. *A p-form or exterior form of degree p on M is alternated or completely antisymmetrical if it is the antisymmetrical part of a multilinear application from M to* $\mathbb{R}$. *Thus, for* t_x *a p-linear form (at point x of M), the operation of antisymmetrization renders*

$$A_p\, t_x\,(V_1, \ldots, V_n) = \frac{1}{p!} \sum_{\sigma} \epsilon_\sigma t_x \left(V_{\sigma(1)}, \ldots, V_{\sigma(p)}\right),$$

with σ *a permutation having the signature* ϵ_σ.

A p-form can be built from the tensorial product of n one-forms on M, according to the rule: the tensorial product of p 1-forms is the p-form, the components of which are identified with the components of the tensorial product if the p associated vectors.

EXAMPLE 4. Consider $\alpha(x_1\, x_2) = 3x_2 - x_1$ and $\beta(x_1\, x_2) = 2x_2 + x_1$; one then has

$$\alpha \otimes \beta = (x_1, x_2) \left[\begin{pmatrix} -1 \\ 3 \end{pmatrix} \otimes \begin{pmatrix} 1 \\ 2 \end{pmatrix} \right] \begin{pmatrix} x_1 \\ x_2 \end{pmatrix} =$$

$$= (x_1\, x_2) \begin{pmatrix} -1 & -2 \\ 3 & 6 \end{pmatrix} \begin{pmatrix} x_1 \\ x_2 \end{pmatrix} = -x_1^2 + x_1 x_2 + 6x_2^2$$

DEFINITION 6. *The exterior product (notation* $\wedge$*) of p 1-forms* A_{ik}*, is the p-form obtained by the anti symmetrization of the tensorial product, viz*

$$A_{i1} \wedge A_{i2} \ldots \wedge A_{ip} = \delta^{i_1 \ldots i_p}_{I_1 \ldots I_p} A_{I_1} \otimes \ldots \otimes A_{I_p}$$

(summation of the indices I_k*), with*

$$\delta^{i_1 \ldots i_p}_{I_1 \ldots I_p} = \begin{cases} 0 \text{ if the } i_k \text{ are not a permutation of the } I_k \\ 1 \text{ if the } i_k \text{ are an even permutation of the } I_k \\ -1 \text{ if the } i_k \text{ are an odd permutation of the } I_k \end{cases}$$

EXAMPLE 5. One has in $\mathbb{R}^4$ the equality

$$x_3 \wedge x_1 = x_3 \otimes x_1 - x_1 \otimes x_3 = -x_1 \wedge x_3$$

The canonical basis of the set of p-forms of order $p \leq n$ at the point $x \in M$, noted $\Omega_x^p(M)$, is given by the C_n^p exterior products $x_{i_1} \wedge \ldots \wedge x_{i_p}$, with the following ordering of the indices $i_1 < i_2 < \ldots < i_p$.. Thus, one can express any p-form ω in a basis $\theta^{i_1} \wedge \ldots \wedge \theta^{i_1}$ of $\Omega_x^p(M)$ using the *strict components* of the p-form $\omega = \omega_{i_1 \ldots i_p} \theta^{i_1} \wedge \ldots \wedge \theta^{i_p}$, with the summation done only on the ordered indices $i_1 < i_2 < \ldots < i_p$.

EXAMPLE 6. Consider $\omega \in \Omega_x^2(M)$; the action of ω on a couple of tangent vectors $X, Y \in T_x M$ is given by $\omega(X, Y) = \omega\left(X^i e_i, Y^j e_j\right) = \omega_{ij} X^i Y^j$, noting $\omega_{ij} \equiv \omega(e_i, e_j)$ the action of ω on the basis vectors (e_i, e_j). Expanding the result and using the antisymmetry of the matrix $\omega_{ij} + \omega_{ji} = 0$, renders

$$\omega(X, Y) = \sum_{I<j} \left(X^i Y^j - X^j Y^i\right) = \sum_{I<j} \omega_{ij} \theta^i \wedge \theta^j(X, Y).$$

Thus, one has $\omega = \sum_{i<j} \omega_{ij} \theta^i \wedge \theta^j$, and the products $\theta^i \wedge \theta^j$, $i < j$, generate any 2-form.

The exterior product of forms has the following properties: the exterior product $\wedge$ is bilinear, associative, non commutative. For two forms ω of order p, and μ of order q, one has $\omega \wedge \mu = (-1)^{pq} \mu \wedge \omega$. The space exterior product of the two spaces $\Omega_x^p(M)$ and $\Omega_x^q(M)$ is then the vectorial space $\Omega_x^{p+q}(M)$.

DEFINITION 7. *The exterior differentiation is the application d that associates to a p-form ω a $(p+1)$ -form $d\omega$, satisfying:*

- *for a function g from M to $\mathbb{R}$, the exterior derivative dg is simply the differential of g;*

it has the following properties

- *d is a linear operator;*
- *d is 2-nilpotent, viz $d \circ d = 0$ (iteration rule);*
- *d is an antiderivation, viz $d(\omega \wedge \mu) = d\omega \wedge \mu + (-1)^p \omega \wedge d\mu$.*

A practical formula for the calculus of the exterior derivative is given in the following

THEOREM 1. *Set $\omega = \omega_{i_1 \ldots i_p} dx_{i_1} \wedge \ldots \wedge dx_{i_p}$ a p-form; its exterior derivative is given by $d\omega = d\omega_{i_1 \ldots i_p} \wedge dx_{i_1} \wedge \ldots \wedge dx_{i_p} = \dfrac{\partial \omega_{i_1 \ldots i_p}}{\partial x_r} dx_r \wedge dx_{i_1} \ldots \wedge dx_{i_p}$.*

EXAMPLE 7. On $\mathbb{R}^3$, consider the 2-form $\omega = x_3 x_1 \, dx_2 \wedge dx_3$. One has

$$d\omega = x_3 \, dx_1 \wedge dx_2 \wedge dx_3.$$

It is interesting to relate exterior differentiation on $\mathbb{R}^3$ to classical vector calculus. Given a vector field $X = \xi_1 \frac{\partial}{\partial x} + \xi_2 \frac{\partial}{\partial y} + \xi_3 \frac{\partial}{\partial z}$, one defines the work form and the flux form of X respectively, as $\omega_X := \xi_1\, dx + \xi_2\, dy + \xi_3\, dz$, and $\phi_X := \xi_1\, dy\, dz + \xi_2\, dz\, dx + \xi\, dx\, dy$. These coinages come from the fact that the line integral of a one-form along a path measures the work done by X, while the surface integral of the flux form measures the flux of the field through the surface. Lastly, let define the density form of a smooth function f on the open set $U \subset \mathbb{R}^3$, as $\rho_f := f\, dx\, dy\, dz$. The table 2.1 then gives the correspondence between the differential forms ω_X, ϕ_X, ρ_f, and the vector components given as components of the exterior derivatives of ω_X, ϕ_X.

Differential form ω	Exterior derivative $d\omega$	Vectorial operator
$f = f(x, y, z)$	$df = \omega_{grad\ f} = f_{,x}dx + f_{,y}dy + f_{,z}dz$	$grad$
Work form $\omega_X := \xi_1\, dx + \xi_2\, dy + \xi_3\, dz$	$d\omega_X = \phi_{curl\ X} = \left(\frac{\partial \xi_3}{\partial y} - \frac{\partial \xi_2}{\partial z}\right) dy\, dz + \left(\frac{\partial \xi_1}{\partial z} - \frac{\partial \xi_3}{\partial x}\right) dz dx + \left(\frac{\partial \xi_2}{\partial x} - \frac{\partial \xi_1}{\partial y}\right) dx\, dy$	$curl$
Flux form $\phi_X := \xi_1 dydz + \xi_2 dzdx + \xi_3 dxdy$	$d\phi_X = \rho_{div X} = \left(\frac{\partial \xi_1}{\partial x} + \frac{\partial \xi_2}{\partial y} + \frac{\partial \xi_3}{\partial z}\right) dxdydz$	Div
$f\, dx\, dy\, dz$	0	

Table 2.1: exterior differentiation of forms and vector calculus

The set of differential forms of arbitrary order on a manifold M defines the *exterior algebra* on M, otherwise called the Grasmann algebra. The exterior algebra $\Omega_x(M)$ at M is the direct sum $\Omega_x(M) = \Omega^0_x(M) \oplus \Omega^1_x(M) \oplus \ldots \oplus \Omega^n_x(M)$. Elements in $\Omega^0_x(M)$ are functions, and the maximum order is $p = n$ (having only one element, the volume form). The dual to the tangent space to a manifold is called the *cotangent space*; it consists of the 1-forms (otherwise called *covectors* or covariant vectors - the tangent vectors being called contravariant) acting on the tangent space.
Another notion of differentiation of forms is given in the following

DEFINITION 8. *The vertical differential of a function $f = f(q_i, \dot{q}_i)$ (notation d_v) expresses locally as $d_v f = \frac{\partial f}{\partial \dot{q}_i} dq_i$, with $d_v(dq_i) = 0 = d_v(d\dot{q}_i)$.*

The inverse operation of decreasing the order of forms is given in the following

DEFINITION 9. *Consider a vector field X defined on M, and a p-form $\omega = \omega_{i_1 \ldots i_p}\, dx_{i_1} \wedge \ldots \wedge dx_{i_p}$. The interior product of ω by X, noted $i_X\omega$, is the*

$(p-1)$-*form* $i_X\omega := \dfrac{1}{(p-1)!}\,\omega_{ki_2\ldots i_p} X_k\, dx_{i_2} \wedge \ldots \wedge dx_{i_p}$.

EXAMPLE 8. consider on $\mathbb{R}^2$ the 1-form $\omega = x_2\, dx_1$ and the vector field

$$X = x_2 \frac{\partial}{\partial x_1} + \frac{\partial}{\partial x_2};$$

the direct application of previous definition gives $i_X\,\omega = \omega_k\, X_k = x_2^2$.

Properties

The following identity is often referred to as *Cartan identity*

$$L_v\omega = i_v d\omega + d\,(i_v\omega)\,.$$

One further list some basic properties (without proof):

$$i_v(\omega \wedge v) = (i_v\omega) \wedge v + (-1)^p \omega \wedge (I_v v)$$

$$L_v d\omega = d L_v\omega;\; L_v\,(i_u\omega) = i_{[v,\mu]}\omega + i_u L_v\omega;$$

$$L_{f v}\alpha = f\, L_v\alpha + df \wedge (i_v\alpha)$$

$$L_v(\omega \wedge v) = (L_v\omega) \wedge v + \omega \wedge (L_v v)\,.$$

The pullback of a p-form ω defined on the manifold W_m by the differentiable function $f : V_n \to W_m; x \mapsto z = f(x)$ is the *induced p-form*, $f^* : \Omega^p\,(W_m) \to \Omega^p\,(V_n)$, s.t.

$$\forall x \in V_n, \forall V_1, \ldots, V_p \in T_x V_n,\; \left(f^*\omega\right)_x \left(V_1, \ldots, V_p\right) = \omega_z \left(df_x V_1, \ldots, df_x V_p\right)$$

The representation of $f^*\omega$ in local coordinates is given by

$$f^*\omega = \omega_{j_1\ldots j_p}\,(z(x))\, \frac{D\left(z^{j_1}, \ldots, z^{j_p}\right)}{D\left(x^{j_1}, \ldots, x^{j_p}\right)}\, dx^{i_1} \wedge \ldots \wedge dx^{i_p}$$

with $\dfrac{D\left(z^{j_1},\ldots,z^{j_p}\right)}{D\left(x^{j_1},\ldots,x^{j_p}\right)}$ the Jacobean of the transformation from the $\left(x^i\right)_i$ to the $\left(z^j\right)_j$. The operators d and f^* commute, viz $d \circ f^* = f^* \circ d$.

EXAMPLE 9. The pullback of the 3-form $dx\,dy\,dz$ (omitting here the symbol $\wedge$) under the change of coordinates $x = r\,\cos\theta$, $x = r\,\sin\theta$, $z = z$ (cylindrical coordinates $r,\ \theta,\ z$) is $f^*(dx\,dy\,dz) = d(r\,\cos\theta)\,d(r\,\sin\theta)\,dz \equiv r\,dr\,d\theta\,dz$ (the Jacobean is thus r).

The pullback of forms is used to evaluate integrals on manifolds (change of variables). Both the differential and the pullback operation find simple interpretations in terms of the Jacobean matrix: suppose $\omega = A_1\,dy^1 + \ldots + A_1\,dy^m$ is a 1-form on the open set $V \subset \mathbb{R}^n$, and $\eta = \phi^*\omega$ expresses as $\eta = B_1\,dx^1 + \ldots + B_n\,dx^n$ as an

1-form on the open set $U \subset \mathbb{R}^n$, with $\phi : U \to V$ a diffeomorphism. Representing ω and η as the row vectors $\vec{\omega} = [A_1, \ldots, A_m]$ and $\vec{\eta} = [B_1, \ldots, B_n]$ then gives

$$[B_1, \ldots, B_n] = [A_1, \ldots, A_m] \begin{bmatrix} D_1\phi^1 & \ldots & D_n\phi^1 \\ \ldots & \ldots & \ldots \\ D_1\phi^m & \ldots & D_n\phi^m \end{bmatrix}$$

Thus, the pullback of a 1-form corresponds to matrix post-multiplication. As an application, when $p = n = m$, one recovers the change of variable formula used in the theory of integration, viz $\omega = A\left(dy^1 \wedge \ldots \wedge dy^n\right) \Rightarrow \phi^*\omega = |D\phi|\, A\left(dx^1 \wedge \ldots \wedge dx^n\right)$. The exterior derivative of a 1-form corresponds to the pre-multiplication by the Jacobean matrix, since the operation corresponds to the tangent mapping associated to the differential. The pullback of 1-forms is related to the dual operation of the push-forward of vector fields: for X a vector field on U, the *push-forward* of X under ϕ is defined as the vector field $\phi \cdot X$ on V, s.t. $\phi \cdot X(y) = d\phi(x)\left(X\left(\phi^{-1}(y)\right)\right)$ The pullback of the 1-form ω then relates to the *push-forward* of X as: $(\phi^*\omega).X(x) = \omega.\phi \cdot X(y)$.

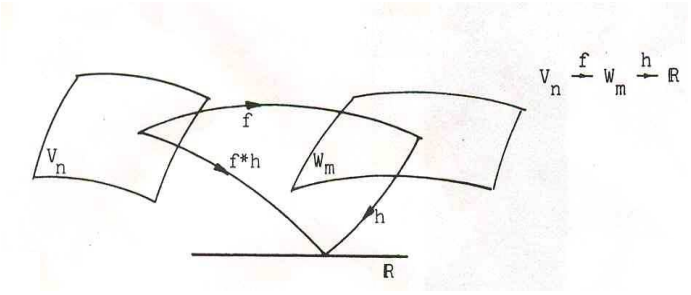

Figure 3: Diagrammatic representation of the pullback operation.

These two operations find useful applications in continuum mechanics, see [1].

The Hodge star operator

Let V_n be an n-dimensional vector space equipped with an inner product $\langle ., . \rangle$. Since $dim\left(\Omega^{n-p}(V_n)\right) = \dim(\Omega^p(V_n))$, for $p \leq n$, one can define a natural isomorphism between both these spaces. For any $\lambda \in \Omega^p(V_n)$, and assuming a given choice of the orientation of space has been done, there exists a unique element - noted ${}^*\lambda \in \Omega^{n-p}(V_n)$ - s.t. $\forall \mu \in \Omega^{n-p}(V_n)$, $\lambda \wedge \mu = \langle {}^*\lambda, \mu \rangle_{n-p} \sigma$, with σ the volume form on V_n. The Hodge star operator is the application that sends $\lambda \to^* \lambda$.
As an application, the correspondence between the exterior algebra and the 3D vector algebra is shown in the following Table.

Further applications of the Hodge star operator shall be given later on. Note lastly that differential forms receive a geometrical interpretation [31]. So, for instance, a 1-form can be represented by two parallel lines (planes in $3D$) in $2D$, representing the density of lines being cut. Just think of the gradient of a function as the 1-form giving the intensity of the slope between neighboring contours on a topographic map

Vector algebra expression	Exterior algebra expression
Cross product $(u \times v)$	$^*(u \wedge v)$
Triple product $u.(v \times w)$	$^*(u \wedge v \wedge w)$
$\lvert u \times v\rvert^2 = \lvert u\rvert^2\lvert v\rvert^2 - (u.v)w$	$\langle u \wedge v,\ u \wedge v\rangle = \langle u,\ u\rangle\langle v,\ v\rangle - \langle u,\ v\rangle^2$
$u \times (v \times w) = (u.w)v - (u.v)w$	$u \wedge^* (v \wedge w) = \langle u,\ w\rangle\ (^*v) - \langle u,\ v\rangle\ (^*w)$

Table 2.2: relation between the exterior algebra and the 3D vector algebra

[31]. The gradient of the function f (here the height of the contour) is orthogonal to the 1-form representation. The condition $i_v df = 0$ for a vector v then means that v is orthogonal to the components $grad\ f$ of the 1-form df. In electricity, a 2-form in $3D$ space (represented by a box aligned by the current flow direction) gives the current density (section of the box).

2.4. Contact structures and symplectic mechanics

The contact structure is a manifold suitable for the description of unparameterized curves. The line element contact bundle, called CM in the sequel, consists of a pair, namely a point in the manifold and a line element at that point. The line element itself gives the local approximation of the unparameterized curve, as a tangent vector of unspecified length (in fact a class of equivalence of tangent vectors, under the relation $v \sim kv$). Considering a submanifold - the pair $(N,\ \psi)$ - as being represented by a map $\psi : N \to M$ (s.t. both ψ and its differential are one-to-one), the first order contact between two submanifolds $(N,\ \psi)$ and $(N',\ \psi')$ at a common point $\psi(p) = \psi'(p')$ is traduced by the equality of tangent mappings $T_\psi\left[T_p(N)\right] = T\psi'\left[T_{p'}(N')\right]$ (this is not a point by point equality, but rather an equality between sets). The equivalence class of submanifolds in contact at a point $q \in M$ is called a *contact element* at q, and is noted $[N,\ \psi]$, for any submanifold N; it is in fact a linear subspace of the tangent space. Note that this notion of contact is weaker than the related notion of tangency. The contact structure is both a bundle (it has a projection onto the base space) and it has a contact structure: for each n-dimensional submanifold $(N,\ \psi)$ in M, one can define the natural lift $\sigma : M(M,\ n);\ q \mapsto (q,\ [N,\ \psi])$, with $[N,\ \psi]$ a contact element.

A simple chart for $C(M,\ N)$ is given by selecting n of the coordinates of M (labeled q^μ), and considering the remaining $(m - n)$ coordinates Y^a as functions of

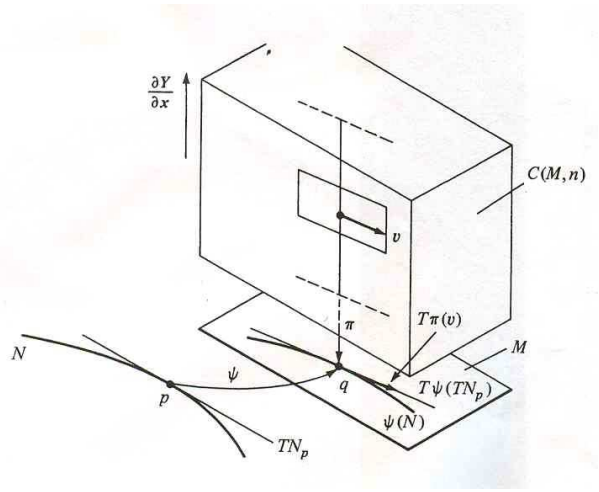

Figure 4: the geometric structure of the contact bundle (from [31]).

the q^μ. The contact elements are then represented by the partial derivatives $p^a_\mu = \frac{\partial Y^a}{\partial q^\mu}$ (note that the index position is here coherent with that chosen for the manifolds CM and C^*M).

DEFINITION 10. *Note that not all curves are lifts; a lifted submanifold is a submanifold for which the p^a_μ coincide with the partial derivatives, as written above. This condition can be expressed using the* 1*-forms $\theta^a = dy^a - p^a_\mu dq\mu$, that we pull-back onto a submanifold of $C(M,\ N)$, with $\psi : N \to C(M,\ N)$; $q \mapsto (q,\ Y(q),\ P(q))$. Using the pull-backs $\psi^* \cdot dq = dq = dq$; $\psi^* \cdot dy^a = \frac{\partial Y^a}{\partial q^\mu} dq^\mu$, one gets $\psi^* \cdot \theta^a = \left(\frac{\partial Y^a}{\partial q^\mu} - P^a_\mu\right)$. These pull-backs do vanish when N is a lifted submanifold; these lifted submanifolds shall then be called integral submanifolds of the contact ideal.*

EXAMPLE 10. Consider functions on the plane as the maps $F : \mathbb{R}^2 \to \mathbb{R}$. The graphs of these functions are the sections described by the map $\psi : \mathbb{R}^2 \to \mathbb{R}^3$; $(x,\ y) \mapsto (x,\ y,\ F(x,\ y))$, that define 2-sumanifolds on $\mathbb{R}^3$. A contact element at the point
$p\,(x_0,\ y_0,\ F\,(x_0,\ y_0))$ is an equivalence class of 2-submanifolds that have first order contact at p. It can be represented by the linear submanifold

$$(x,\ y) \mapsto \left(x,\ y,\ F + \frac{\partial F}{\partial x}\,(x - x_0) + \frac{\partial F}{\partial y}\,(y - y_0)\right)$$

The partial derivatives (here evaluated at the point $(x_0,\ y_0)$) are natural coordinates for the contact elements; the coordinates for the jet bundle are here $\left(x,\ y,\ f,\ f_x\ f_y\right)$, in

which f_x, f_y are coordinates of the contact element (and not partial derivatives). The pull-back of the contact 1-form $\theta := df - f_x dx - f_y dy$ onto a submanifold defined by the application $\psi : (x, y) \mapsto \left(x,\ y,\ F,\ F_x\ F_y\right)$ gives $\psi^* \cdot \theta = \frac{\partial F}{\partial x} dx + \frac{\partial F}{\partial y} dy - F_x dx - F_y dy$, which vanishes when $F_x = \frac{\partial F}{\partial x}$; $F_y = \frac{\partial F}{\partial y}$. The geometric approach to the calculus of variations presents some interest because of its originality, compared to the standard approach. The standard formulation of the classical mechanics of unconstrained conservative systems states the existence of a Lagrangian function L, depending upon the state variables and possibly upon time, such that the action integral $\int L\, dt$ is extremized. On the contact bundle of the configuration space, having the natural coordinates $(t,\ q,\ \dot{q})$, the integrand $\int L\, dt$ is a one-form. The possible motions of the system are then described by the curves in the contact bundle on which the contact 1-forms $\alpha := dq - \dot{q}\, dt$ pull back to zero. The variation of the action integral around the extrema is further performed, using the vector field $v = Q(t)\dfrac{\partial}{\partial q} + \dot{Q}(t)\dfrac{\partial}{\partial \dot{q}}$, restricting to isochronal variations. Restricting further to variations with fixed end conditions, the variation is given by

$$\int_\Gamma L_v\,(L\, dt) = \int_\Gamma i_v\,(dL\, dt) = \int_\Gamma \left[Q\frac{\partial L}{\partial q} dt + \dot{Q}\frac{\partial L}{\partial q} dt \right]$$

In order now for the variations to satisfy the previous constraint condition, the vector field v has to move the initial path into a path that is parallel to the α; instead of pushing the path forward, one can equivalently pull back the 1-forms α, as $\alpha(\epsilon) = \alpha + \epsilon L_v \alpha$. The condition that the 1-form $\alpha(\epsilon)$ pulls backs to zero on the integral curve, viz $i_{\dot\gamma}\alpha(\epsilon) = 0$, renders $i_{\dot\gamma} L_v \alpha = 0$, thus $i_{\dot\gamma}\left(dQ - \dot{Q}\, dt\right) = 0$. Since integration over the optimal path is equivalent to contracting the integrand with $\dot\gamma$, using the previous equation allows to replace $\dot{Q}\, dt$ by dQ, thus

$$L_v \int_\Gamma L\, dt = \int_\Gamma \left[Q\frac{\partial L}{\partial q} dt + \frac{\partial L}{\partial \dot{q}} dQ \right]$$

Integrating the second term by part and omitting the perfect differential (since we consider fixed ends) renders

$$L_v \int_\Gamma L\, dt = \int_\Gamma Q\left[\frac{\partial L}{\partial q} dt + d\left(\frac{\partial L}{\partial \dot{q}}\right) \right]$$

The arbitrariness in the choice of the functions $Q(t)$ then leads to the condition

$$i_{\dot\gamma}\left\{ \frac{\partial L}{\partial q} dt + d\left(\frac{\partial L}{\partial \dot{q}}\right) \right\} = 0$$

for $\dot\gamma$ to be tangent to the path.
This condition together with the constraint

$$I_{\dot\gamma}\,(dq - \dot{q} dt) = 0$$

gives $2n$ relations for the $2n$ components of the line element.
Since $L\, dt$ is not a general 1-form (its exterior derivative $dL\, dt$ being in the differential

ideal generated by $L\,dt$) , and $d\alpha$ also is in the ideal generated by $L\,dt$, a more general viewpoint is needed. Let then enlarge the previous considerations, starting first from the extemum condition of unconstrained integrals of the form $I = \int_\gamma \omega$, with the smooth enough 1-form ω defined on a manifold M, and Γ a curve in M (between two points A and B) s.t. the integral I does not vary at the first order as Γ is deformed. Considering a curve parameterized by s, the tangent vector to the curve $\dot{\gamma}$ expresses as the push forward of the basis vector $\dfrac{\partial}{\partial s}$, viz $\dot{\gamma} = \Gamma_*.\left(\dfrac{\partial}{\partial s}\right)$. Let then continuously deform the curve Γ by a vector field v; the previous condition that the integral I does not change under this deformation expresses as

$$\int_\Gamma L_v \omega$$

Using the properties of the Lie derivatives further renders

$$\int_\Gamma i_v\, d\omega + \int_\Gamma i_v\, \omega = 0$$

Since v vanishes at the end points (A and B being fixed), the boundary term vanishes. From the definition of a line integral, we further have

$$\int_\Gamma i_v\, d\omega = \int_a^b \Gamma^*.\left(i_v\left(i_{\dot{\gamma}\, d\omega}\right)\right) ds = 0, \forall v,$$

thus the local condition $i_v\left(i_{\dot{\gamma}\, d\omega}\right) = 0$, $\forall v$, that further gives $i_{\dot{\gamma}\, d\omega} = 0$, which is an ordinary differential equation for Γ.

Using the local coordinates $x^\mu = x^\mu(s)$ along the curve, one can further elaborate previous condition: the integral $I = \int \omega_\mu\, dx^\mu ds$ renders the Euler-Lagrange equations $\omega_{\mu,v}\dot{x}^\mu - \dfrac{d}{ds}\omega_v = 0$ thus giving the Schwarz condition $\left(\omega_{\mu,v} - \omega_{v,\mu}\right)\dot{x}_\mu = 0$. A first insight into Noether's theorem can here be given: suppose an infinitesimal symmetry exists, having the vector field k, such that $L_k\omega = 0$. This clearly gives $\int_\Gamma L_k\omega = 0$; along any piece of a curve that satisfies the Euler-Lagrange equations, the condition $i_{\dot{\gamma}} d\omega = 0$ gives

$$\int_\Gamma L_k\omega = \int_\Gamma d\,(i_k\omega) + \int_\Gamma i_k d\omega = \int_\Gamma i_k\omega = 0$$

which means that the quantity $i_k\omega$ is constant along the solution curves. This is an illustration of Noether's theorem, articulating infinitesimal symmetries and conservation laws.

The case of constrained variations is next treated, whereby the constraint is expressed by the vanishing of some function $\phi : M \to \mathbb{R}$, in the case of holonomic variations: we require that the variation of the integral $I = \int_\Gamma \omega$ vanishes, viz $L_v \int_\Gamma \omega = 0$, for all deformations of the curve that satisfy the constraint $L_v\phi = i_v d\phi = 0$. Summarizing, the variation of the integral must vanish at any point, viz $i_v\left(i_{\dot{\gamma}} d\omega\right) = 0$, $\forall v$, for all v

satisfying the condition $i_v d\phi = 0$. This implies the existence of a multiplier function $\lambda = \lambda(s)$, s.t. the following condition holds along the curve: $i_{\dot\gamma} d\omega = \lambda d\phi$, where $\phi = 0$.
This condition forms a set of determining equations for the curve and the Lagrange multiplier λ. In the case of anholonomic variations, the constraints can be expressed in the form $i_{\dot\gamma}\alpha = 0$, for a set of prescribed 1-forms α. The extension of the vector field $\dot\gamma$ off the curve is done using the condition $L_v\dot\gamma = 0$, thus the constraint condition $i_{\dot\gamma} L_v\alpha = L_v\left(i_{\dot\gamma}\alpha\right) = 0$.
The optimal path Γ is again determined by the condition $i_{\dot\gamma} d\left(\omega + \lambda\alpha\right) = 0$, along with $i_{\dot\gamma}\alpha = 0$. To be complete, one can evidence a Lagrange multiplier λ s.t. an unconstrained minimum exists for the problem having the one-form $\omega + \lambda\alpha$, see e.g [31]. For that purpose, a vector field w is selected s.t. the deformation of the curve can be written in the form $v = v_c + \xi w$, where v_c satisfies the constraint, and ξ is a scalar function that restores the degree of freedom lost in the constraint: it is found $\xi = \dfrac{i_{\dot\gamma} L_v\epsilon}{i_{\dot\gamma}\left(i_w d\alpha\right)}$, under the condition $i_w d\alpha \neq 0$ (with $d\alpha \neq 0$, otherwise the constraint would be integrable). Using next Cartan identity and neglecting the exact differentials gives the multiplier $\lambda = -\dfrac{i_{\dot\gamma}\left(i_w d\omega\right)}{i_{\dot\gamma}\left(i_w d\alpha\right)}$.

EXAMPLE 11. The dynamic equations of motion of a conservative system described by a Lagrangian $L\left(q,\ \dot q,\ t\right)$ is given as the stationary conditions of the functional $\int_\Gamma L\left(q,\ \dot q,\ t\right) dt$, under the constraints $i_{\dot\gamma}\left(\dot q dt - dq\right) = 0$. Application of previous general methodology renders the multiplier $\lambda = -\dfrac{\partial L}{\partial \dot q}$, and the equivalent unconstrained problem is $\displaystyle\int_\Gamma \left[L dt - \frac{\partial L}{\partial \dot q}\left(\dot q dt - dq\right)\right]$, the Euler-Lagrange equations of which being

$$i_{\dot\gamma}\left\{ dL dt - d\left(\tfrac{\partial L}{\partial \dot q}\right)\left(\dot q dt - dq\right) - \tfrac{\partial L}{\partial \dot q}\right\} = i_{\dot\gamma}\left\{ \tfrac{\partial L}{\partial q} dq\, dt - d\left(\tfrac{\partial L}{\partial \dot q}\right)\left(\dot q dt - dq\right)\right\} = 0.$$

It holds true that

$$i_{\dot\gamma} dq\, dt = i_{\dot\gamma}\left(dq - \dot q dt\right) dt = -\left(dq - \dot q dt\right) dt = -\left(dq - \dot q dt\right)\left(i_{\dot\gamma} dt\right)$$

the previous equation then gives

$$i_{\dot\gamma}\left\{ dL dt - d\left(\tfrac{\partial L}{\partial \dot q}\right)\left(\dot q dt - dq\right) - \tfrac{\partial L}{\partial \dot q} d\dot q dt\right\} = i_{\dot\gamma}\left\{ \tfrac{\partial L}{\partial q} dq dt - d\left(\tfrac{\partial L}{\partial \dot q}\right)\left(\dot q dt - dq\right)\right\} = 0$$

$$i_{\dot\gamma}\left\{ \frac{\partial L}{\partial q} dt - \left(\frac{\partial L}{\partial \dot q}\right)\right\}\left(\dot q dt - dq\right) = 0$$

Consequently, the extremals are the integral curves of the 1-forms $\dfrac{\partial L}{\partial q} dt - d\left(\dfrac{\partial L}{\partial \dot q}\right)$ and $dq - \dot q dt$.

The invariance of the constrained problem under infinitesimal symmetries again leads to the evidence of a conservation law: let indeed the vector k be an infinitesimal symmetry of both the variational principle and of the constraint, viz $L_v\omega = 0$ and $L_v\alpha = 0$. Thus, the Lie derivative of the one-form α has to be in the ideal generated by α (since $i_{\dot{\gamma}}\alpha = 0$). Incorporating the multiplier into the Lie differentiation then gives the condition $L_k(\omega + \lambda\epsilon) \subset I[\alpha]$, which traduces into a differential format as $\int_\Gamma \{d(\omega + \lambda\alpha) + i_k d(\omega + \lambda\alpha)\} = 0$. The second term is identified as the Euler-Lagrange equation (it vanishes), thus one obtains the conservation law $i_k d(\omega + \lambda\alpha) = constant$, along the extremals.

3. Lagrangian formalism and irreversibility

3.1. Differential structure of thermodynamics

A few words related to the geometrical setting of thermodynamics are first in order. Thermodynamic systems are described in the contact bundle sustained by the following coordinates:

- The total energy and entropy;
- the extensive variables (such as the volume, the number of particle, or the electric charge), that are the measurable degrees of freedom;
- the intensive associated variables, which are forces or potentials that describe the energy transfer between the various extensive variables.

EXAMPLE 12. An ideal gas is described in a 2D state space, with coordinates entropy and volume. An open gaseous system would require the additional coordinate of the amount of gas present in the system.

A thermodynamic system shall then be described by a linear structure, a contact structure and a convexity structure: the *linear structure* is a model for the physical idea of short-range interactions and existence of homogeneous systems with a scaling symmetry. The *contact structure* is associated with the energy conservation (first law of thermodynamics), while the *convexity structure* accounts for the Second Law and the entropy increase due to mixing. As a starting point, the *fundamental equation* consists of the expression of the stored internal energy of the system for all possible states, versus the set of state variables. For instance, the fundamental equation of an aggregate of N molecules of an ideal gas is

$$U(S\,V) = N^{5/3}V^{-2/3}\exp(2S/3NK),$$

with k the Boltzmann's constant. Linear structures rely on the assumption that the system size is much larger than the range of its interactions, thus the internal energy is proportional to the size of any subsystem (the shape of the subsystem does not matter):

by Euler's theorem (traducing here the homogeneity of degree one), this scaling symmetry gives $U = S\dfrac{\partial U}{\partial S} + V\dfrac{\partial U}{\partial V}$. Contrary to the status of the extensive variables, the intensive variables do not change versus size (homogeneity of degree zero). The graph of the fundamental equation is an n-surface in an $(n-1)$-space, with the potentials (partial derivatives of the internal energy w.r. to the extensive variables) the components of the contact elements to that surface. The contact bundle consists of the $(2n+1)$-space with coordinates the extensive variables, their associated intensive variables, and the internal energy. The contact ideal is generated by the 1-form

$$\alpha = dU + \sum (\text{forces})\, d\,(\text{extensive variables})\,.$$

EXAMPLE 13. The previously introduced ideal gas is modeled in the 5-dimensional contact bundle with coordinates $(U,\ T,\ S,\ P,\ V)$, and a contact ideal generated by the 1-form $\alpha = dU - TdS + Pdv$, with $P = -\partial - VU$; $T = \partial_S U$. The previous homogeneity condition becomes $U = TS - PV$, which is the *Gibbs-Duhem relation*. In addition to the fundamental equation, the equation of state expressing the intensive variables has to be specified. As an example, consider the ideal gas, which obeys the relation $PV = NkT$, together with the internal energy expression $U = 3/2NkT$. In the contact manifold, the system is described by the following map

$$\psi : (S,\ V) \mapsto (U,\ T,\ S,\ P,\ V) = (U\,(S,\ V)\,,\ T\,(S,\ V)\,,\ S,\ P\,(S,\ V)\,,\ V)$$

which expresses as

$$\psi : (S,\ V) \mapsto (U,\ T,\ S,\ P,\ V) = (3/2NkT,\ T\,(S,\ V)\,,\ S,\ NkT/V,\ V)\,.$$

The functions $U,\ Y,\ P$ shall satisfy the two previous conditions, as well as $\psi^*.\theta = 0$, with the 1-form $\theta = dU - U_V\, dV - u_p\, dP = dU - TdS + PdV$. Accounting for the pullbacks

$$\psi^*.dU = (3/2)\, Nk\left(\frac{\partial T}{\partial S}dS + \frac{\partial T}{\partial V}dV\right);\ \ \psi^*.dS = dS;\ \ \psi^*.dV = dV$$

one obtains

$$\psi^*.\theta = (3/2)\, Nk\left(\frac{\partial T}{\partial S}dS + \frac{\partial T}{\partial V}dV\right) - TdS + \left(\frac{NkT}{V}\right)dV \equiv 0$$

The independence of the differential elements $(dV,\ dT)$ then implies

$$\frac{1}{T}\frac{\partial T}{\partial S} = 2/3Nk;\ \ \frac{1}{T}\frac{\partial T}{\partial V} = -2/3V$$

The integration of these two equations gives $T = AV^{-2/3}exp(2S/3Nk)$, thus we recover the fundamental equation $U\,(U,\ V) = N^{5/3}V^{-2/3}exp\,(2S/3Nk)$. Note that the factor $N^{5/3}$ therein ensures the satisfaction of the homogeneity condition of U (a system of twice the volume, with twice the number of molecules has twice the energy).

Having so far developed what could be called a differential thermodynamics [31], the use of Frobenius theorem closes the characterization of the structure of thermodynamics: consider for instance the energy 2-surface as the map $\mathbb{R}^2 \to \mathbb{R}^3$; $(S,\ V) \mapsto (U,\ S,\ V)$, with the intensities given by $T = \partial_S U$ and $-P = \partial_V U$. The symmetry of the partial derivatives also leads to $\partial_V T + \partial_S P = 0$. The system can locally be described by a 2D surface element, spanned by the two vectors $A = a\dfrac{\partial}{\partial U} + \dfrac{\partial}{\partial T} + b\dfrac{\partial}{\partial S} + c\dfrac{\partial}{\partial P}$ and $A = d\dfrac{\partial}{\partial U} + \dfrac{\partial}{\partial T} + e\dfrac{\partial}{\partial S} + f\dfrac{\partial}{\partial V}$, that must lie in the zero surface of α, thus the conditions: $i_A\alpha = 0 = i_B\alpha$. This gives $a = bT$ and $d = eT - fP$. The fact that it is a differential ideal also implies that $d\alpha$ is one generator of the ideal, thus $i_B\,(i_A d\alpha) = 0$. Combining the previous relations gives the Maxwell relation $(c_V - C_P)\,/T + \left(\dfrac{dV}{dT}\right)_P \left(\dfrac{dP}{dT}\right)_V = 0$, with C_V, C_P the heat capacities at constant volume and pressure respectively.

3.2. Differential geometric setting for dynamical systems

Noether's theorem embodies the fact that to every symmetry is associated a conservation law. For an exterior differential system, a conservation law is a differential form whose restriction to the integral manifold is closed. Any closed generator of the ideal leads to a conservation law.

EXAMPLE 14. [31] The heat-equation $\kappa\dfrac{\partial^2\phi}{\partial x^2} + \dfrac{\partial\phi}{\partial t} = 0$ (with $\phi = \phi(x,\ t)$ the temperature, κ the specific thermal diffusivity), can be equivalently rephrased as the first order system $u = \kappa\dfrac{\partial\phi}{\partial x};\ \dfrac{\partial u}{\partial x} - \dfrac{\partial\phi}{\partial t} = 0$. The last equation of this system rewrites as $d\alpha = 0$, having defined the 1-form $\alpha = \phi\,dx + u\,dt$, that represents the *heat flux*. T hus, the equation $d\alpha = 0$ describes the *conservation of energy*. The geometrical picture of the heat transport equation can be given, using the following sharp operator: $\sharp dx = \dfrac{\partial}{\partial x};\ \sharp dt = 0$, leading to the Hodge star operator ${}^*1 = dx\,dt;\ {}^*dt = 0;\ {}^*dx = dt;\ {}^*dx\,dt = 0$. We then have ${}^*\alpha = \phi\,dt;\ d{}^*\alpha = \phi_{,x}dx\,dt$. The heat flux can further be written $u = i_{\frac{\partial}{\partial t}}\alpha$. Therefore, the geometric form of the heat equation is given by the following differential system

$$\left|\begin{array}{c} d\alpha = 0 \\ d\kappa{}^*\alpha = i_{*\lambda}\alpha \end{array}\right.$$

Note that the 1-form field α describes a field of conserved flux lines, but the 1-form ${}^*\alpha$ is not the gradient of any function, thus the flux lines are not cut by a regular family of orthogonal hypersurfaces. The problem can further be formulated as the integral submanifold of the ideal generated by the two 2-forms $\omega = d\phi\,dx + du\,dt$ and $\beta = u\,dx\,dt - \kappa\,d\phi\,dt$: for a $2D$ submanifold $\psi : (t,\ x) \mapsto (t,\ x,\ \phi,\ u)$, the condition of zero pull-back, viz $\phi^*\dot{\beta} = 0$, traduces the relationship $u = \kappa\,\phi_{,x}$. Note that the ideal

generated by the previous 2-forms is a differential ideal, due to the relationship

$$d\beta = du\,dx\,dt = -dx \wedge \omega.$$

In the ideal defined by the forms $\omega,\ \beta$, the form ω is closed, and the 1-form $j := i_S\omega$ satisfies the differential identity $dj = L_S\omega - i_S d\omega$ which vanishes for every isovector S, since $d\omega$ pulls back to zero. This leads to conservation laws, for instance the conservation of heat, viz

$$i_{\phi\frac{\partial}{\partial\phi}+u\frac{\partial}{\partial u}}\omega = \phi\,dx + u\,dt.$$

One of the approaches suitable for the generalization of the Lagrange formalism to dissipation is the differential geometry of manifolds: the interest of this generalized Lagrangian formulation lies in the fact that it follows from the structure of the chosen manifold, and naturally introduces the notion of a Rayleigh potential. In order to illustrate this method, let consider a discrete system of n punctual masses m_I, having the d.o.f. $q = \{q_I(t),\ I = 1\ldots 3n\}$ in $3D$ Euclidean space. Such a mechanical system is characterized by (Godbillon):

- a differentiable manifold generated by the d.o.f. $q = \{q_i(t),\ i = 1\ldots 3n\}$, called configuration manifold (the integer $m = 3n$ is the number of d.o.f.);
- a differentiable function K on the tangent space to M (here noted $T(M)$), called kinetic energy;
- a pfaffian π (differential form of degree one) defined on $T(M)$, that takes the form of the work $\pi = F_i\,(q,\ \dot{q})\,dq_i$ of the force F_i. The fundamental form of the mechanical system is defined as the exterior differential of the vertical differential of K, viz

$$\omega = \frac{\partial^2 K}{\partial q_k \partial \dot{q}_i} dq_k \wedge dq_i + \frac{\partial^2 K}{\partial \dot{q}_k \partial \dot{q}_i} d\dot{q}_k \wedge dq_i$$

Assuming this 2-form is closed and regular, and introducing the Liouville vector field $v = \dot{q}_i \dfrac{\partial}{\partial \dot{q}_i}$, the manifold structure implies the following

THEOREM 2. *There is a unique vector field* $X = a_i \dfrac{\partial}{\partial q_i} + b_i \dfrac{\partial}{\partial \dot{q}_i}$ *defined on* $T(M)$ *s.t.*

$$\begin{aligned} i_X\omega &= \frac{\partial^2 K}{\partial q_k \partial \dot{q}_i} a_k\,dq_i - \frac{\partial^2 K}{\partial q_k \partial \dot{q}_i} a_i\,dq_k + \frac{\partial^2 K}{\partial \dot{q}_k \partial \dot{q}_i} b_k\,dq_i \\ &- \frac{\partial^2 K}{\partial \dot{q}_k \partial \dot{q}_i} a_i\,d\dot{q}_k = d\,(K - vK) + \pi \end{aligned}$$

The integral curve of X (as a dynamical system) are solutions of the Lagrange equations

$$\frac{d}{dt}\frac{\partial K}{\partial q_i} - \frac{\partial K}{\partial q_i} = F_i\,(q,\,\dot{q})$$

The force field π is further decomposed into a contribution due to conservative forces F_I^C, deriving from a potential energy V, according to
$-dV = F_i^c\,dq_i \rightarrow F_i^c = -\dfrac{\partial V}{dq_i}$, and a non conservative contribution $F_i^{nc}dq_i$, viz

$$\pi = -dV + F_i^{nc}dq_i.$$

Introducing the Lagrangian of the system given by $L := K - V$, previous equation rewrites as

$$\frac{d}{dt}\frac{\partial L}{\dot{q}_i} - \frac{\partial L}{\partial q_i} = F_i^{nc}\,(q,\,\dot{q}) \tag{1}$$

EXAMPLE 15. **Differential geometry of the oscillatory mass**
In the case of single mass m evolving on a straight line, with position $q = q(t)$, submitted to an elastic force $F^c = -kq = -\dfrac{\partial V}{\partial q}$ (with clearly $V = \dfrac{1}{2}kq^2$) and a viscous force $F^{nc} = -\lambda\dot{q}$ (with λ a constant), the kinetic energy is $K = \dfrac{1}{2}m\dot{q}^2$, and the force field associated to F^c and F^{nc} is $\pi = -\lambda\dot{q}\,dq - k\,q\,dq$. Thus, the fundamental form ω and the Liouville vector field are respectively given by
$\omega = m\,d\dot{q} \wedge dq$; $v = \dot{q}\dfrac{\partial}{\partial\dot{q}}$.
Application of previous Theorem then leads to the search of a vector field X under the form

$$X = a\,(q,\,\dot{q})\,\frac{\partial}{\partial q} + b\,(q,\,\dot{q})\,\frac{\partial}{\partial\dot{q}}$$

satisfying the differential form identity

$$\begin{aligned} i_X\omega &= -m\,a\,(q,\,\dot{q})\,d\dot{q} + -m\,b\,(q,\,\dot{q})\,d\dot{q} \\ &= d\,(K - vK) + \pi = -m\,\dot{q}d\dot{q} + (-\lambda\dot{q} - kq)\,dq. \end{aligned}$$

The identification of the coefficients of the one-forms dq and $d\dot{q}$ then leads to

$$X = \dot{q}\frac{\partial}{\partial q} - \left(\frac{\lambda}{m}\dot{q} + \frac{k}{m}q\right)\frac{\partial}{\partial\dot{q}}$$

The integral curves of X are the solutions of the differential system
$\dfrac{dq}{dt} = d\dot{q}$; $\dfrac{d\dot{q}}{dt} = -\dfrac{\lambda}{m}\dot{q} - \dfrac{k}{m}q$ that condenses into the dynamical equation of motion
$m\ddot{q} + \lambda\dot{q} + kq = 0$.

Defining the Lagrangian as the difference $L = K - V = \frac{1}{2}m\dot{q}^2 - \frac{1}{2}kq^2$, the equivalence between the Lagrange equation and the integral curves of X easily appears:

$$\frac{d}{dt}\frac{\partial L}{\partial \dot{q}} - \frac{\partial L}{\partial q} = F^{nc} \Leftrightarrow m\ddot{q} + kq = -\lambda\dot{q}$$

Previous theorem can be considered as a generalization of the Lagrangian formalism, since the previous equation (1) results from the Lagrange-d'Alembert principle

$$(2) \quad \delta \int_{t_0}^{t_1} L\,(q,\,\dot{q})\;dt + \int_{t_0}^{t_1} F_i^{nc}\,(q,\,\dot{q})\,\delta q_i\,dt = 0 \Rightarrow \frac{d}{dt}\frac{\partial L}{\partial \dot{q}_i} - \frac{\partial L}{\partial q_i} = F_i^{nc}\,(q,\,\dot{q})$$

In the conservative case ($\pi = -dV$), previous equation resumes to the stationary condition of the action integral. Note furthermore that the non conservative forces are usually supposed to derive from a pseudo-potential dissipation (also called Rayleigh potential) R, as $R = -\frac{1}{2}\lambda\dot{q}^2 \Rightarrow F_i^{nc} = \frac{\partial R}{\partial \dot{q}_i}\ (= -\lambda\dot{q})$
The application of the Lagrange-d'Alembert principle also shows that the variation of the action integral $\int_{t_0}^{t_1} L\,(q,\,\dot{q})\;dt$ does not vanish, evidencing thereby a closure defect of the pfaffian $L\,(q,\,\dot{q})\;dt$ along its extremal (topological torsion of the configuration manifold, according to [21]).

The notion of Rayleigh potential introduced in the dynamics evokes the nearby concept of dissipation potential, that plays a role essentially in the thermomechanics of continuous media. Various attempts towards the formulation of the state laws and evolution equations of a viscoelastic and / or viscoplastic solid under a Lagrangian form have been addressed in the literature. Those approaches rely on the setting up of the Helmholtz free energy - here noted ψ that essentially depends upon two types of variables:

- observable variables (one can measure them), being in general the temperature T and a deformation like variable ϵ;
- hidden variables that describe the internal state of the material. These variables are otherwise called internal variables, here noted α (of a scalar or tensorial nature).

Accordingly, the potential takes a priori the general expression $\psi = \psi\,(\epsilon,\,\alpha,\,T)$, from which the state laws follow from the use of Clausius-Duhem inequality, as

$$\sigma_r = \rho_0\psi_{,\epsilon};\;\; A = -\rho_0\psi_{,\alpha};\;\; s = -\rho_0\psi_{,T}$$

with ρ_0 the density in the reference configuration, σ_r the reversible part of the stress, A the thermodynamical affinity (conjugated to the internal variables), and s the entropy density. These state laws shall be completed in the case of dissipative media by the information related to the irreversible behavior, via a pseudo potential of dissipation

$\Omega(\dot{\epsilon})$, s.t. the irreversible part of the stress is given by $\sigma_{ir} = \Omega_{,\dot{\epsilon}}$, considering the additive decomposition $\sigma = \sigma_r + \sigma_{ir}$. Adopting a viscoelastic behavior, the affinity A derives from a second pseudo-potential $\Phi(\dot{\alpha})$, as $A = \Phi_{,\dot{\alpha}}$.
The Lagrangian formalism established in [33] relies on the definition of a pseudo-potential D, being the sum $D = \Omega(\dot{\epsilon}) + \Phi(\dot{\alpha})$. The author next defines a functional $S = S[u,\ \dot{u},\ \alpha,\ T]$ with

$$\begin{aligned} S &:= \int_{t_0}^{t_1} \left(\int_V \left[\frac{1}{2}\rho_0 \left(\frac{du}{dt} \right)^2 - \rho_0 \psi(\epsilon(u),\ \alpha,\ T) \right] dV \right) dt \\ &+ \int_{t_0}^{t_1} \left(\lambda \int_{S_f} T^d . u\, dS \right) dt \end{aligned}$$

with T^d the given imposed traction on the portion of boundary S_f, and λ a loading parameter that explicitly depends upon time. The variational principle associated to the extremality conditions of S can be viewed as a generalization of the Lagrange d'Alembert principle to continuous dissipative media; its formulation w.r. to the sole displacement is

$$\delta S + \int_{t_0}^{t_1} \left[\int_V \left(\frac{\partial D}{\partial \dot{\epsilon}} \epsilon\, \delta u \right) dV \right] dt = 0$$

leading to a relation analogous to (2):

$$\frac{\partial L}{\partial u} - \frac{d}{dt}\frac{\partial L}{\partial \dot{u}} = \frac{\partial D}{\partial \dot{\epsilon}} \epsilon$$

This equation in turn leads to the dynamical equations of equilibrium

$$div(\sigma_r + \sigma_{ir}) = \rho_0 \frac{d^2 u}{dt^2};\ (\sigma_r + \sigma_{ir}) . n = \lambda T^d$$

with n the outward normal to S_f. The complementary information relative to the thermodynamic forces (that traduces the internal evolution of the body) is given by the Lagrange equations relative to the internal variables, viz

$$\frac{\partial L}{\partial \alpha} = \frac{\partial L}{\partial \dot{\alpha}} \Leftrightarrow A = -\rho_0 \frac{\partial \psi}{\partial \alpha} = \frac{\partial \Phi}{\partial \dot{\alpha}}$$

One shall note the strong analogy between the description of the dynamics of a discrete system of dissipative punctual masses and the writing of the Lagrange equations in presence of non conservative forces F^{nc}: the first involves a Rayleigh potential R, while the second approach requires the functional S to be supplemented by the pseudo-dissipation potential D.
Going further in that direction, an attempt to extend the Lagrange formalism for dissipative media is further elaborated, in connection with the associated variational symmetries.

4. Lagrange formalism and TIP

Following the axioms of classical thermodynamics as stated in [4], let assume the existence of a functional E, called the internal energy, being extensive w.r. to its arguments, viz $E = (E\,(V\epsilon,\ S,\ N)$, whereby the introduced arguments reflect the different forms of energy:

- mechanical energy (we here focus on small deformations ϵ, with a nearby constant volume V);
- calorific energy, represented by the total entropy S;
- chemical energy, represented by the number of moles $N = \{N_k,\ k = 1 \ldots n\}$ of the various species.

The extensity of E (homogeneity of degree one) expresses as (Euler's theorem):

$$E\,(\lambda V\epsilon,\ \lambda S,\ \lambda N) = \lambda E\,(V\epsilon,\ S,\ N)\,, \quad \forall \lambda \in \mathbb{R}$$

Deriving previous equation w.r. to λ at $\lambda = 1$ leads to the Euler identity

$$\frac{\partial E}{\partial\,(V\epsilon)} : (V\epsilon) + \frac{\partial E}{\partial S} S + \frac{\partial E}{\partial N} N = E\,(V\epsilon,\ S,\ N) \Rightarrow$$

$$E\,(V\epsilon,\ S,\ N) = \sigma\,(V\epsilon,\ S,\ N) : (V\epsilon) + T\,(V\epsilon,\ S,\ N)\,S + \mu\,(V\epsilon,\ S,\ N)\,.N$$

wherein the intensive quantities conjugated to the independent intensities have been introduced: the stress $\sigma\,(V\epsilon,\ S,\ N)$, the temperature $T\,(V\epsilon,\ S,\ N)$, and the chemical potentials $\mu\,(V\epsilon,\ S,\ N)$. Accounting for these relationships then leads to the fundamental Gibbs relation:

$$dE = \sigma : d\,(V\epsilon) + TdS + \mu.dN$$

The differentiation of Euler's identity leads to the Gibbs-Duhem relation

$$(V\epsilon) : d\sigma + SdT + N.d\mu = 0$$

Both the Gibbs and Gibbs-Duhem relations are at the roots of thermodynamics; Gibbs-Duhem relation expresses the adjustment of the intensive variables during the variation of the extensities. When sufficient mechanical energy is brought to the system as input, may lead to a change of the internal configuration of the body, due to the fact that the system escapes from equilibrium. Assuming that the internal energy still has the status of a potential function, and replacing the variables N_k by extensive internal variables Ω_i, one has $E = E\,(V\epsilon,\ S,\ \Omega)$. The thermodynamic driving force A (or affinity in the language of De Donder) associated to the internal variable α expresses as $A_i\,(V\epsilon,\ S,\ \Omega) = -\dfrac{\partial E\,(V\epsilon,\ S,\ \Omega)}{\partial \Omega_i}$. In the sequel, we shall rather work with densities, thus writing the generalized fundamental Euler's relation as

$$e\,(\epsilon,\ s,\ \alpha) = \sigma\,(\epsilon,\ s,\ \alpha) : \epsilon + T\,(\epsilon,\ s,\ \alpha)\,s - A\,(\epsilon,\ s,\ \alpha)\,.\alpha$$

here introducing the energy and entropy density e and s respectively, and the density of the internal variables extensities Ω, noted α. The Gibbs-Duhem relation then rewrites as

$$\epsilon : d\sigma + sdT - \alpha.dA = 0$$

The state laws that give the constitutive behavior of the body then express in rate form as

$$\left(\begin{array}{c} \dot{\sigma} \\ \dot{T} \\ -\dot{A}_i \end{array} \right) = \left(\begin{array}{ccc} e_{,\epsilon\epsilon} & e_{,\epsilon s} & e_{,\epsilon\alpha_k} \\ e_{,s\epsilon} & e_{,ss} & e_{,s\alpha_k} \\ e_{,\alpha_k\epsilon} & e_{,\alpha_k s} & e_{,\alpha_k\alpha_k} \end{array} \right) . \left(\begin{array}{c} \dot{\epsilon} \\ \dot{s} \\ -\dot{\alpha}_k \end{array} \right), \tag{3}$$

In the vicinity of equilibrium, the matrix of second order partial derivatives can be considered as made of constant entries. In order to be synthetic, let introduce the vector $y = (\epsilon,\ s)^t$ of the controlled extensities (their densities), being conjugated to the dual observable, noted $Y = (\sigma,\ T)^t$. Previous system then rewrites $P = 0$, with

$$P := \left\{ \begin{array}{c} P_Y(y,\ \alpha) = Y - e_{,yy}.\dot{y} - e_{,y\alpha}.\dot{\alpha} = 0 \\ P_A(y,\ \alpha) = -\dot{A} - e_{,\alpha y}.\dot{y} - e_{,\alpha\alpha}.\dot{\alpha} = 0 \end{array} \right. \tag{4}$$

Elementary calculations show that the previous system satisfies the self-adjunction condition of the Frechet derivative of P, viz $D_p = D^* P$, being equivalent to the Maxwell's relations for the internal energy e [19, 32]. Recall that the *Frechet derivative* of a vector of functions $P_i\left(x,\ u^{(n)}\right)$, depending upon the independent variable x and the dependent variable u, up to its derivatives to the order n, is the differential operator D_p given by $\left(D_p\right)_{ij} = \sum_J \dfrac{\partial P_i}{\partial u_{j,J}} D_J,\ i = 1 \ldots r,\ j = 1 \ldots q$. The multiindex J of dimension k consist of a set of k indices each less than 4, viz $J = (j_1, \ldots,\ j_k),\ 1 \leq j_k \leq 4$. Accordingly, one expresses the partial derivative $u_{i,j} = \dfrac{\partial^k u_i}{\partial x_{j1} \ldots . \partial x_{jk}}$.

EXAMPLE 16. For $P = u + u_x^2$, one has $D_p = \dfrac{\partial P}{\partial u} + \dfrac{\partial P}{\partial u_x} D_x = 1 + 2u_x D_x$, with D_x the total derivative operator w.r. to x.

THEOREM 3. *The adjunct of the Frechet derivative is the matrix of differential*

$$\left(D^* P\right)_{ij} = \sum_J (-D)_J \frac{\partial P_j}{\partial u_{i,J}},\ i = 1 \ldots q;\ \ j = 1 \ldots r$$

Given the scalar products of two elements $P = \left\{P_i\left(x,\ u^{(n)}\right)\right\},\ Q = \left\{Q_i\left(x,\ u^{(n)}\right)\right\}$ *as* $\langle P,\ Q\rangle := \int_\Omega \sum_{I=1}^{q} P_i Q_i dx$, *the adjunct satisfies the following condition*

$$\langle P,\ DQ\rangle = \langle Q,\ D^* P\rangle,\ \forall P = \left\{P_i\left(x,\ u^{(n)}\right)\right\},\ \forall Q = \left\{Q_i\left(x,\ u^{(n)}\right)\right\}$$

EXAMPLE 17. For $D = \dfrac{d}{dt}$ the operator acting on functions with compact support in $\Omega =]0,\ 1[$, one writes

$$\langle u,\ Dv\rangle = \int_0^1 v\frac{dv}{dt}dt = -\int_0^1 u\frac{dv}{dt}dt + [uv]_0^1 = \langle v,\ D^*u\rangle,$$

thus the adjunct $D^* \equiv -\frac{d}{dt}$.

The existence and construction of a Lagrangian for a system described by a set of PDE's is expressed in the following

THEOREM 4. [27] *A system of PDE on the dependent variables u of the form $P(u) = \left\{P_i\left(x,\ u^{(n)}\right),\ I = 1\ldots q\right\} = 0$ realizes the extremum of a functional integral $S = \int_\Omega L\, d\Omega$, i.e. $P_i = E_i(L)$, with $E_i(.)$ the Euler-Lagrange operator, iff its Frechet derivative is self-adjunct. In this case, a possible Lagrangian is given by the line integral $\int_0^1 \sum_{i=1}^{q} u_i.P_i(\lambda u)d\lambda$. Equivalent Lagrangian are obtained up to the generalized divergence of a vector $P = \{P_t,\ P_X,\ P_Y,\ P_z\}$, defined as $Div\ P = \sum_{i=1}^{4} \dfrac{\partial P_i}{\partial x_i}$.*

EXAMPLE 18. (The vibrating string) The transverse vibrations of a string of length l_0 are described by the PDE $\lambda\, u_{tt} - T\, u_{xx} = 0$, with λ the lineic mass, and T the tension applied to the string. It is immediate to see that this EDP is self-adjunct, and a possible Lagrangian is set up as $L = \dfrac{1}{2}u\left(\lambda\, u_{,tt} - T\, u_{,xx}\right)$, however lacking a physical significance. It can further be worked out as

$$L = -\frac{1}{2}\lambda\, u_{,t}^2 + \frac{1}{2}T\, u_{,x}^2 + \frac{d}{dt}\left(\frac{1}{2}\lambda\, u\, u_{,t}\right) - \frac{d}{dx}\left(\frac{1}{2}T\, u\, u_{,x}\right).$$

An equivalent Lagrangian is $L = \dfrac{1}{2}\lambda\, u_{,t}^2 - \dfrac{1}{2}T\, u_{,x}^2$, thus the action integral

$$S = \int_0^\tau dt \int_0^{l_0}\left(\frac{1}{2}\lambda\, u_{,t}^2 - \frac{1}{2}T\, u_{,x}^2\right) dx = K - V,$$

difference of the kinetic energy $K = \displaystyle\int_0^\tau dt \int_0^{l_0}\left(\frac{1}{2}\lambda\, u_{,t}^2\right) dx$ and of the potential energy V, which itself results from the linearization of the expression

$$V = T\,(l - l_0) \equiv T\left(\int_0^{l_0}\sqrt{1 + u_x^2}dx - l_0\right).$$

Application of the previous theorem shows that the self-adjunction condition of the state laws is satisfied, thus the Lagrangian

$$L = \int_0^1 \left[y.P_Y\,(\lambda y,\ \lambda\alpha) + \alpha.P_A(\lambda y,\ \lambda\alpha)\right] d\lambda.$$

Accounting for the homogeneity of degree -1 of the second order partial derivatives of $e(y,\ \alpha)$, and the homogeneity of degree zero of the intensities $Y(y,\ \alpha)$ and $A(y,\ \alpha)$ then leads to

$$L = y.\dot{Y} - \alpha.\dot{A} + e_{,y}.\dot{y} + e_{,\alpha}.\dot{\alpha} - \frac{d}{dt}\left(e_{,y}.y + e_{,\alpha}.\alpha\right)$$

The last contribution can be removed (it is a total derivative), and the first contribution vanishes, according to Gibbs-Duhem relation, thus an equivalent Lagrangian is given by $L = e_{,y}.\dot{y} + e_{,\alpha}.\dot{\alpha}$, as independently obtained in [23].The stationarity of the action integral

$$S = \int e_{,y}.\dot{y} + e_{,\alpha}.\dot{\alpha} = \int \frac{de}{dt} \equiv e[y,\ \alpha]$$

(it is indeed a functional, due to the history dependence of the potential $e = e(y,\ \alpha)$ upon the internal variables α) simply means that the internal energy keeps its status of potential function during the evolution of the system. The postulate of existence of a thermodynamic potential E outside equilibrium thereby generates a stationarity principle, equivalent to the state laws. Note that adapted potentials can be built using the Legendre transformation, when a given set of control variables have been chosen. The Lagrangian so far established incorporates the thermodynamical information related to the state laws, but it does not consider the evolution laws of the internal variables. These can be written for GSM (generalized standard material) as the following subdifferential identities: $(-\dot{\alpha}) = \partial_A \phi^*\ (\sigma,\ T,\ A)$, with $\phi^*\ (\sigma,\ T,\ A)$ the pseudo-potential of dissipation [14]. Thus, using this last equation as a constraint via a set of Lagrange multipliers yields the unconstrained problem:

$$\delta \int_{t_0}^{t} \left[\dot{e} + \sum_{k=1}^{n} \lambda_k \left(\dot{\alpha}_k - \partial_{A_k} \phi^*\ (\sigma,\ T,\ A) \right) \right] dt = 0$$

where the subdifferential is taken w.r. to the affinity A_k, for the augmented Lagrangian

$$\dot{e} + \sum_{k=1}^{n} \lambda_k \left(\dot{\alpha}_k - \partial_{A_k} \phi^*\ (\sigma,\ T,\ A) \right)$$

sum of a thermodynamic Lagrangian $L_{thermo} := \dot{e}$ and a kinetic Lagrangian

$$L_{kin} := \sum_{k=1}^{n} \lambda_k \left(\dot{\alpha}_k - \partial_{A_k} \phi^*\ (\sigma,\ T,\ A) \right).$$

Note that the subdifferential reduces to the partial derivative in a 'smooth' case.

4.1. Continuous symmetries of dissipative constitutive laws and master curves

A reminder of variational symmetries is first in order: when a differential problem admits a variational formulation in terms of the stationarity of a functional, Noether's

theorem associates to each variational symmetry a conservation law. Recall that the one-parameter (μ is the parameter) Lie group of transformations $G : \bar{x_i} = \bar{x_i}(x,\ u,\ \mu)$; $\bar{u_i} = \bar{u_i}(x,\ u,\ \mu)$ is a symmetry group for the functional integral

$$S = \int_\Omega L\left(x,\ u^{(n)}\right)\, d\Omega$$

iff S keeps the same value in the set of transformed variables, viz

$$\bar{S} = \int_{\bar{\Omega}} \bar{L}\left(\bar{x},\ \bar{u}^{(n)}\right)\, d\Omega = S = \int_\Omega L\left(x,\ u^{(n)}\right)\, d\Omega$$

The vector field (symmetry generator)

$$v = \sum_{k=1}^{4} \xi_k(x,\ u)\frac{\partial}{\partial x_k} + \sum_{k=1}^{q} \phi_k(x,\ u)\frac{\partial}{\partial u_k} \equiv \sum_{i=1}^{4} \frac{\partial \bar{x_i}}{\partial \mu_{|\mu=0}}\frac{\partial}{\partial u_i}$$

defines a variational symmetry group iff the following condition is satisfied:

$$pr^{(n)} + L div\, \xi = 0.$$

The prolongation of the vector field v, alias $pr^{(n)}$, is defined as the extended vector field

$$pr^{(n)} v = v + \sum_{k=1}^{q}\sum_{J} \phi_k^J\left(x,\ u^{(n)}\right)\frac{\partial}{\partial u_{k,J}}$$

$$\phi_k^J\left(x,\ u^{(n)}\right) = D_J\left(\phi_k - \sum_{I=1}^{4} \xi_i u_{k,i}\right) + \sum_{I=1}^{4} \xi \frac{\partial}{\partial x_i}\left(D_J u^k\right)$$

J being an arbitrary multiindex or order less than 4.

THEOREM 5 (E. Noether, [20]). *When v generates a symmetry group for the functional $S[u] = \int_\Omega L\left(x,\ u^(1)\right)\, d\Omega$, the conservation law*

$$Div\, P = D_1 P_1 + \cdots + D_4 P_4 = 0$$

is satisfied, with the quadruplet $\{P_i,\ i = 1 \ldots 4\}$ given by

$$P_i = \sum_{k=1}^{q}\sum_{j=1}^{4} \xi_j u_{k,j}\frac{\partial L}{\partial u_{k,j}} - \sum_{j=1}^{q} \phi_j \frac{\partial L}{\partial u_{j,i}} - \xi_i L,\ \forall x \in \Omega.$$

Going back to the finding of the variational symmetries associated to the Lagrangian $L = L_{thermo} + L_{kin}$, the group generator

$$v = \xi\,\partial_t + \phi_\epsilon \partial_\epsilon + \phi_T \partial_T + \phi_{\alpha_k}\partial_{\alpha_k} + \phi_\sigma \partial_\sigma + \phi_S \partial_S + \phi_{A_k}\partial_{A_k}$$

maybe elaborated in such a way that the variational symmetry for L_{thermo} is automatically satisfied: just compute the components of the intensive variables s.t. they satisfy

the state laws. Previous symmetry condition then simplifies to [19, 32]

$$pr(n)v + L_{kin}Div\xi = 0 \text{ with } \mathrm{div}\xi \equiv D_t\xi$$

Using TIP and the elegant formalism of differential geometry, balance laws for intrinsically dissipative continuous media can then be formulated, in articulation with symmetries. These can be obtained in the following manner: the variation of the functional S under an arbitrary group of transformations expresses as

$$\delta S = \mu \int_\Omega \left(\frac{\partial L}{\partial u_k} - D_i \frac{\partial L}{\partial u_{k,i}} \right) \left(\phi_k - \xi_j u_{k,j} \right) d\Omega + \mu \int_{\partial\Omega} \left(L\xi_I + \left(\phi_k - u_{k,j}\xi_j \right) \right) n_i \, d(\partial\Omega)$$

This form can be transcribed into the compact differential form identity (Cartan formula):

$$L_X\omega = i_X \, d\omega + d \, (i_X\omega)$$

which allows a condensed writing of Noether's theorem: under the conditions $L_X\omega = 0$ (invariance of $\int_\Omega \omega \equiv \int_\Omega L \, dx \, dt$ by the group generated by X) and $i_X d\omega = 0$ (validity of the Euler-Lagrange equations), the following conservation law is obtained:

$$Div \left(L\xi_i + \left(\phi_k - u_{k,j}\xi_j \right) \frac{\partial L}{\partial u_{k,i}} \right) = 0$$

This identity appears as a balance law for dissipative media, wherein the Lagrangian describes the kinetics of evolution of the internal variables (according to previous developments). This approach seems more natural compared to the work in [5], since the authors do not truly consider dissipative media per se.

EXAMPLE 19. (Conservation of Deborah number in linear viscoelasticity) As a simple illustrative example, let consider the linear viscoelasticity law relating the Cauchy stress rate $\dot{\sigma}$ to the strain and strain rates, written as the following first order PDE with initial condition:

$$Delta := \left| \begin{array}{c} \frac{\partial\sigma}{\partial t} - E^0\dot{\epsilon} + \frac{\sigma - E^\infty\epsilon(t)}{\tau(T)} = 0 \\ \sigma(0) = 0 \end{array} \right.$$

wherein $\tau(T)$ is a temperature dependent relaxation time, and E^0, E^∞ denote the instantaneous and relaxed moduli respectively. The parameters τ, ϵ are here considered as dependent variables, whereas the time t is the independent variable. An equivalence principle is defined as the prescription of two groups of transformations G_1, G_2, s.t.

$$G_1(t, \sigma, \mu_1) = G_2(t, \sigma, \mu_2)$$

when $\mu_1 = \mu_2$, with σ solution of Δ. In terms of the generators, previous condition is rephrased as $pr^{(1)}v_1(\Delta) = pr^{(2)}v_2(\Delta)$, when $\Delta = 0$. As a specific generator that satisfies the previous condition together with the initial condition $\sigma(0) = 0$, one

obtains the time dilatation group (expressing the equivalence principle and integrating the resulting system of ODE satisfied by the coefficients of the two selected generators

$$v_1 = \xi\,(t,\ \tau,\ \dot{\epsilon})\,\frac{\partial}{\partial t} + \alpha\,(t,\ \tau,\ \dot{\epsilon})\,\frac{\partial}{\partial \dot{\epsilon}} \qquad \text{and} \qquad v_2 = \beta\,(t,\ \tau,\ \dot{\epsilon})\,\frac{\partial}{\partial t},$$

having the generators

$$v_1 = t\frac{\partial}{\partial t} - \dot{\epsilon}\frac{\partial}{\partial \dot{\epsilon}}; \qquad v_2 = -\tau\frac{\partial}{\partial \tau}.$$

They correspond to the two symmetry groups

$$G_1\,(t,\ \sigma,\ \mu) := \left| \begin{array}{c} \bar{t}_1 = e^{\mu_t} \\ \bar{\tau}_1 = \tau \\ \bar{\dot{\epsilon}}_1 = e^{-\mu_{\dot{\epsilon}}} \\ \bar{\sigma}_1 = \sigma \end{array} \right. \text{ and } G_2\,(t,\ \sigma,\ \mu) := \left| \begin{array}{c} \bar{t}_2 = t \\ \bar{\tau}_2 = e^{-\mu_\tau} \\ \bar{\dot{\epsilon}}_2 = \dot{\epsilon} \\ \bar{\sigma}_2 = \sigma \end{array} \right.$$

denoting the transformed variables with an over bar. Traducing the equivalence condition as $\bar{\sigma}_1\left(\bar{t}_1,\ \bar{\sigma}_1,\ \bar{\dot{\epsilon}}_1\right) = \bar{\sigma}_2\left(\bar{t}_2,\ \bar{\sigma}_2,\ \bar{\dot{\epsilon}}_2\right)$ gives the relation $\sigma\left(\frac{t}{\alpha},\ \alpha\tau,\ \dot{\epsilon}\right)$, with $\alpha = e^{\mu}$. Thereby, it appears that an identical response of the material is obtained, when a time contraction and a strain rate dilatation are operated, with the factors $1/\alpha$ and α respectively. This equivalence between time and strain rate leads to the conservation of Deborah number, defined as the ratio of the internal relaxation time (microscopic time) to the observer (macroscopic) time scale, viz

$$n_D := \frac{\tau}{t_{obs}} = \frac{\tau}{\epsilon/\,(\alpha\dot{\epsilon})} \equiv \frac{\alpha\tau}{t}$$

Applications of this methodology to the time-temperature equivalence principles have been further done [19], within a thermodynamic framework of relaxation [6]. Thereby, a systematic and predictive methodology for the setting up of master curves of dissipative media has been elaborated. Note that the symmetry groups act in the space of both independent variables (space and time) and dependent variables (that itself depend upon the selected thermodynamic framework); these symmetries shall further be exploited.

References

[1] ABRAHAM R, MARSDEN J.E AND RATIU T., *Manifolds, tensor analysis, and applications*, Springer, New York 1988.

[2] ANTHONY K.H., *Hamilton's action principle and thermodynamics of irreversible processes. A unifying procedure for reversible and irreversible processes*, J. Non-Newtonian Fluid. Mech. **96** (2001), 291–339.

[3] BIOT M.A., *Variational and lagrangian methods in viscoelasticity*, Springer-Verlag, New York 1956.

[4] CALLEN H., *Thermodynamics: an introduction to the physical theories of equilibrium thermostatics and irreversible thermodynamics*, Wiley, New York 1960.

[5] CHEN N., HONEIN T. AND HERMANN G., *Dissipative systems, conservation laws and symmetries*, Int. J. Solids Struct. **33** (20-22) (1993), 2959–2968.

[6] CUNAT C., *The DNLR approach and relaxation phenomena. Part I: historical account and DNLR formalism* , J. Mech. Time Dependent Mat. **5** (2001), 1013–1032.

[7] FEYNMANN R., *The strange history of light and matter*, Penguin, London 1990.

[8] GAO D.Y., *Duality principles in nonconvex systems*, Kluwer Academic Publishers, Dordrecht-Hardbound 1999.

[9] BERGER M. AND GOSTIAUX B., *Differential geometry: manifolds, curves, and surfaces*, Springer, New York 1988.

[10] CARTAN H., *Differential forms*, Hermann, Paris 1970.

[11] CURTIS W. D. AND MILLER F.R., *Differential manifolds and theoretical physics*, Academic Press, New York 1985.

[12] EDELEN D.G.B., *Applied exterior calculus*, Wiley, New York 1985.

[13] COLEMAN B.D. AND GURTIN M.E., *Thermodynamics with internal state variables*, J. Chem. Phys. **47** (1967), 597–613.

[14] GERMAIN P., NGUYEN Q.S. AND SUQUET P., *Continuum thermodynamics*, J. Appl. Mech. **50** (1983), 1010–1020.

[15] TRUESDELL C. AND NOLL W., *The non-linear field theories of mechanics*, Handbuch der Physik **III/3**, Springer-Verlag, Berlin 1965.

[16] FLANDERS H., *Differential forms with applications to the physical sciences*, Dover, New York 1989.

[17] LAGRANGE J.L., *Mecanique analytique*, Editions Jacques Gabay, Paris 1989.

[18] MAUGIN G.A., *Internal variables and dissipative structures*, J. Non-equ. Thermod. **15** (1990), 173–192.

[19] MAGNENET V., GANGHOFFER J.F., RAHOUADJ R. AND CUNAT C., *Master curves for viscous media predicted from symmetry analysis*, Proc. STAMM, Darmstadt 2004.

[20] OLVER P., *Applicaton of Lie group to differential equations*, Springer Verlag 1989.

[21] KIEHN R.M., *An extension of Hamilton's principle to include dissipative sys*, J. Math. Phys., **15** (1974), 9–13.

[22] KRUPKOVA O., *Hamiltonian field theory*, J. of Geometry and Physics, **778** (2001), 1–40.

[23] RAHOUADJ R., GANGHOFFER J.F. AND CUNAT C., *A thermodynamic approach with internal variables using Lagrange formalism. Part I and II*, Mech. Res. Comm. **30** (2003), 109–123.

[24] REIWE F., *Nonconservative Lagrangian and Hamiltonian mechanics*, Phys. Rev. E **53** (2) (1996), 1890–1899.

[25] POINCARE H., *Methodes nouvelles de la mecanique celeste*, Dover publications, 1957.

[26] LANG S., *Differentiable manifolds*, Addison-Wesley, Reading, MA. 1972.

[27] SANTILLI R. M., *Variational approach to self adjointness for tensorial field equations*, Annals of Phys. **103** (1977), 354–408.

[28] SPIVAK M., *A comprehensive introduction to differential geometry*, Vol. I-IV. Berkeley 1979.

[29] STRUIK D., *Lectures on classical differential geometry*, Dover, New York 1988.

[30] TALPAERT Y., *Lecons et applications de geometrie differentielle et de mecanique analytique*, Cepadues Editions 1993.

[31] BURKE W.L., *Applied differential geometry*, Cambridge University Press 1985.

[32] MAGNENET V., *Formulation thermodynamique de lois de comportement hors-equilibre: groupes de symmetries continues issus dune approce lagrangienne irreversible*, Ph.D. Thesis, INPL, Nancy 2005.

[33] STOLZ C., *Sur les equations generales de la dynamique des milieux continues anelastiques*, C.R. Acad. Sci. Serie II **307** (1988), 1997–2000.

AMS Subject Classification: 53DXX, 74A20, 80M30.

Jean-François GANGHOFFER, LEMTA - ENSEM, 2, Avenue de la Foret de Haye, BP 160. 54504 Vandoeuvre les Nancy Cedex, FRANCE
e-mail: jean-francois.Ganghoffer@ensem.inpl-nancy.fr

Rend. Sem. Mat. Univ. Pol. Torino - Vol. 65, 2 (2007)
ISASUT Intensive Seminar

G.A. Maugin

BASICS OF THE MATERIAL MECHANICS OF MATERIALS (M3) FOR ARBITRARY CONTINUA

Abstract. It is shown that the canonical balance of momentum of continuum mechanics can be formulated in a general way, but not independently of the usual balance of linear momentum, even in the absence of specified constitutive equations. A parallel construct can be made for the accompanying time-like canonical energy equation. On specifying the energy, previous particular cases can be deduced including pure elasticity, inhomogeneous thermoelasticity of conductors, and the case of dissipative solid-like materials described by means of a diffusive internal variable (such as in damage or weakly nonlocal plasticity). A redefinition of the entropy flux is necessarily accompanied by a redefinition of the Eshelby stress tensor.

1. Introduction

There exist two opposite viewpoints concerning the status of the equation of material (or canonical) momentum in continuum mechanics. The viewpoint of the author [1]-[2] is that this equation is never independent of the classical (physical) equation of linear momentum, in Cauchy or Piola-Kirchhoff form, being essentially deduced from the latter by a complete pull-back to the reference configuration whenever constitutive equations are known for the material. It is, therefore, an identity at all regular material points - but it still is extremely useful on any singular manifold [3]. This is in agreement with the application of Noether's identity [4] when one considers a variational formulation for a nondissipative material, a point of view shared by J.D.Eshelby in his original works, e.g.,[5]. The second viewpoint is that of Gurtin [6] who claims that this equation is an a priori statement independent of the classical balance laws although in the end it is, for sure, always shown to be related to the physical balance of momentum so that Gurtin's statement is somewhat inappropriate.

Let us be more inclusive. Several phantasms and fallacies are at work in the field that is our concern. The present work has for main purpose to correct these by pondering the basics of the material formulation of continua. First, it was for long thought that canonical equations of motion or equilibrium such as obtained initially by Eshelby can be deduced only when a variational formulation is at hand to start with, i.e., in the absence of dissipation and when the kinetic and potential energies are prescribed since a Lagrangian density is needed to start with. This is the belief of, if we may say, those who know "too much". Indeed these authors know elements of field theory including the celebrated theorem of Noether [4] according to which a "conservation law" is associated with any of the parameters describing the field theory under study when a variational basis is considered to formulate balance laws. One must obviously distinguish between the **field equations** (one for each scalar component of the involved fields) - these are the Euler-Lagrange equations of motions, and the **conservation laws**

that follow from Noether's identity. In pure continuum mechanics the fields are the actual components of the placement or of the displacement. The description parameters are a set of coordinates - usually the so-called material coordinates in order to avoid any confusion with any other system of coordinates-, and Newtonian time, a scalar. Infinitesimal variations of the latter generate the so-called equation of canonical - or material momentum - and the equation of energy conservation (Maugin and Trimarco [7]). If there are more fields, then there are more field equations, as many as fields, but the space-time parametrization remaining unchanged, the canonical conservation equations are still four in number (the three components of the canonical momentum equation, and the scalar energy equation). Accordingly, in general and working in Newtonian physics, there may be 3 + n field equations and 4 scalar conservation laws. In classical continuum mechanics where the medium involves no inner structure (such as in micropolar, Cosserat or micromorphic media), it happens that the three field equations left for the displacement and the material momentum equation can, at all regular material points, be placed in a one-to-one correspondence by the operations of material convection (pull-back and push-forward). Accordingly, one has the correct feeling that nothing is gained from having a conservation of canonical momentum -as a pure identity - in addition to that of momentum in physical space. The situation is altogether different when (i) there exist material points in the spatial domain of interest where the fields suffer a singularity of an appropriate order. The writing of the global canonical balance laws will then make additional terms emerge that correspond to the driving force (a **material** or **configurational** force acting on the singularity set - this may be a line or a surface) and an energy sink (so-called **energy-release rate**) such as at a crack tip line or at a surface of phase change) [8]-[9]. The situation is also more interesting even in the case (ii) where there are more fields than three but no singularity present, because both the canonical momentum conservation, then remaining essentially three dimensional, and the energy equation, as it should, but simultaneously with the canonical momentum conservation, involve all fields. This fact is exploited in perturbations of solutions of systems of partial differential equations (such as in soliton theory) [10] and also for checking the accuracy of numerical schemes of various nature [11]. Notice that when there are more fields than the classical placement, the canonical momentum equation is obtained by constructing a linear combination of field equations, each of these being first multiplied in the appropriate way by the material gradient of the corresponding field. In that sense the "canonical momentum" concept is additive and will include contributions from all fields including those of an electromagnetic nature [1] or even more surprisingly, rotational internal degrees of freedom although the canonical momentum itself reflects a translational invariance in material space (this is most nicely illustrated by the case of polar continua [12] and liquid crystals [13]). All these aspects have been duly examined in works by the author and co-workers. Still, one keeps on mind that constitutive equations have been suggested, perhaps only through a proposed dependence of the potential energy, in the relevant construct.

The view point of Gurtin [6] adopted by some authors is that there exists a priori a balance of configurational forces, in a sense, a new law of physics. We would say that this represents the view point of the philistines because they seem to ignore that the number of descriptive parameters, and therefore the number of balance laws of

classical continuum mechanics, is limited so that there should not exist a balance law of the momentum type independently of the one already and generally first written in the spatial framework. These authors generally ignore these rules of invariance that are the tenets of modern physics. They are thus led to introducing the energy pressure-like term in the Eshelby material stress through a dubious argument. They claim, to their defense, that this is a way to arrive at the material momentum equation, or its jump in the case of a singular surface, without previous knowledge of the constitutive equations of the medium, and, therefore, even in the presence of dissipation.

Here we expand the view that the balance of canonical or material momentum, albeit following from the balance of physical momentum, can be formulated independently of any constitutive behavior. Moreover, accounting for the fact that this equation is the space-like equation associated with a particular form of the energy equation, it is shown that the former and the latter can be used in parallel to build a consistent thermomechanics of many behaviors, especially in the presence of dissipation. It in fact is dissipative terms that help us construct a true invariant thermomechanics of rather general continua. In other words we would like to show how far one can first proceed in the construction of canonical material conservations laws without previous specialization to a certain behavior, it being understood that dissipation is not an obstacle to the formulation of such equations.

2. Reminder of classical local balance laws of continuum mechanics

We shall use the standard notation of nonlinear continuum mechanics such as in Eringen [14] and Eringen and Maugin [15], and a fortiori in Maugin [1]-[2]. In particular, $\mathbf{x} = \bar{\mathbf{x}} = (\mathbf{X}, t)$ is the time-parametrized motion mapping of material space onto physical Euclidean space. ∇_R and div_R denote the referential (material) nabla and divergence, and $d/dt = \partial/\partial t|_X$ or a superimposed dot denote the material time derivative. We suppose that the following three local balance laws have been deduced from a global statement for sufficiently smooth fields (see any book on the thermomechanics of continua). Here we consider the Piola-Kirchhoff formulation of the balance of mass, physical (linear) momentum, and energy (no external supply of energy apart from that related to the body force) at any regular material point X in a continuous body in the presence of a body force $\mathbf{f}_0$ per unit reference volume

$$\left.\frac{\partial \rho_0}{\partial t}\right|_X = 0 \tag{1}$$

$$\left.\frac{\partial (\rho_0 \mathbf{v})}{\partial t}\right|_X - div_R \mathbf{T} = \mathbf{f}_0 \tag{2}$$

$$\left.\frac{\partial (K+E)}{\partial t}\right|_X - \nabla_R(\mathbf{T}.\mathbf{v} - \mathbf{Q}) = \mathbf{f}_0.\mathbf{v}, \tag{3}$$

where ρ_0 is the mass density, $\mathbf{v} = \partial\bar{\mathbf{x}}\partial t|_X$ is the physical velocity, $\mathbf{T}$ is the first Piola-Kirchhoff stress, $K = \rho_0 v^2/2$ is the kinetic energy, E is the internal energy per unit reference volume, and $\mathbf{Q}$ is the material heat flux. This is complemented by the second law of thermodynamics written as

$$\left.\frac{\partial S}{\partial t}\right|_X + \nabla_R.\mathbf{S} \geq 0, \ \mathbf{S} = (\mathbf{Q}/\theta) + \mathbf{K}, \tag{4}$$

where S is the entropy density, θ is the absolute temperature ($\theta > 0, \ \inf\theta = 0$), and $\mathbf{S}$ is the entropy flux. The "extra entropy flux" $\mathbf{K}$ vanishes in most cases. We note $\mathbf{F} = \partial\bar{\mathbf{x}}/\partial X|_t = \nabla_R\bar{\mathbf{x}}$ the deformation gradient.

3. Canonical balance laws of momentum and energy

3.1. A canonical form of the energy conservation

First we shall formulate an interesting form of the energy conservation equation. A part of the reasoning is standard. In effect, taking the scalar product of both sides of eqn. (2) by $\mathbf{v}$ and performing some elementary manipulations we obtain the so-called *theorem of the kinetic energy* as

$$\frac{dK}{dt} - \nabla_R.(\mathbf{T}.\mathbf{v}) + \mathbf{T} :\dot{\mathbf{F}} - \mathbf{f}_0.\mathbf{v} = 0. \tag{5}$$

Combining this with the first law of thermodynamics (3) we obtain the so-called *theorem of internal energy*:

$$\frac{dE}{dt} - \mathbf{T} :\dot{\mathbf{F}} + \nabla_R.\mathbf{Q} = 0. \tag{6}$$

Further, in the case where $\mathbf{K} = \mathbf{0}$, introducing the Helmholtz free energy function by $W = E - S\theta$, we transform the inequality $(4)_1$ into the celebrated *Clausius-Duhem inequality*

$$-\left(\frac{dW}{dt} + S\frac{d\theta}{dt}\right) + \mathbf{T} :\dot{\mathbf{F}} - \mathbf{S}.\nabla_R\theta \geq 0. \tag{7}$$

As we know, this is exploited as a constraint in the formulation of thermodynamically admissible constitutive equations, while the "conservation equation " (6) is the equation governing heat propagation in a disguise. This can be given several transformed forms. A most interesting form is obtained straightforwardly by noting that $E = W + S\theta$, yielding

$$\frac{d(S\theta)}{dt} + \nabla_R.\mathbf{Q} = h^{int}, \quad h^{int} := \mathbf{T} :\dot{\mathbf{F}} - \left.\frac{\partial W}{\partial t}\right|_X \tag{8}$$

This is of special interest because of the expression in the right-hand side which a priori appears as an *internal heat source*. Indeed, for a typically thermodynamically reversible behavior such as pure nonlinear elasticity (hyperelasticity), where $W = \bar{W}(\mathbf{F})$

depends only on **F**, we have from the exploitation of (7),

$$\mathbf{T} = \frac{\partial W}{\partial \mathbf{F}} \Rightarrow h^{int} \equiv 0 \tag{9}$$

Note that in the situation where (8) holds good, the inequality (7) can also be written in the following enlightening form

$$S\dot{\theta} + \mathbf{S}.\nabla_R \theta \leq h^{int} \tag{10}$$

We claim that $(8)_1$ in fact is the most interesting form of the energy conservation equation for our purpose (i.e., establishing canonical equations). This we discover by constructing the canonical equation of momentum as follows.

3.2. Canonical (material) momentum conservation

Guided by what is valid for pure finite-strain elasticity (Noether's identity; see Maugin [1]), we apply **F** to the right of eqn. (2) and note that (T = transpose)

$$\left(\frac{\partial(\rho_0 \mathbf{v})}{\partial t}\right).\mathbf{F} = -\left.\frac{\partial \mathbf{P}}{\partial t}\right|_X - \nabla_R\left(\frac{1}{2}\rho_0 \mathbf{v}^2\right) + \left(\frac{1}{2}\mathbf{v}^2\right)(\nabla_R \rho_0), \tag{11}$$

and

$$(div_R \mathbf{T}).\mathbf{F} = div_R(\mathbf{T}.\mathbf{F}) - \mathbf{T} : (\nabla_R \mathbf{F})^T, \tag{12}$$

where we have set

$$\mathbf{P} := -\rho_0 \mathbf{v}.\mathbf{F} \tag{13}$$

the material momentum. Introducing plus and minus the material gradient of an (unspecified) free energy density $W = \bar{W}(.,.,...,\mathbf{X})$, we then check that eqn. (2) yields the following material balance of momentum

$$\frac{d\mathbf{P}}{dt} - div_R \mathbf{b} = \mathbf{f}^{int} + \mathbf{f}^{ext} + \mathbf{f}^{inh}, \tag{14}$$

in which we have defined the material *Eshelby stress* **b**, the material *inhomogeneity force* $\mathbf{f}^{inh}$ (cf. [1]-[2] for this notion), the material *external* (or body) force $\mathbf{f}^{ext}$, and the material *internal* force $\mathbf{f}^{int}$ by

$$\mathbf{b} = -(L_W \mathbf{1}_R + \mathbf{T}.\mathbf{F}), \quad L_W := K - W \tag{15}$$

$$\mathbf{f}^{inh} := \left.\frac{\partial L_W}{\partial \mathbf{X}}\right|_{expl} \equiv \left.\frac{\partial L_W}{\partial \mathbf{X}}\right|_{fixed\ fields} = (\mathbf{v}^2/2)\nabla_R \rho_0 - \left.\frac{\partial \bar{W}}{\partial \mathbf{X}}\right|_{expl}, \tag{16}$$

$$\mathbf{f}^{ext} := -\mathbf{f}_0.\mathbf{F}, \quad \mathbf{f}^{int} := \mathbf{T} : (\nabla_R \mathbf{F})^T - \nabla_R W|_{impl}, \tag{17}$$

where the subscript notations *expl* and *impl* mean, respectively, the material gradient keeping the fields fixed (and thus extracting the explicit dependence on **X**), and taking the material gradient only through the fields present in the function.

Equation (14) is the *canonical* balance of momentum of continuum mechanics *in the absence of specification of constitutive equations*. It is a mathematically strict conservation equation only when all source terms in its right-hand side vanish. Here the new notion is that of *material internal force* which appears in parallel and total analogy with the internal heat source $(8)_2$, the action of the material gradient replacing that of the material time derivative. We note that there is no "time-like" scalar equivalent to $\mathbf{f}^{inh}$ in equation $(8)_1$ because this inhomogeneity force which is automatically captured by that equation, has no dissipative nature. An explicit dependence of W on time (in a nonholonomous system) would yield a nonzero term h^{inh}, but this is hardly considered in continuum mechanics except perhaps in growing and ageing materials such as soft tissues (inhomogeneity of the material in time!). Similarly, there is no equivalent to the external material force $\mathbf{f}^{ext}$ in $(8)_1$ because this equation governs essentially the internal energy. It would be easy to rewrite eqns. $(8)_1$ and (14) as a single four-dimensional space-time equation (see [8]) but this serves no special purpose, except for an aesthetic satisfaction, in engineering applications. Still the *consistency* between the space-like co-vectorial equation (14) and the time-like equation $(8)_1$ is a fundamental requirement in the thermodynamical study of the progress of singularity sets (e.g., defects).

Still, in the present approach, in order to proceed further we need to specify the full functional dependence of W. The general expressions $(8)_1$ and (14) are the most general canonical equations for momentum and energy we can write down without a postulate of the full dependency of W. However, just like for other equations if continuum mechanics, we could also write the jump relations associated with $(8)_1$ and (14) at a singular surface by using elements of the theory of hyperbolic systems or a more naive method such as the pill-box method. But since the "conservation laws" $(8)_1$ and (14) already exhibit source terms in the bulk (i.e., they are not conservation laws in a strict mathematical sense), the associated jump relations will also contain surface source terms. The latter, a priori unknown but responsible for the dissipation at the singularity, have to be computed with the help of the standard jump relations associated with eqns. (1)-(3).

3.3. Case $\mathbf{K} \neq \mathbf{0}$

Without reporting the whole algebra, starting with $(4)_2$, we let the reader check that the thermodynamical inequality (7) is replaced by

$$-\left(\frac{dW}{dt} + S\frac{d\theta}{dt}\right) + \mathbf{T} :\dot{\mathbf{F}} + \nabla_R.(\theta\mathbf{K}) - \mathbf{S}.\nabla_R\theta \geq 0, \tag{18}$$

where $\mathbf{S}$ is still give by the general expression $(4)_2$. Equations (8) and (14) are left unchanged:

$$\frac{d(S\theta)}{dt} - \nabla_R.\mathbf{Q} = h^{int}, \quad h^{int} := \mathbf{T} :\dot{\mathbf{F}} - \left.\frac{\partial W}{\partial t}\right|_X, \tag{19}$$

$$\frac{d\mathbf{P}}{dt} - div_R\mathbf{b} = \mathbf{f}^{int} + \mathbf{f}^{ext} + \mathbf{f}^{inh}; \tag{20}$$

On account of (18), eqn. (10) is replaced by

$$S\dot{\theta} + \mathbf{S}.\nabla_R\theta \leq h^{int} + \nabla_R.(\theta\mathbf{K}). \tag{21}$$

Now let us illustrate these general equations by specific cases; some trivial, and some nontrivial ones.

4. Examples without body force

4.1. Pure homogeneous elasticity

In that case $\rho_0 = const.$, and $W = \bar{W}(\mathbf{F})$ only. We have $h^{int} \equiv 0$, $\mathbf{f}^{int} \equiv 0$ since (9) holds good, and also $\mathbf{f}^{inh} = \mathbf{0}$, $\mathbf{Q} \equiv \mathbf{0}$ since the body is homogeneous and non conducting. Equations (8) and (14) reduce to the following [in fact Hamiltonian for a (3+1)-dimensional canonical momentum $(\mathbf{P}, \theta_0 S)$] system ($\theta_0 = const.$):

$$\frac{d\mathbf{P}}{dt} - div_R\mathbf{b} = \mathbf{0}, \quad \theta_0\frac{dS}{dt} = 0. \tag{22}$$

In four-dimensional form this is the formulation of Kijowski and Magli [16].

4.2. Inhomogeneous thermoelasticity of conductors

In that case $\rho_0 = \bar{\rho}_0(\mathbf{X})$, and $W = \bar{W}(\mathbf{F}, \theta; \mathbf{X})$. We have the constitutive equations

$$\mathbf{T} = \frac{\partial\bar{W}}{\partial\mathbf{F}}, \quad S = -\frac{\partial\bar{W}}{\partial\theta} \tag{23}$$

that follow from a standard exploitation of the Clausius-Duhem inequality. Accordingly, we obtain that

$$\mathbf{f}^{int} \equiv \mathbf{f}^{th}, \quad h^{int} \equiv h^{th} := S\dot{\theta} \tag{24}$$

where

$$\mathbf{f}^{th} := S\nabla_R\theta \tag{25}$$

is the material thermal force first introduced by Bui in small strains [17] and independently by Epstein and Maugin in their geometrical considerations [18], so that (8) and (14) are replaced by the following canonical (*non*-Hamiltonian) system of balance of momentum and energy:

$$\frac{d\mathbf{P}}{dt} - div_R\mathbf{b} = \mathbf{f}^{inh} + \mathbf{f}^{th}, \quad \frac{d(S\theta)}{dt} + \nabla_R.\mathbf{Q} = h^{th}, \tag{26}$$

as first found in by Maugin [8].

4.3. Homogeneous dissipative solid material described by means of a diffusive internal variable

Let α the internal variable of state whose tensorial nature is not specified. This may relate to damage, or anelasticity of some sort with a possible diffusion of the said variable so that its material gradient must be taken into account (e.g., in strain-gradient plasticity). This is in the spirit of the thermodynamics developed at length in a book [19]. Then W is specified as the general sufficiently regular function

$$W = \bar{W}(\mathbf{F}, \theta, \alpha, \nabla_R \alpha). \tag{27}$$

First we assume that $\mathbf{K}$ vanishes. The *equations of state* (in a sense, mere definitions of the partial derivatives of the free energy) are given by *Gibbs'equation* as

$$\begin{aligned} \mathbf{T} &= \frac{\partial \bar{W}}{\partial \mathbf{F}} \qquad S = -\frac{\partial \bar{W}}{\partial \theta} \\ A &:= -\frac{\partial \bar{W}}{\partial \alpha} \quad \mathbf{B} := -\frac{\partial \bar{W}}{\partial (\nabla_R \alpha)} \end{aligned} \tag{28}$$

Accordingly, we find that

$$\mathbf{f}^{int} = \mathbf{f}^{th} + \mathbf{f}^{intr}, \quad h^{int} = h^{th} + h^{intr}, \tag{29}$$

where the thermal sources have already been defined and the "intrinsic" sources are given by

$$\mathbf{f}^{intr} := A(\nabla_R \alpha)^T + B\left(\nabla_R (\nabla_R \alpha)^T\right)^T, \quad h^{intr} := A\dot{\alpha} + \mathbf{B}.(\nabla_R \dot{\alpha})^T, \tag{30}$$

so that we have the following consistent (non-Hamiltonian) system of canonical balance laws:

$$\frac{d\mathbf{P}}{dt} - div_R \mathbf{b} = \mathbf{f}^{th} + \mathbf{f}^{intr}, \quad \frac{d(S\theta)}{dt} + \nabla_R.\mathbf{Q} = h^{th} + h^{intr}, \tag{31}$$

while the dissipation reads

$$\Phi = h^{intr} - \mathbf{S}.\nabla_R \theta \geq 0, \quad \mathbf{K} \equiv \mathbf{0}. \tag{32}$$

Here the thermodynamical forces A and $\mathbf{B}$ are purely dissipative by virtue of the "internal" character of the state variable α.

This approach with $\mathbf{K}$=$\mathbf{0}$ favors the *continuum mechanics* (Coleman-Noll) *standard viewpoint* by accepting the classical relationship between heat and entropy flux, and assuming that α and its material gradient are essentially independent. A more *field-theoretic* viewpoint is to envisage the set of eqns.(18) through (21) as holding true and selecting the non-zero $\mathbf{K}$ such that the divergence term in (18) be identically zero, after computation of dW/dt on account of (27), i.e.,

$$\mathbf{K} = -\theta^{-1}\mathbf{B}\dot{\alpha}. \tag{33}$$

This follows the scheme originally developed in [20] for materials with *diffusive* dissipative processes described by means of internal variables of state.

We let the reader check that eqns. (31) and (32) are then replaced by the following equations:

$$\frac{d\mathbf{P}}{dt} - div_R\tilde{\mathbf{b}} = \mathbf{f}^{th} + \tilde{\mathbf{f}}^{intr}, \quad \frac{d(S\theta)}{dt} + \nabla_R.\tilde{\mathbf{Q}} = h^{th} + \tilde{h}^{intr}, \tag{34}$$

and

$$\Phi = \tilde{h}^{intr} - \tilde{\mathbf{S}}.\nabla_R\theta \geq 0, \quad \tilde{h}^{intr} := \tilde{A}\dot{\alpha} \tag{35}$$

where we have introduced the new definitions

$$\tilde{A} \equiv:= -\frac{\delta\bar{W}}{\delta\alpha} := -\left(\frac{\partial\bar{W}}{\partial\alpha} - \nabla_R.\frac{\partial\bar{W}}{\partial(\nabla_R\alpha)}\right) = A - \nabla_R.\mathbf{B}, \tag{36}$$

$$\tilde{\mathbf{S}} := \theta^{-1}\tilde{\mathbf{Q}}, \quad \tilde{\mathbf{Q}} = \mathbf{Q} - \mathbf{B}\dot{\alpha}$$

and

$$\tilde{\mathbf{b}} = -(L\mathbf{1}_R + \mathbf{T}.\mathbf{F} - \mathbf{B}.(\nabla_R\alpha)^T), \quad \tilde{\mathbf{f}}^{intr} := \tilde{A}\,(\nabla_R\alpha)^T\,. \tag{37}$$

The two thermodynamical approaches just illustrated are to be compared to the recent constructive comments of Ireman and Nguyen Quoc-Son [21]. Here we additionally show that alteration in the entropy flux definition goes along with a parallel alteration in the expression of the Eshelby stress tensor, thus reinforcing the space-like complementarity of eqn. (34). More on this with the possible interpretation of α as an additional degree of freedom when it is equipped with its own inertia in a recent work [22].

5. Conclusion

The above-reported formal developments had for main purpose to show that, guided by an admissible form of the energy conservation, we are naturally led to the construction of the corresponding canonical equation of conservation for the material momentum, with no specific information on the functional dependence of the free energy. This obviously accommodates a large spectrum of dissipative behaviors, in particular when we adopt the thermodynamics of internal variables to formulate complex irreversible behaviors. This generality is encapsulated in the general expression (27). For instance, in finite-strain elastoplasticity, we would select only the elastic deformation "gradient" $\mathbf{F}^e$ instead of the full $\mathbf{F} = \mathbf{F}^e.\mathbf{F}^p$ and the set of internal variables α can be built up of the plastic deformation gradient $\mathbf{F}^p$ itself and a set β of hardening variables, yielding a sufficiently general framework.

The resulting canonical equations of conservation of material momentum and energy are those to be exploited to determine the driving forces on defects in materially homogeneous or inhomogeneous materials, including appropriate generalizations of

the J integral of fracture and the driving force on shock waves of different types (true shock waves and phase-transition fronts). To do this one can follow the line taken in a paper by Dascalu and Maugin [23] for cracks and the author [3], [9] for singularity surfaces.

What we finally learn from the above analysis is to make a clear distinction between various concepts of field theory applied to continuum mechanics. These concepts are those of (i) field equations, (ii) balance laws, (iii) conservation laws, and (iv) strict conservation laws. The first type are those equations which govern the fields, the latter being understood in the sense of field theory, i.e., selected form the start. This procedure is particularly well defined in the Lagrangian-Hamiltonian variational approach. The second type relates to a scrupulous examination of what makes a basic physical quantity (which is not necessarily a basic field) vary in time and space on account of prescribed external actions in the bulk and at the surface of a body. The result of this generally is a partial differential equation exhibiting a time derivative, a divergence term, and source terms. A conservation law in the present setting is generated by a variation in the describing parameters of the fields. This is related to an invariance requirement. A strict conservation law involves no source terms and is typically written as a four-dimensional space-time divergence. The four types of equations have been illustrated in this paper on the case of continuum mechanics. In some problems such as in the theory of exactly integrable systems in soliton theory, the number of balance equations is usually small, the (scalar) components of the field equations may usually be few, and the conservation laws may be infinite in number! (see, e.g., [24]). The relationship between some of the members of this infinite series and the conservation equations addressed in the present paper has been examined by the author in the context of the wave mechanics of solids (see, e.g., [25]).

6. Acknowledgment

The author thanks S.N.Gavrilov of the R.A.S. in St Petersburg for fruitful discussions about the material balance of momentum which inspired the present formulation.

References

[1] MAUGIN G.A., *Material inhomogeneities in elasticity*, Chapman, London 1993.

[2] MAUGIN G.A., *Material forces: concepts and applications*, A.S.M.E. Appl. Mech. Rev. **48** (1995), 213–245.

[3] MAUGIN G.A., *Thermomechanics of inhomogeneous-heterogeneous systems: application to the irreversible progress of two- and three-dimensional defects*, ARI **50** (1997), 41–56.

[4] NOETHER W., *Invariante variationsproblem*, Klg-Ges. Wiss. Nach. Göttingen. Math. Phys. **2** (1918).

[5] ESHELBY J.D., *Elastic energy-momentum tensor*, J. of Elasticity **5** (1975), 321–335.

[6] GURTIN M.E., *Configurational forces as basic concepts of continuum physics*, Springer, New York 1999.

[7] MAUGIN G.A. AND TRIMARCO C., *Pseudo-momentum and material forces in nonlinear elasticity: variational formulations and application to brittle fracture*, Acta Mechanica **94** (1992), 1–28.

[8] MAUGIN G.A., *On the universality of the thermomechanics of forces driving singular sets*, Arch. Appl. Mech. **70** (2000), 31–45.

[9] MAUGIN G.A., *On Shock waves and phase-transition fronts in continua*, ARI **50** (1998), 141–150.

[10] MAUGIN G.A., *Eshelbian continuum mechanics and nonlinear waves*, in: "Computational fluid dynamics (Anniversary Volume of K. Roesner)" (Eds. Leutloff D. and Srivastava R.C.), Springer-Verlag, Berlin 1995, 269–287.

[11] MAUGIN G.A., *Geometry of material space: its consequences in modern numerical means*, Technische Mechanik (Magdeburg) **20** (2000), 95–104.

[12] MAUGIN G.A., *On the structure of the theory of polar elasticity*, Phil. Trans. Roy. Soc. Lond., **A356** (1998), 1367–1395.

[13] MAUGIN G.A. AND TRIMARCO C., *On material and physical forces in liquid crystals*, Int. J. Engng. Sci. **33** (1995), 1663–1678.

[14] ERINGEN A.C., *Mechanics of continua*, Krieger, Melbourne, Florida 1980.

[15] ERINGEN A.C. AND MAUGIN G.A., *Electrodynamics of continua*, Vol. I, Springer-Verlag, New York 1990.

[16] KIJOWSKI J. AND MAGLI G., *Unconstrained hamiltonian formulation of general relativity with thermo-elastic sources*, Classical Quantum Grav. **15** (1998), 3891–3916.

[17] BUI H.D., *Mécanique de la rupture fragile*, Masson, Paris 1978.

[18] EPSTEIN M. AND MAUGIN G.A., *Thermoelastic material forces: definition and geometric aspects*, C. R. Acad. Sci. Paris, **II-320** (1995), 63–68.

[19] MAUGIN G.A., *Thermdynamics of nonlinear irreversible behaviors*, World Scientific, Singapore 1999.

[20] MAUGIN G.A., *Internal variables and dissipative structures*, J. Non-Equilib. Thermod. **15** (1990), 173–192.

[21] IREMAN P. AND NGUYEN QUOC-SON, *Using the gradients of the temperature and internal parameters in continuum thermodynamics*, C. R. Mécanique **332** (2004), 249–255.

[22] MAUGIN G.A., *On the thermodynamics of continuous media with diffusion and/or weak locality*, Arch. Appl. Mech. (Anniversary issue) **75** (2006), 723–738.

[23] DASCALU C. AND MAUGIN G.A., *Forces matérielles et taux de restitution de l'énergie dans les corps élastiques homogènes avec défauts*, C. R. Acad. Sci. Paris **II-317** (1993), 1135–1140.

[24] ABLOWITZ M.J. AND SEGUR H., *Solitons and the inverse scattering transform*, S.I.A.M., Philadelphia 1981.

[25] MAUGIN G.A. AND CHRISTOV C.I., *Nonlinear waves and conservation laws (Nonlinear Duality Between Elastic waves and Quasi-particles)*, in: "Topics in nonlinear wave mechanics", (Eds. Christov C.I. and Guran A.), Birkhauser, Boston 2002, 117–160.

AMS Subject Classification: 74AXX, 74A30.

Gérard A. MAUGIN, Laboratoire de Modélisation en Mécanique, UMR 7607 CNRS, Université Pierre et Marie Curie, Tours 55-65, case 162, place Jussieu 4, 75252 Paris cedex O5, FRANCE
e-mail : gam@ccr.jussieu.fr

Rend. Sem. Mat. Univ. Pol. Torino - Vol. 65, 2 (2007)
ISASUT Intensive Seminar

A.V. Porubov

ANALYTICAL SOLUTIONS AND UNSTEADY PROCESSES GOVERNED BY NON-LINEAR NON-INTEGRABLE EQUATIONS

Abstract. The benefit of finding particular exact and asymptotic solutions of non-integrable non-linear partial differential equations is considered. It is shown how explicit analytical solutions predict important features of the waves behavior even outside their formal applicability. In particular, an arbitrary initial pulse splits in a numerical solution into the train of localized waves each described by the analytical travelling wave solution. This happens both for the bell-shaped and kink-shaped localized waves. Also numerical simulations demonstrate an incident wave amplification/attenuation to a stable wave with the amplitude and velocity defined by the relationships obtained via an asymptotic solution. Physically reasonable equations are used to illustrate above mentioned statements.

1. Introduction

It would be nice to obtain an analytical solution of a governing non-linear equation. Most of the mathematical work in the realm of non-linear phenomena refers to integrable equations and their exact solutions. In this case rather general methods may be employed to obtain general solutions, see, e.g., [1, 2, 3]. Unfortunately, most of non-linear equations are non-integrable, and only particular solutions may be found.

Of special interest are the solutions that keep their shape on propagation. One of them is a bell-shaped solitary wave, see Fig. 1(a), that arises thanks to a balance between nonlinearity and dispersion. Another one is a shock wave or a kink-shaped wave, see Fig. 1(b), that usually appears due to a balance between nonlinearity and dissipation. One can find a lot of papers where particular exact solutions of these kinds are obtained. However, most of them do not consider an application of the solutions to the real physical problems. Indeed, exact travelling wave solutions of non-integrable equations are obtained as a rule. Hence, they require specific initial conditions. Moreover, some solutions do not contain free parameters, and special relationships between the equation coefficients are needed for their existence. Asymptotic solutions of non-linear equations are not travelling wave ones without fail. However, they usually describe a particular process, e.g., evolution of a single solitary wave [1]. Real physical problem requires a more general solution, in particular, evolution of an initial pulse of arbitrary shape. Usually such a problem may be solved only numerically. That is why people prefer to deal with numerical simulations. However, a solution of a non-linear equation is very sensitive to the values of the equation coefficients and to the initial conditions; this may be missed in a numerical modelling. Also numerical results may happen to be unusual, and its justification is needed. So, a natural question arises: may one employ particular analytical solutions to predict a behavior in the general problem when only numerical solution may be obtained? May the relationships between the coefficients

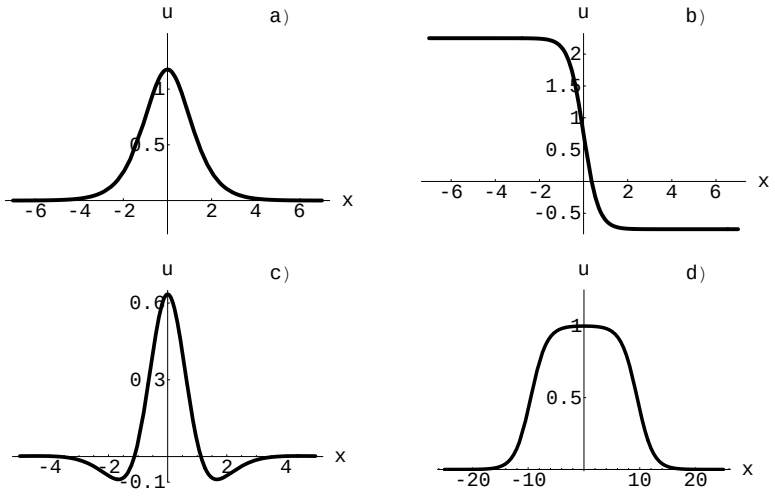

Figure 1: Various profiles of travelling wave solutions: a) bell-shaped solitary wave; b) kink-shaped wave; c) oscillatory vanishing solitary wave ; d) ”fat” solitary wave.

of the equation obtained via analytical solutions describe the conditions when one or another stable profile of permanent shape is realized in numerics?

An attempt is done in this paper to answer these questions. Since the size of the paper does not allow to study the whole problem, the presentation is designed using some instructive examples that illustrate main ideas. First, the employment of exact solutions is considered. Usually exact solutions of nonlinear non-integrable partial differential equations are obtained using various direct methods. Here the attention is paid to one of them- the method of an ansatz. It looks the most efficient for non-integrable equations and rather simple in use. More information and useful references regarding direct methods may be found in [1, 2, 3, 4, 5]. Some exact solutions are presented to illustrate the power of the ansatz method. Then it is shown how the solutions obtained may help to understand some results of numerical simulations. Next section is devoted to the employment of asymptotic solutions in the same manner. The procedure used for finding asymptotic solutions is familiar [1, 5], hence it is not explained here in details. Instead, again some examples are considered where the asymptotic solutions describe important numerical results. The evolution of the bell-shaped solitary wave is studied on the basis of one seismic waves model. Then the attention is paid to the use of the kink-shaped solutions of the Burgers equation modified by weak dispersion and higher-order nonlinearity. It is important to mention that the moderate values of the small parameter responsible for the weak dissipation or dispersion may be formally used in numerics. It is found that even in this case the features of the asymptotic solutions remain valid.

2. Exact solutions

2.1. Direct methods for finding exact solutions

Sometimes, a solution may be obtained using a transformation of variables that allows us to reduce our equation to an equation whose solution is known. Another method, method of ansatz, allows us to reduce our differential equation to algebraic equations for the parameters of the solution.

Important steps in employment of these methods are:

• Reduce non-linear partial differential equation (PDE) to an ordinary differential equation (ODE) considering only travelling wave solutions (or self-similar);

• Reduce the obtained ODE to an ODE whose solution is already known, by means of a suitable transformation of variables or

• Reduce ODE to coupled algebraic equations for the parameters of the solution by means of a suitable ansatz.

As an example, consider the double-dispersive equation (DDE) [4, 5],

$$u_{tt} - \alpha_1 u_{xx} - \alpha_2 (u^2)_{xx} - \alpha_3 u_{xxtt} + \alpha_4 u_{xxxx} = 0. \tag{1}$$

that describes, in particular, longitudinal strain waves evolution in an elastic rod. Its travelling wave solution depending on the phase variable $\theta = x - V t$ is obtained from the ODE reduction of Eq.(1),

$$(V^2 - \alpha_1) u_{\theta\theta} - \alpha_2 (u^2)_{\theta\theta} + (\alpha_4 - \alpha_3 V^2) u_{\theta\theta\theta\theta} = 0 \tag{2}$$

Using substitution of variables,

$$u = \frac{6(\alpha_3 V^2 - \alpha_4)}{\alpha_2} v(\theta) + \frac{V^2 - \alpha_1}{2\alpha_2},$$

equation (2) is transformed to the Weierstrass equation,

$$\{v'(\zeta)\}^2 = 4v^3 - g_2 v - g_3,\ g_2 = \frac{(V^2 - \alpha_1)^2}{12(\alpha_4 - \alpha_3 V^2)} \tag{3}$$

whose known exact solution is expressed through the elliptic Weierstrass function, $v = \wp(\theta,\ g_2,\ g_3)$.

In order to transform the problem of finding exact solutions of ODE to the problem of finding solutions of algebraic equations, it would be nice to express an ansatz through the functions whose derivatives are expressed only through these functions. That is why various elliptic functions are widely used to obtain periodic solutions. One possibility is to use the set of the Weierstrass function $\wp$ and its first derivative $\wp_\theta$. Indeed, we have $\wp_{\theta\theta} = 6\wp^2 - 0.5 g_2$, $\wp_{\theta\theta\theta} = 12\wp_\theta$ etc. An important limit of the Weierstrass function corresponds to the choice $g_2 = 8k^4/3$, $g_3 = -8k^6/27$. In this case $\wp = k^2/3 - k^2 \mathrm{Sech}^2(k\theta)$ that accounts for a bell-shaped solitary wave solution. Also the solitary wave solutions are obtained directly

using the hyperbolic functions for an ansatz. One can find a lot of papers where the hyperbolic tangent is employed. Indeed, we have $\mathrm{Tanh}(k\theta)_\theta = k(1-\mathrm{Tanh}(k\theta)^2)$, $\mathrm{Sech}^2(k\theta)_\theta = 2(\mathrm{Tanh}^3(k\theta)-\mathrm{Tanh}(k\theta))$ etc. A more complicated ansatz through the Ricatti functions was suggested in [6]. These functions satisfy the Riccati equations,

$$\sigma^{'} = -\sigma\tau,\ \tau^{'} = -\tau^2 - A\sigma + 1. \tag{4}$$

Certainly any derivatives of the Riccati functions σ and τ are expressed through themselves. Eqs. (4) possess the exact solution that allows us to express the Riccati functions through the hyperbolic functions,

$$\sigma = \frac{1}{A + C_1\mathrm{Cosh}(k\theta) + C_2\mathrm{Sinh}(k\theta)},\ \tau = \frac{C_2\mathrm{Cosh}(k\theta) + C_1\mathrm{Sinh}(k\theta)}{A + C_1\mathrm{Cosh}(k\theta) + C_2\mathrm{Sinh}(k\theta)} \tag{5}$$

A power series in Tanh or/and in Sech is often used to construct the ansatz. Use of the power series in the Riccati functions allows us to look for a solution as a rational function of the hyperbolic functions while power series approximation in terms of the hyperbolic functions appears as a special case. Indeed, when $C_1 = A$, $C_2 = 0$, we get from Eq. (5)

$$\sigma = \frac{1}{2A}\mathrm{Sech}^2(\frac{k\theta}{2}),\ \tau = \mathrm{Tanh}(\frac{k\theta}{2}).$$

However, substitution of an infinite power series into the equation yields a complicated algebra to find the coefficients of the series. Further simplification may be done using the pole analysis of the solution to define the functional form of the ansatz. One can see that the critical points of the elliptic and hyperbolic functions are poles (in the complex plane). Let us consider the DDE (1), for example, and assume that its solution possesses a pole of order n, $u \sim \theta^{-n}$. Then $u_{\theta\theta}^2 \sim \theta^{-2n-2}$, $u_{\theta\theta\theta\theta} \sim \theta^{-n-4}$. Comparing higher order derivative (dispersion) and nonlinear terms one finds $n = 2$. This provides a balance between nonlinearity and dispersion required for existence of localized bell-shaped solitary wave solution. Then the ansatz may be suggested,

$$u = B\ \mathrm{Sech}^2(k\theta). \tag{6}$$

Substituting (6) into (2) integrated two times one obtains

$$\mathrm{Sech}^2(k\theta)B[\alpha_1 - V^2 - 4k^2(\alpha_4 - \alpha_3 V^2)] +$$
$$\mathrm{Sech}^4(k\theta)B[\alpha_2\ B + 6k^2(\alpha_4 - \alpha_3 V^2)] = 0$$

Equating to zero combinations at each power of Sech, one obtains *algebraic* equations for B, and k whose solutions are

$$B = \frac{3(V^2-\alpha_1)}{2\alpha_2},\ k^2 = \frac{\alpha_1 - V^2}{4(\alpha_4 - \alpha_3 V^2)}. \tag{7}$$

There may be more than one higher-order derivative or non-linear terms in the equation. Consider the Korteweg-de Vries-Burgers (KdVB) equation,

$$u_t + u_x^2 + b\,u_{xx} + s\,u_{xxx} = 0, \tag{8}$$

In this case we get $n = 2$ comparing nonlinearity and dispersion u_{xxx} and $n = 1$ comparing nonlinearity and dissipation u_{xx}. We have to satisfy both possibilities in order to provide a common balance between nonlinearity, dispersion and dissipation. Hence the solution should contain both the second and the first order poles. The suitable ansatz is

$$u = B\ \mathrm{Sech}^2(k\theta) + F\ \mathrm{Tanh}(k\theta) + C. \tag{9}$$

It allows us to find the well-known kink-shaped solution of the KdVB equation with parameters defined by

$$B = 6k^2 s,\ F = \frac{6b\,k}{5},\ C = \pm\frac{3b^2}{25s},\ k = \pm\frac{b}{10s},\ V = \pm\frac{6b^2}{25s}.$$

More examples regarding the method of ansatz may be found in Refs. [3, 4, 5].

2.2. Exact bell-shaped solitary wave solutions

Following the procedure described before one can find exact solutions to many non-integrable equations. However, most of them are single travelling wave solutions that require special initial conditions. In particular, the form of the initial condition for the exact solitary wave solution of the DDE is defined by Eq. (6), (7) with $t = 0$ in θ. What happens when an initial condition differs from the "Sech" shape? Certainly, it is unlikely to describe *whole* evolution of an arbitrary input analytically. But if we find such a solution numerically, what is the reason for finding special exact travelling wave solution?

Numerical simulation of the DDE has been performed in [5]. It was found that for $\alpha_2 > 0$ rather arbitrary initial pulse with positive amplitude splits into a train of solitary waves with different amplitudes while negative input is dispersed, and no travelling localized wave appears. The higher is the amplitude of the wave, the larger is its velocity. The distance between the localized waves increases in time, hence the waves interaction becomes weaker and weaker. Hence each wave may be considered as a single travelling wave and comparison with the exact solution may be done. It is found that each localized wave generated by positive input evolves according to the exact travelling wave solution (6), (7). Moreover, reality of the parameters in (7) gives rise to the conclusion that only positive amplitude solitary waves may exist for $\alpha_2 > 0$. Similarly, negative amplitude solitary waves arise from a negative amplitude input for $\alpha_2 < 0$ Hence exact solution allows us to choose suitable sign of the input amplitude to provide generation of localized stable solitary waves and to describe each solitary wave thus confirming numerical results.

Sometimes numerical simulations yield rather unusual results. Recently, the Gardner equation,

$$u_t + a\,u_x^2 + cu_x^3 + bu_{xxx} = 0, \tag{10}$$

was studied in [8]. It was found that a train of solitary waves appears from certain initial pulse. However, there is an input that produces rather wide solitary wave followed by

a sequence of usual bell-shaped waves. These results may be explained using known solitary wave solution of the Gardner equation [7]:

$$u_s = \frac{3b\,k^2}{a(B_1\mathrm{Cosh}(k\theta)+1)}, \tag{11}$$

where

$$B_1 = \sqrt{1+\frac{9bck^2}{2a^2}}, \theta = x - bk^2\,t.$$

The solution has an interesting feature for negative c: tendency to the extensive or "fat" shape at $k \to \sqrt{-2a^2/(9b\,c)}$. The amplitude of the wave tends to the limiting value equal to $-2a/3c$, while the width growths without limits, see Fig.1(d). Like in the case of the DDE, numerical simulations are successfully checked by the exact solution (11) both to account for the usual bell-shaped waves and the "fat" solitary wave [8].

Even more interesting unusual profiles appear studying numerically the equation

$$u_t + 2b\,u\,u_x + 3c\,u^2u_x + r\,u\,u_{xxx} + s\,u_x\,u_{xx} + d\,u_{3x} + f\;u_{5x} = 0, \tag{12}$$

which is often called the extended KdV equation [5, 9]. A review of its exact bell-shaped solitary wave solutions may be found in [3, 5]. An appearance of the solitary waves described by the exact solutions from rather arbitrary input was studied numerically in [5, 9]. It was found that sometimes there is a good agreement with the exact solutions, namely, in the shape of generated solitary waves and in dependence of their parameters upon the equation coefficients. Also the conditions required for existence of exact solutions were realized in numerics. At the same time, the localized waves were obtained that differ from those described by the analytical solutions. In particular, an oscillatory vanishing at infinity, see Fig.1(c), and a multi-humps localized waves have been discovered in [5, 9] as well as the "fat" solitary wave [9]. One has to note that all known exact solutions of Eq.(12) either do not contain free parameters or exist under special relationships between the equation coefficients. So the absence of free parameters or additional restrictions do not allow us to use exact solutions so efficiently as in the case of the DDE whose solution (6) contains the free parameter V and in the case of the Gardner equation having free parameter k.

2.3. Kink-shaped solutions

The Burgers equation

$$u_t + (u^2)_x + bu_{xx} = 0, \tag{13}$$

is widely used in many physical problems [10, 11]. In particular, it possesses the well-known shock-wave solution (or a kink),

$$u_0 = b\;p\;\mathrm{Tanh}(p(x - Vt)) + V/2. \tag{14}$$

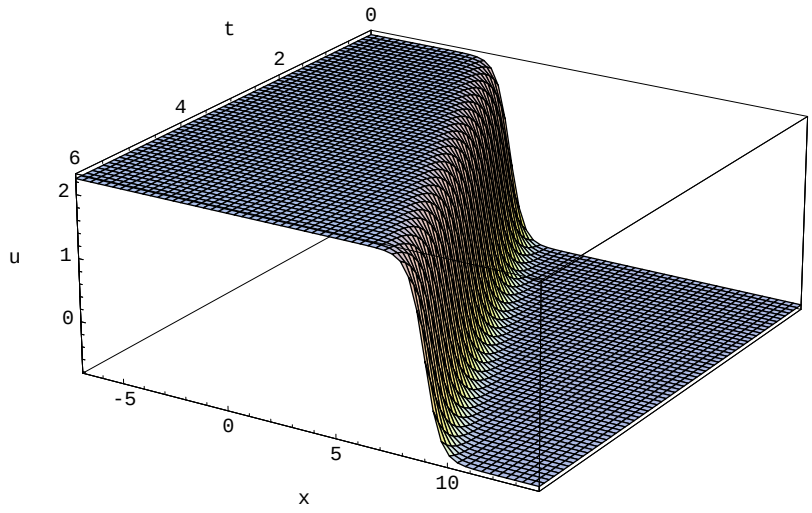

Figure 2: Evolution of the exact solution of the Burgers equation for $b < 0$.

where p and V are free parameters to be defined by the boundary conditions for x. The Burgers equation is integrable, and a more general solution of the Cauchy problem may be obtained. However, integrability fails for most of its generalizations caused by an inclusion of the additional terms like dispersion, higher-order non-linearity etc.

Figure 2 shows stable movement of the kink wave of permanent shape (14). This is because the shock-wave solution of the Burgers equation arises as a result of a balance between nonlinearity and dissipation.

The same simulations for the KDVB equation (8) yield a profile different from that of the exact solution since it contains oscillations on the upper or on the lower parts of the step depending upon the sign of s, see Fig.3. A possible reason of it lies in the fact that the exact solution of the KDVB equation (9) does not contain free parameters in contrast to the two-parameter solution of the Burgers equation (14).

In order to check this idea let us add an additional non-linear term to the KdVB equation,

$$u_t + u_x^2 + b\, u_{xx} + s\, u_{xxx} + q\, u_{xx}^2 = 0. \tag{15}$$

Its exact kink-shaped solution

$$u_0 = \frac{s\ p}{q}\mathrm{Tanh}(p(x - Wt)) + W/2, \tag{16}$$

contains is a free parameter p and fixed velocity

$$W = \frac{s - b\, q}{q^2}.$$

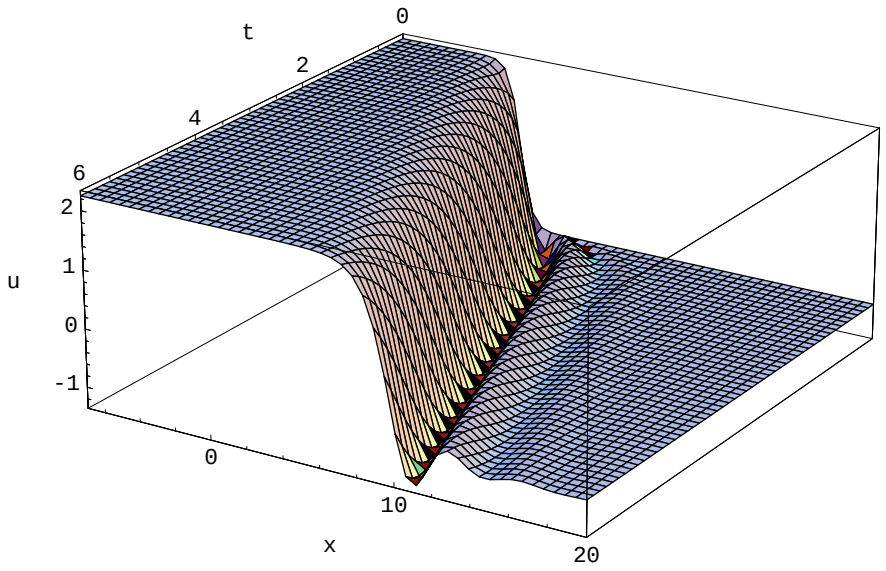

Figure 3: Evolution of the initial Burgers shock wave for $b < 0, s > 0$.

The solution (16) never coincides with the Burgers kink solution (14) since the equality in the amplitudes, $b = s/q$ yields $W = 0$ for the velocity in the solution (16). Now numerical simulation of Eq.(16) demonstrate almost identical to the Burgers kink evolution for certain values of s and q. However, the amplitude in the solution (16) does not depend on the value of b. It means that the wave shown in Fig.2 might propagate for positive values of b, and this prediction of the exact solution is realized also. There exist domains of the values of s and q where initial Burgers kink evolves like in the case of the KdVB equation with oscillations on the profile, see Fig.3. Another scenario is the smoothness of the initial profile shown in Fig.4. It is very likely that oscillations are caused by dispersion while higher-order nonlinearity is responsible for the smoothness, and observed deviations in the kink shape are caused by breach of the balance between dispersion and higher-order nonlinearity. So, addition of the higher-order nonlinearity allows us to provide two balances *separately*, between nonlinearity and dissipation and between higher-order nonlinearity and dispersion. In contrast to it, the solution (9) of the KdVB equation should satisfy two balances *simultaneously* that fixes its parameters and prevents the appearance of the solution from an arbitrary input.

3. Asymptotic solutions

The balance between nonlinearity and dispersion may be destroyed due to the influence of dissipation and/or accumulation. When this influence is weak, asymptotic solutions may be obtained to account for the bell-shaped solitary wave evolution. Introduction of the fast (usually phase) and slow (time or space) variables allows us to study more

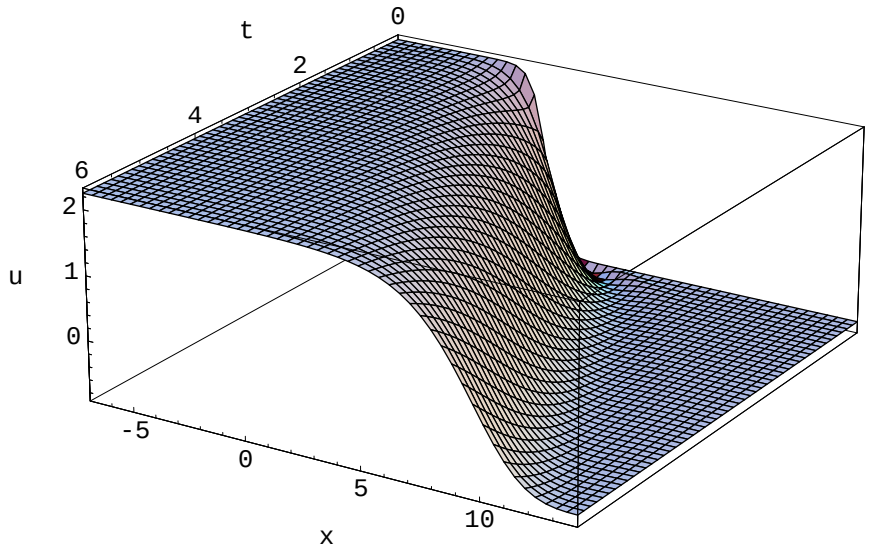

Figure 4: Smoothness of the initial Burgers shock wave.

general processes than those described by exact travelling wave solutions. In particular, asymptotic solutions may account for an amplification or attenuation of a wave. The ODE describing the solitary wave amplitude variation may predict the case when an increase or a decrease in the amplitude happens to some finite value defined by the values of the coefficients of the original PDE. We call this process the solitary wave selection. Selection from *below* is accompanied by the growth of the initial amplitude while selection from *above* is provided by the decrease of the initial solitary wave amplitude.

Similarly the case may be studied when the balance between nonlinearity and dissipation is destroyed by the presence of dispersion and higher-order nonlinearities. In this case, the asymptotic solution allows us to account for a propagation of a kink with stationary deviations on its front and to establish a connection between the shape of these deviations and the structure of the perturbation terms in the equation. Both for the bell-shaped and kink-shaped waves the features of the asymptotic solutions are realized in numerics even when the small parameter characterizing weak perturbations achieves moderate values.

3.1. Evolution of the bell-shaped waves

The asymptotic solution allows us to describe seismic waves selection on the basis of the model equation obtained in [12]:

$$u_t + u\,u_x + d\;u_{xxx} = -\varepsilon\left(a_1 u - a_2 u^2 + a_3 u^3\right), \tag{17}$$

a_1, a_2, a_3 are positive constants and ε is a small parameter. One can see that Eq.(17) is nothing but the disturbed KdV equation that possesses exact bell-shaped solitary wave solution in the absence of disturbances. In the general case, Eq. (17) may describe an appearance of microseisms. Following [5, 13] assume the function u depends upon a fast variable ξ and a slow time T , such as

$$\xi_x = 1,\ \xi_t = -V(T),\ T = \varepsilon\, t.$$

The asymptotic solution is sought of the form

$$u(\xi, T) = u_0(\xi, T) + \varepsilon\, u_1(\xi, T) + ... \tag{18}$$

The bell-shaped solitary wave solution of the KdV equation arises in the leading order,

$$u_0 = 12\, d\ k(T)^2 \mathrm{Sech}^2\ (k(T)\, \xi) \tag{19}$$

However, now its parameters depend upon the slow time T. Next order solution yields the equation for the wave amplitude $Q = 12\, d\ k(T)^2$ of the form [5, 13]:

$$Q_T = -\frac{4}{105}\, Q(24a_3 Q^2 - 28a_2 Q + 35a_1). \tag{20}$$

The behavior of the solitary wave amplitude, Q, depends on the value of $Q_0 \equiv Q(T = 0)$. Indeed, Q will diverge at $Q_0 < Q_1$, when $Q_1 < Q_0 < Q_2$, Q will grow up to Q_2, while if $Q_0 > Q_2$, it will decrease by Q_2. Here $Q_1 < Q_2$ are the roots of equation $24a_3 Q^2 - 28a_2 Q + 35a_1 = 0$. Hence parameters of the solitary wave tends to the finite values prescribed by the equation coefficients a_i, and the *selection* of the solitary wave takes place.

Despite this solution requires special initial condition, numerical simulations [5, 13] confirm the behavior of the wave predicted by the theory even when an initial condition is arbitrary or in the presence of solitary waves interaction. In the former case, the situation is close to that of the DDE when the input is transformed into the train of solitary waves each separately being described by the asymptotic solution. In the latter case, it is found that the interaction does not prevent solitary waves amplification, vanishing or selection that are realized for the coefficients of Eq.(17) prescribed by the asymptotic solution. It is important that the amplitudes of the resulting localized waves in the numerical solution are equal to those of the selected waves obtained from the asymptotic solution. Moreover, the value of the amplitude of the selected solitary wave remain valid when ε is not small.

Similarly the amplification, attenuation and selection of the bell-shaped nonlinear waves may be studied using an equation

$$v_{tt} - v_{xx} - \varepsilon\alpha_1 (v^2)_{xx} - \gamma\alpha_2\, v_{xxt} + \delta(\alpha_3\, v_{xxxx} - \alpha_4\, v_{xxtt}) +$$

$$\gamma\delta(\alpha_5\, v_{xxxxt} + \alpha_6\, v_{xxttt}) + \gamma^2\alpha_7 v_{xxtt} = 0, \tag{21}$$

that appears to account for the strain waves $v(x, t)$ in a microstructured medium [5, 14]. When $\delta = O(\varepsilon)$, $\gamma << 1$, this equation is nothing but the DDE disturbed by

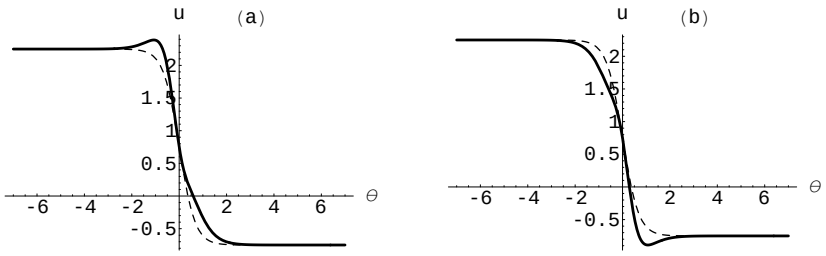

Figure 5: Influence of the weak dispersion on the Burgers kink for $b < 0$: a) $s > 0$; b) $s < 0$.

dissipative/active terms. Its asymptotic solution is obtained in [5, 14] similar to the solution of Eq. (17).

The same procedure may be applied to study the bell-shaped localized wave evolution in the two-dimensional case. An example of the two-dimensional selection of the lump of the Kadomtsev-Petviashvili equation may be found in [15].

3.2. Evolution of the kink-shaped waves

Let us consider the KdVB equation

$$u_t + (u^2)_x + bu_{xx} = -\delta s u_{xxx}, \tag{22}$$

when δ is a small parameter. The asymptotic solution accounting for the perturbation of the kink-shaped wave is sought in the form

$$u(\theta) = u_0(\theta) + \delta u_1(\theta) + ...$$

where $\theta = x - Vt$, and $u_1 \to 0$ for $\theta \to \pm\infty$. Substituting this series into Eq.(22) we obtain in the leading order an ordinary differential equation (ODE)

$$(-Vu_0 + u_0^2 + b\, u_{0,\theta})_\theta \;=\; 0,$$

which is satisfied by the travelling wave solution of the Burgers equation (14). In the next order an inhomogeneous linear ODE appears for the function u_1,

$$(-Vu_1 + 2u_0u_1 + b\, u_{1,\theta})_\theta \;=\; -su_{0,\theta\theta\theta},$$

whose solution is

$$u_1 = 2p^2 s\ \mathrm{Sech}^2(p\theta)\mathrm{Log}(\mathrm{Cosh}(p\,\theta)).$$

Figure 5 demonstrates affect of the weak dispersion on the shape of the Burgers shock wave, $u = u_0 + \delta u_1$. Here and in the following the unperturbed solution is shown by dashed line. One can note non-symmetric influence on the upper and lower parts of the wave. For positive s, a "hat" appears at the upper part while the lower one is subjected

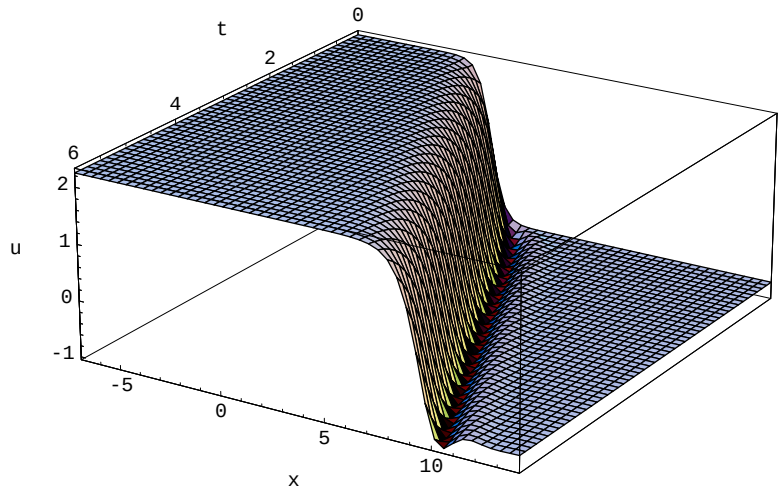

Figure 6: Evolution of the initial Burgers shock wave for $s > 0$ and small δ.

to a smoothness of the wave front. The mirror profile appears for negative values of s. We see that all deviations are concentrated around the wave front.

Our travelling wave asymptotic solution requires special initial condition in the form of already perturbed kink, $u(t = 0)$. However, one can check numerically that the Burgers unperturbed kink transforms into another one whose shapes agrees well with that described by our solution, see Fig. 6. One can see that perturbations of the shock wave profile are stable, they are located near the wave front and do not evolve far from it. Moreover, even for $\delta = O(1)$, the initial Burgers kink wave still evolves into the profile predicted by the asymptotic solution which is not valid in this case in a strict mathematical sense (δ is not small). Typical evolution is shown in Fig.3, where this new wave continues to propagate with one and same velocity and the shape. Hence asymptotic solution explains what was not covered by the exact solution (9).

Next equation to be considered is similar to the extension of the KdVB equation (15),

$$u_t + (u^2)_x + bu_{xx} = -\delta(su_{xxx} + qu_{xx}^2). \tag{23}$$

Its asymptotic solution is

$$u = u_0 + \delta p^2 \mathrm{Sech}^2(p\theta)\left[2(s - b\,q)\mathrm{Log}(\mathrm{Cosh}(p\,\theta)) - V\,q\,\theta\right]$$

An influence of the higher-order quadratic nonlinearity is seen in Fig. 7 for $s = 0$. A smoothness is achieved for $q < 0$ the same happens for the numerical solution shown in Fig. 4. Again the asymptotic solution reveals the features was not discovered by the exact solution (16).

Similarly one can study an influence of the higher-order dissipation u_{xxxx} and other linear and non-linear perturbations on the kink solution of the Burgers equation.

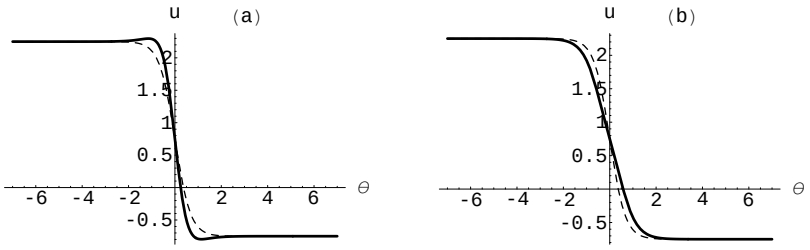

Figure 7: Influence of the weak higher-order nonlinearity on the Burgers kink for $b < 0$: a) $q > 0$; b) $q < 0$.

4. Conclusions

One can see that exact travelling solitary wave solutions with free parameters arise in a more general numerical solution, they may predict important features of an arbitrary input evolution. However, exact solutions with fixed parameters are not necessary realized in computations. In the case when exact solution with free parameters is unlikely to find, an asymptotic solution depending upon the fast and the slow variables may help to understand the behavior of the wave, in particular, amplification and selection of the bell-shaped solitary wave.

Even more special, *travelling wave* asymptotic solutions predict deviations in the profile of the Burgers shock wave that are realized in numerical simulations of unsteady processes. Like for the bell-shaped waves, these predictions remain valid even outside the formal applicability of the asymptotic solution at moderate values of the small parameter.

Both the exact and asymptotic solutions provide us with the relationships between the coefficients of the equation required to achieve one or another kind of the wave evolution. One can use this information in advance for a design of numerical study, it does not allow us to miss one or another scenario of the waves localization. On the other hand, analytical solutions may be used as a testing point for a design of numerical scheme. To sum up, they deserve time required for their finding.

5. Acknowledgment

The author thanks Professor F. Pastrone for his kind invitation to attend the Intensive Seminar and for his warmest hospitality during the work of the Seminar.

References

[1] ABLOWITZ M. AND SEGUR H., *Solitons and inverse scattering transform*, SIAM, Philadelphia 1981.

[2] BULLOUGH R.K. AND COUDREY P.J., *Solitons*, Springer, Berlin 1980.

[3] KUDRYASHOV N.A., *Analytical theory of nonlinear differential equations (in russian)*, Moscow-Izhevsk: Institute of Computation Studies 2003.

[4] SAMSONOV A.M., *Strain soltons in solids and how to construct them*, Chapman & Hall/CRC, 2001.

[5] PORUBOV A.V., *Amplification of nonlinear strain waves in solids*, World Scientific, Singapore 2003.

[6] CONTE R. AND MUSETTE M., *Link between solitary waves and projective Riccati equations*, J. Phys. A **25** (1992), 5609–5623.

[7] KAKUTANI T. AND YAMASAKI N., *Solitary waves on a two-layer fluid*, J. Phys. Soc. Japan **45** (1978), 674–679.

[8] SLYUNIAEV A.V. AND PELINOVSKY E.N., *Dynamics of large-amplitude solitons*, JETP **89** (1999), 173–181.

[9] PORUBOV A.V., MAUGIN G.A., GURSKY V.V. AND KRZHIZHANOVSKAYA V.V., *On some localized waves described by the extended KdV equation*, C. R. Mécanique **333** (2005), 528–533.

[10] WHITHAM G., *Linear and nonlinear waves*, John Wiley & Sons, New York 1974.

[11] SACHDEV P.L., *Nonlinear diffusive waves*, Cambridge Univ. Press, Cambridge 1987.

[12] ENGELBRECHT J., *Nonlinear wave dynamics. Complexity and simplicity*, Kluwer, The Netherlands 1997.

[13] PORUBOV A.V., GURSKY V.V. AND MAUGIN G.A., *Selection of localized nonlinear seismic waves*, Proc. Estonian Acad. Sci., Phys. Math. **52** (2003) 85–93.

[14] PORUBOV A.V. AND PASTRONE F., *Nonlinear bell-shaped and kink-shaped strain waves in microstructured solids*, Intern. J. Nonl. Mech. **39** (2004) 1289–1299.

[15] PORUBOV A.V., PASTRONE F. AND MAUGIN G.A., *Selection of two-dimensional nonlinear strain waves in micro-structured media*, C. R. Mécanique **332** (2004), 513–518.

AMS Subject Classification: 35Q51, 35Q53, 37K40.

Alexey PORUBOV, A.F.Ioffe Physical Technical Institute of the Russian Academy of Sciences
Polytekhnicheskaya st., 26, 194021, Saint-Petersburg, RUSSIA
e-mail: porubov@math.ioffe.ru

Rend. Sem. Mat. Univ. Pol. Torino - Vol. 65, 2 (2007)
ISASUT Intensive Seminar

M. Bonadies*

THERMOELASTIC STRESS ANALYSIS FOR LINEAR THERMOELASTIC BODIES

Abstract. The thermoelastic stress analysis for linear thermoelastic bodies is developed as a mathematical support to the infra-red radiometric method (SPATE) applied to structures under cyclic loading conditions.

1. Introduction

The use of high-tech materials for structural applications has shown in recent years that the study of mechanical behaviour of such materials is often inadequate. Studies on the interaction between mechanical and thermal effects in solid bodies have therefore received considerable attention.

Thermographic stress analysis has been adopted as a particularly convenient mean of experimental stress analysis based on the thermoelastic effect. The thermoelastic stress analysis tecnique is based upon the use of the SPATE (Stress Pattern Analysis by the measurement of Thermal Emission) equipment for the radiometric monitoring of the temperature changes induced by cyclic loading in the elastic range [1], [2], [9], [10], [11].

In [8] a theoretical analysis of the thermoelastic effect has been developed in order to provide a mathematical model as a support to SPATE and the results of tests carried out on concrete and mortar [1] are reported as experimental evidences of the theory described.

The aim of this paper is to generalize the results obtained in [8] : the intrinsic formulation of the linear theory of thermoelasticity is adopted [3] and the linear relations given in [8] between the variation of temperature and the variation of stress are obtained after suitable assumptions.

In Section 2, within the linear theory of elasticity for an isotropic continuum body, we deduce from the First Law of Thermodynamics a differential equation which gives a relation between stress and temperature.

In Section 3 we integrate this equation and we remark that if the principal stress components are two and three the solution depends on the first and the second invariant of the stress while the second invariant vanishes in the case of one component of the principal stress.

In Section 4 we show that if we linearize the equations obtained in Section 3, we get, at least for the case of dimension one, the same results of [9].

*This work was supported by the Italian M.U.R.S.T. research project “Modelli matematici per la scienza dei materiali” (Cofin 2002).

In Section 5 we apply the results obtained in Section 3 to the SPATE model considering sinusoidal principal components of stress.

2. The mathematical equations

Let us consider a continuum body as defined in [4] and let us assume the bounded regular region of space occupied by the body in a fixed reference configuration be closed with respect to mass transfer and open with respect to energy transfer. The body can be considered a thermodynamical closed system.

According to [3] we recall that the local form of the First Law of Thermodynamics for the system considered is:

$$\rho \dot{e} = \mathbf{S} \cdot \dot{\mathbf{F}} - \mathrm{div}\mathbf{q} + \rho r, \tag{1}$$

where e is the internal energy per unit mass, $\mathbf{q}$ is the heat flux vector per unit surface area and unit time, r is the heat supply per unit mass and unit time, ρ is the mass density, $\mathbf{S}$ and $\mathbf{F}$ are respectively the first Piola-Kirchhoff stress tensor and the deformation gradient.

If η is the entropy per unit mass and ϑ the absolute temperature, we introduce the free energy per unit mass [3]

$$\psi = e - \eta\vartheta. \tag{2}$$

If we assume that the body is elastic, the Second Law of Thermodynamics implies the following restrictions:

$$\psi = \hat{\psi}(\mathbf{F}, \vartheta), \qquad \mathbf{S} = \hat{\mathbf{S}}(\mathbf{F}, \vartheta), \qquad \eta = \hat{\eta}(\mathbf{F}, \vartheta) \tag{3}$$

$$\hat{\mathbf{S}}(\mathbf{F}, \vartheta) = \rho \partial_{\mathbf{F}} \hat{\psi}(\mathbf{F}, \vartheta), \qquad \hat{\eta}(\mathbf{F}, \vartheta) = -\partial_{\vartheta} \hat{\psi}(\mathbf{F}, \vartheta). \tag{4}$$

If we differentiate (2) and $(3)_1$ with respect to time, by means of (4), from (1) we get:

$$\rho \eta \dot{\vartheta} = -\mathrm{div}\mathbf{q} + \rho r. \tag{5}$$

Defining the finite strain tensor $\mathbf{D}$ by [3], [4]:

$$\mathbf{D} = \frac{1}{2}\left(\mathbf{F}^T\mathbf{F} - \mathbf{1}\right), \tag{6}$$

where $\mathbf{1}$ is the unit tensor, the restrictions (3) and (4) are substituted by:

$$\psi = \tilde{\psi}(\mathbf{D}, \vartheta), \qquad \mathbf{S} = \mathbf{F}\tilde{\mathbf{S}}(\mathbf{D}, \vartheta), \qquad \eta = \tilde{\eta}(\mathbf{D}, \vartheta) \tag{7}$$

and

$$\tilde{\mathbf{S}}(\mathbf{D}, \vartheta) = \rho \partial_{\mathbf{F}} \tilde{\psi}(\mathbf{D}, \vartheta), \qquad \tilde{\eta}(\mathbf{D}, \vartheta) = -\partial_{\vartheta} \tilde{\psi}(\mathbf{D}, \vartheta), \tag{8}$$

as a consequence of material frame indifference [3], [4].

By differentiating $(8)_2$ with respect to time and introducing the specific heat at constant deformation [3]:

$$c = \vartheta \partial_\vartheta \tilde{\eta}(\mathbf{D}, \vartheta), \tag{9}$$

from (5) we get:

$$-\vartheta \partial_\vartheta \tilde{\mathbf{S}} \cdot \dot{\mathbf{D}} + \rho c \dot{\vartheta} = -\mathrm{div}\mathbf{q} + \rho r. \tag{10}$$

Now we assume that the gradient displacement $\nabla \mathbf{u}$ and its rate of change $\nabla \dot{\mathbf{u}}$ are small and that the body is subjected to small increment of temperature.

Nevertheless the stress tensor $\tilde{\mathbf{S}}$ depends on the temperature through the material functions which appear in the constitutive equations.

Therefore, introducing the infinitesimal strain tensor [3], [4]:

$$\mathbf{E} = \frac{1}{2}\left(\nabla \mathbf{u} + \nabla \mathbf{u}^T\right), \tag{11}$$

if

$$\mathbf{F} = \mathbf{1} + \nabla \mathbf{u}, \tag{12}$$

from (6) we get:

$$\mathbf{D} = \mathbf{E} + \frac{1}{2}\nabla \mathbf{u}^T \nabla \mathbf{u}. \tag{13}$$

If we assume that the body is isotropic, then the constitutive equation is [3]:

$$\mathbf{S} = 2\mu \mathbf{E} + [\lambda \mathrm{tr}\mathbf{E} - \beta(\vartheta - \vartheta_0)]\mathbf{1}. \tag{14}$$

In the above equation λ and μ are the Lamé moduli, while β is related to the coefficient of linear thermal expansion α by [11]:

$$\beta = (3\lambda + 2\mu)\alpha \tag{15}$$

From the experimental data we deduce that λ and μ are functions of the temperature ϑ ([6], [11]).

Moreover from (13) and the assumption of linear approximation for the gradient displacement we can obtain:

$$\dot{\mathbf{D}} \cong \dot{\mathbf{E}} \tag{16}$$

Therefore by substituting (14) in (10), with the use of (16) we get the following equation:

$$\rho c \dot{\vartheta} = -\mathrm{div}\mathbf{q} + \rho r + \vartheta \{2\partial_\vartheta \mu \mathbf{E} + [\partial_\vartheta \lambda \mathrm{tr}\mathbf{E} - \partial_\vartheta \beta(\vartheta - \vartheta_0) - \beta]\mathbf{1}\}\dot{\mathbf{E}} \tag{17}$$

Let us assume that the thermodynamical process is adiabatic without internal heat sources, that is [3]:

$$-\mathrm{div}\mathbf{q} + \rho r = 0 \tag{18}$$

From experimental results and from the analysis of the order of magnitude we can deduce that $\partial_\vartheta \beta(\vartheta - \vartheta_0)$ is negligible with respect to β, while $\partial_\vartheta \mu \mathbf{E}$ and $\partial_\vartheta \lambda \mathrm{tr}\mathbf{E}$ are relevant, therefore, with the use of (18), equation (17) can be written as:

$$\rho c \frac{\dot{\vartheta}}{\vartheta} = 2\partial_\vartheta \mu \mathbf{E} \cdot \dot{\mathbf{E}} + [\partial_\vartheta \lambda \mathrm{tr}\mathbf{E} - \beta]\,\mathrm{tr}\dot{\mathbf{E}}. \tag{19}$$

Equation (19) represents the thermoelastic coupling between strain and temperature.

Let us now deduce from (19) a similar expression in terms of stress. Because of the isotropy of the material we can assume that $\mu > 0$, $3\lambda + 2\mu > 0$ [5]. Therefore the constitutive equation (14) can be inverted in

$$\mathbf{E} = \frac{1}{2\mu}\,\mathbf{S} - \frac{\lambda}{2\mu(3\lambda + 2\mu)}\,\mathrm{tr}\mathbf{S}\,\mathbf{1} + \alpha(\vartheta - \vartheta_0)\mathbf{1}. \tag{20}$$

Let us now recall the well known relations between the Lamé moduli λ, μ and the Poisson's ratio ν and the Young's modulus E:

$$\begin{cases} \lambda = \dfrac{E\nu}{(1+\nu)(1-2\nu)} \\ \\ \mu = \dfrac{E}{2(1+\nu)} \end{cases} \tag{21}$$

By means of (21) we get $\partial_\vartheta \lambda$ and $\partial_\vartheta \mu$ in terms of $\partial_\vartheta E$ and $\partial_\vartheta \nu$, then with the use of (20) and the assumptions that both $(\vartheta - \vartheta_0)$ and its time-derivative are negligible, from (19) we deduce:

$$\frac{\dot{\vartheta}}{\vartheta} = -\left[\frac{\alpha}{\rho c} - \Gamma_1 \mathrm{tr}\mathbf{S}\right]\mathrm{tr}\dot{\mathbf{S}} + \Gamma_2 \mathbf{S} \cdot \dot{\mathbf{S}} \tag{22}$$

where

$$\begin{cases} \Gamma_1 = \dfrac{1}{\rho c}\left[-\dfrac{\nu}{E^2}\partial_\vartheta E + \dfrac{1}{E}\partial_\vartheta \nu\right] \\ \\ \Gamma_2 = \dfrac{1}{\rho c}\left[\dfrac{1+\nu}{E^2}\partial_\vartheta E - \dfrac{1}{E}\partial_\vartheta \nu\right] \end{cases} \tag{23}$$

Let us now set:

$$\begin{cases} \sigma = I_1 = \mathrm{tr}\mathbf{S} \\ \dot{\sigma} = \mathrm{tr}\dot{\mathbf{S}} \\ \sigma_i = (\mathbf{S})_i \\ \dot{\sigma}_i = (\dot{\mathbf{S}})_i \end{cases} \qquad \text{with } i = 1, 2, 3 \tag{24}$$

where $(\mathbf{S})_i$ are the principal stresses with respect to an orthonormal basis $(\mathbf{e}_i)$. If we recall that $\mathbf{S} \cdot \dot{\mathbf{S}} = \sum_{i=1}^{3} (\mathbf{S})_i (\dot{\mathbf{S}})_i$, with the use of the (24), the relation (22) becomes:

$$\frac{\dot{\vartheta}}{\vartheta} = -\left[\frac{\alpha}{\rho c} - \Gamma_1 \sigma\right] \dot{\sigma} + \Gamma_2 \sum_{i=1}^{3} \sigma_i \dot{\sigma}_i \tag{25}$$

3. Stress-temperature relations

In order to get from (25) a relation between temperature and stress we must suppose that:

i) the mass density ρ is constant during the thermodynamical process;

ii) the partial derivatives with respect to temperature ϑ of the Poisson's ratio ν and of the Young's modulus E are constant with respect to time and temperature.

It follows therefore that Γ_1 and Γ_2 given by (23) are constant. If we introduce the "thermoelastic constant"

$$k = \frac{\alpha}{\rho c} \tag{26}$$

and we denote with τ the second invariant of the stress tensor:

$$\tau = I_2 = \sigma_1 \sigma_2 + \sigma_1 \sigma_3 + \sigma_2 \sigma_3, \tag{27}$$

under the assumption that $\vartheta = \vartheta_0$, $\sigma = \sigma_0$ and $\tau = \tau_0$ for $t = 0$, the integration of (25) with respect to time gives:

$$\ln \frac{\vartheta}{\vartheta_0} = -k(\sigma - \sigma_0) + \frac{1}{2} (\Gamma_1 + \Gamma_2) \left(\sigma^2 - \sigma_0^2\right) - \Gamma_2 (\tau - \tau_0). \tag{28}$$

It is interesting to remark that in the two-dimensional case that is when the principal stresses are:

$$\sigma_1 \neq 0, \qquad \sigma_2 \neq 0, \qquad \sigma_3 = 0 \tag{29}$$

equation (28) still holds assuming $i = 1, 2$ in (24) and replacing (27) by

$$\tau = I_2 = \sigma_1 \sigma_2,$$

while in the one-dimensional case in which

$$\sigma_1 \neq 0, \qquad \sigma_2 = \sigma_3 = 0 \qquad \text{and } \sigma_1 = \sigma \tag{30}$$

the second invariant of the stress tensor vanishes and (28) is replaced by:

$$\ln \frac{\vartheta}{\vartheta_0} = -k(\sigma - \sigma_0) + \frac{1}{2} (\Gamma_1 + \Gamma_2) \left(\sigma^2 - \sigma_0^2\right). \tag{31}$$

Let us remark that the solution of (25) shows a non linear dependence on the first invariant of the stress in all the cases (see (28) and (31)) while only in two and three-dimensional cases a linear dependence on the second invariant appears.

4. The linear case

In classical theory [2], [7] from the generalised heat conduction equation, by assuming that straining occurs adiabatically with no conduction of heat and with no heat supply, the Kelvin formula has been deduced:

$$\frac{\Delta\vartheta}{\vartheta_0} = -k\Delta\sigma \tag{32}$$

with k thermoelastic constant defined in (26).

We shall prove that, from (28) and (31) of the previous section, after suitable linearizations, it is possible to get linear relations between the variation of temperature and the variation of stress which are comparable to (32).

Infact, let us define the average values of the principal stresses, of the stress invariants and of the temperature by the following linear relations:

$$\begin{gathered} \sigma_{im} = \frac{1}{2}(\sigma_i + \sigma_{i0}), \quad \sigma_{i0} = \sigma_i \quad \text{for } t = 0,\ i = 1,2,3 \\ \sigma_m = \frac{1}{2}(\sigma + \sigma_0), \quad \tau_m = \frac{1}{2}(\tau + \tau_0), \quad \vartheta_m = \frac{1}{2}(\vartheta + \vartheta_0) \end{gathered} \tag{33}$$

We assume moreover that the principal stresses, the stress invariants and the temperature are related to their variations by:

$$\begin{gathered} \sigma_i = \sigma_{im} + \Delta\sigma_i, \quad i = 1,2,3 \\ \sigma = \sigma_m + \Delta\sigma, \quad \tau = \tau_m + \Delta\tau, \quad \vartheta = \vartheta_m + \Delta\vartheta \end{gathered} \tag{34}$$

From (33) with the use of (34) we get:

$$\begin{gathered} \sigma_i - \sigma_{i0} = 2\Delta\sigma_i \quad i = 1,2,3 \\ \sigma - \sigma_0 = 2\Delta\sigma, \quad \tau - \tau_0 = 2\Delta\tau, \quad \vartheta - \vartheta_0 = 2\Delta\vartheta \end{gathered} \tag{35}$$

By using the relations (33), (34) and (35) and linearizing the logarithm, as usually done if $|2\Delta\vartheta/\vartheta_0| < 1$:

$$\ln\left(\frac{\vartheta}{\vartheta_0}\right) = \ln\left(1 + \frac{2\Delta\vartheta}{\vartheta_0}\right) \approx \frac{2\Delta\vartheta}{\vartheta_0} \tag{36}$$

we obtain from (29) and (31) the linearized equations:

$$\begin{gathered} \frac{\Delta\vartheta}{\vartheta_0} = [-k + (\Gamma_1 + \Gamma_2)\,\sigma_m]\,\Delta\sigma - \Gamma_2\Delta\tau \\ \frac{\Delta\vartheta}{\vartheta_0} = [-k + (\Gamma_1 + \Gamma_2)\sigma_m]\,\Delta\sigma \end{gathered} \tag{37}$$

Let us remark that $(37)_2$ can be compared with the Kelvin's formula but the coefficient of $\Delta\sigma$ is the thermoelastic constant plus a coefficient depending on σ_m and on an elasticity modulus [9]. We remark also that $(37)_1$ shows a dependence on the variation of the first and the second invariant of the stress and on the Poisson and Young moduli .

5. SPATE model results

The SPATE model allows us to obtain the temperature variation related to the elastic deformation by spectroscopical experimental analysis.

The fundamental ipothesis of the SPATE model are the following:

1) the deformation must be adiabatic,

2) there must not exist other heat sources.

Now the relations obtained in Section 3 will be applied to SPATE model, analysing a cyclic loading [11] in which the temperature variation $(\vartheta - \vartheta_0)$ is small compared to the initial temperature ϑ_0. We assume that the principal stress are:

$$\sigma_i = \sigma_{im} + a_i \sin(\omega t), \quad i = 1, 2, 3 \tag{38}$$

where σ_{im}, with $i = 1, 2, 3$, denote the average stresses and a_i, with $i = 1, 2, 3$, are arbitrary constants. Let us set:

$$\sigma_m = \sum_{i=1}^{3} \sigma_{im}, \qquad a = \sum_{i=1}^{3} a_i \tag{39}$$

The equation (28), with the use of (36), $(37)_1$, (38) and (39), becomes:

$$\frac{2\Delta\vartheta}{\vartheta_0} = A \sin(\omega t) + B[1 - \cos(2\omega t)] \tag{40}$$

where

$$\begin{cases} A = -ka + \Gamma_1 \sigma_m a + \Gamma_2 \displaystyle\sum_{i=1}^{3} \sigma_{im} a_i \\ \\ B = \dfrac{1}{4} (\Gamma_1 + \Gamma_2) a^2 - \dfrac{1}{2} \Gamma_2 (a_1 a_2 + a_1 a_3 + a_2 a_3) \end{cases} \tag{41}$$

Formulas (40), (41) are the generalization of the results given in [11] and include the particular cases of dimension 1 and 2. Infact, if $i = 1, 2$ formulas (38)-(41) are valid replacing $(41)_2$ by

$$B = \frac{1}{4} (\Gamma_1 + \Gamma_2) a^2 - \frac{1}{2} \Gamma_2 a_1 a_2;$$

if $i = 1$ then

$$\sigma_1 = \sigma = \sigma_m + a\sin(\omega t), \quad \sigma_m = \sigma_{1m}, \quad a = a_1, \tag{42}$$

(39) and (40) still hold, with:

$$\begin{cases} A = -ka + (\Gamma_1 + \Gamma_2)\,\sigma_m a \\ \\ B = \dfrac{1}{4}\,(\Gamma_1 + \Gamma_2)\,a^2 \end{cases} \tag{43}$$

Let us remark that, in the case of dimension 1, from (43) and (23) we deduce that the elastic behaviour of the material is described by the Young modulus, while in the cases of dimension 2 and 3 both Poisson and Young modulus are involved, as it turns out from (41) and (23). Moreover in case of dimension 1 it is possible to analyze the relation between the temperature variation and the stress variation. According to [1], let us replace in (42), (43) the constant a by the variation of stress $\Delta\sigma$ and let us assume in $(43)_1$ that the thermoelastic constant k be relevant with respect to the other terms. Then from (40) we observe that according to the first addendum of the right member there is a loss of temperature for an increase of stress and an increase of temperature for a reduction of stress. The second addendum of the right member of (40) is relevant only for large variation of stress. In [1] a detailed discussion of tests performed on various specimens is reported and the conclusions are in agreement with our remarks.

6. Conclusions

The assumption of the dependence of the Poisson and Young moduli of elasticity from the temperature ϑ allows us to get a relation between the temperature variation and the stress variation. This relation presents coefficients which are not only the thermoelastic constant, as in the classical Kelvin's formula, but depend on the average stress, on the first and second invariant of the stress and on the modulus of elasticity. This result is supported by experimental results [11]. The application of our results to the SPATE model gives a solution which is the superposition of two cyclic functions with a phase difference of $\pi/2$ one with respect to the other. The relation between the temperature variation and the stress variation obtained can be compared with the experimental results given in [1].

References

[1] BERRA M. AND BOCCA P., *Thermoelastic stress analysis: temperature - strain relationships in concrete and mortar*, Materials and Stuctures **26** (1993), 395–404.

[2] BOYLE J.T. AND CUMMINGS W.M., *Finite element analysis of SPATE benchmarks*, in: "Applied stress analysis" (Eds. Hyde T.H. and Ollerton E.), Elsevier Applied Science, New York 1990, 150–159.

[3] CARLSON D.E., *Linear thermoelasticity*, in: "Handbuck der Physik, VIa/2 Mechanics of Solids II", Springer, Berlin 1972.

[4] GURTIN M.E., *The linear theory of elasticity*, in: "Handbuck der Physik, VIa/2 Mechanics of Solids II", Springer, Berlin 1972.

[5] GURTIN M.E., *An introduction to continuum mechanics*, Academic Press, Cambridge 1981.

[6] LOVE A.E.H., *A treatise on the mathematical theory of elasticity*, Dover, New York 1927, Cap. III, Art. 74, 108–.

[7] NOWACKI W., *Thermoelasticity* Pergamon Press, New York 1982, sect I.9, 38–.

[8] QUARANTA F., *SPATE: un modello matematico*, (in Italian) Degree Thesis, University of Turin, Turin 1991-92.

[9] STANLEY P., *Thermoelastic stress analysis: progress and prospect*, in: "Proceedings of 9th International Conference on Experimental Mechanics, Copenhagen 1990", 728–747.

[10] STANLEY P. AND CHAN W.K., *The application of thermoelastic stress analysis techniques to composite materials*, Journal of Strain Analysis **23** (3) (1988), 137–143.

[11] WONG A.K., JONES R. AND SPARROW J.G., *Thermoelastic constant or thermoelastic parameter?*, J. Phys. Chem. Solids **48** (8) (1987), 749–753.

AMS Subject Classification: 74A15, 74B05.

Manuelita BONADIES, Department of Mathematics, University of Turin, Via Carlo Alberto 10, 10123, Turin, ITALY
e-mail: manuelita.bonadies@unito.it

Rend. Sem. Mat. Univ. Pol. Torino - Vol. 65, 2 (2007)
ISASUT Intensive Seminar

A. Casasso*

NONLINEAR WAVES IN PLANE COSSERAT SOLIDS

Abstract. As it is well known, the propagation of nonlinear strain waves may be governed by a nonlinear dispersive-dissipative equation. In this work we study models in one or two dimensions. The final purpose is to apply the analytic technique developed by Samsonov [7] to dynamic equations arising in the theory of microstructured solids. To do this we search to reduce the 2 or 4 Euler-Lagrange equations of the model to 1 or 2 p.d.e. each depending only on one field variable.

1. Introduction

Nonlinear wave dynamics in dissipative solids has been discussed in two recent books by A. Porubov [6] and A. Samsonov [7], with the same goal of obtaining and exploiting physically and mathematically meaningful results related to the propagation of solitary waves mostly in complex wave guides. In particular in [7] it is presented a method of reduction of the dynamic p.d.e. to a second order Lie equation, hence to the Abel equation, but only for the 1D-case.

Now, we want to apply the same passages even for the 2D-case. This is possible if, after, we have reduced the 4 Lagrange equations to a couple of partial differential equations each depending only on one field variable. This reduction is the main purpose of this work, and it is used in one-dimensional or bi-dimensional models.

We want to remark that in our model the non linearity is due to a strain energy density which depends on the deformation variables, both macro and micro, the dissipation is introduced trough a linear combination of strain velocities.

2. Method of reduction

The aim of this work is to find the travelling wave solution (TW) of the initial p.d.e., that depends only upon the phase variable $z = \pm Vt$ and describes the wave propagation along the x-axis in time t and velocity V. The process used can be resumed in two principal steps. In the first we reduce the Euler-Lagrange equations to one or two p.d.e. equations each depending only on one field variable. To do this we choose a suitable form of the potential energy W, we calculate the Euler-Lagrange equations (two for the one-dimensional case and four for the two-dimensional case) and then we reduce this system to the wanted partial differential equation using the method of the "slaving principle", (for a general treatment of this principle, see, for instance, [4]).

The second step requirs to distinguish the one- from the two-dimensional case. For the one-dimensional case we introduce the phase variable $z = x + Vt$, where V is

*This work was supported by the Italian M.U.R.S.T. research project "Modelli matematici per la scienza dei materiali" (Cofin 2002).

the wave's velocity. We consider the vector

$$\mathbf{r} = \mathbf{r}(x, t) = u(x, t)\mathbf{i}$$

for the macrostructure and the vector

$$\mathbf{d} = \mathbf{d}(x, t) = \varphi(x, t)\mathbf{i}$$

for the microstructure. So we transform the function u(x,t) in a function u(z) that depends only on the variable z:

$$u(x, t) = u(z)$$

For the two-dimensional case, the procedure is a bit more difficult. To simplify it, we suppose that the components of vectors **r** and of vector **d** depend only on one direction, such that we have:

$$\mathbf{r}(x, y, t) = u(x, t)\mathbf{i} + v(y, t)\mathbf{j}$$

and

$$\mathbf{d}(x, y, t) = \varphi(x, t)\mathbf{i} + \chi(y, t)\mathbf{j}.$$

Hence two phase variables z and z'

$$z = x \pm Vt, \quad z' = y \pm V't$$

and two new functions $u(z)$ and $v(z')$ are introduced:

$$u(x, t) = u(z), \quad v(y, t) = v(z')$$

Thereafter, we reduce the starting partial diferential equation to an ordinary differential equation using the funtion $u(z)$ for the one-dimensional case and $u(z)$ and $v(z')$ for the two-dimensional case. Then we reduce this ordinary differential equation to a second order Lie equation, we pass to an Abel equation, a first order equation, and, last step, we reduce, if possible, the Abel equation to the Weierstrass equation and we integrate it to find the solution called "soliton".

3. One-dimensional case

We consider now an example of model in one dimension. We deal with the vector **r** and **d** defined above and we choose the following form for the kinetic energy K and for the strain energy W:

$$K = \frac{1}{2}\left[\rho\dot{u}^2 + I\dot{\varphi}^2\right]$$

$$W = \frac{1}{2}\alpha u_x^2 + \frac{1}{6}\beta u_x^3 - A\varphi u_x + \frac{1}{2}B\varphi^2 + \frac{1}{2}C\varphi_x^2 + \frac{1}{6}D\varphi_x^3$$

With the above mentioned formulas, the Euler-Lagrange equations which in general read

$$\begin{cases} \rho u_{tt} = \left(\dfrac{\partial W}{\partial u_x}\right)_x - \dfrac{\partial W}{\partial u} \\ I\varphi_{tt} = \left(\dfrac{\partial W}{\partial \varphi_x}\right)_x - \dfrac{\partial W}{\partial \varphi} \end{cases}$$

become

$$\text{(1)} \qquad \begin{cases} \rho u_{tt} = \alpha u_{xx} + \beta u_x u_{xx} - A\varphi_x \\ I\varphi_{tt} = C\varphi xx + D\varphi_x \varphi_{xx} + Au_x - B\varphi \end{cases}$$

To reduce this system to one partial differential equation depending only on the funtion u, we introduce the dimensionless form of the variables u, x, t and two new parameters:

$$U = \frac{u}{U_0},\ X = \frac{x}{L},\ T = \frac{c_0 t}{L},\ \delta = \left(\frac{l}{L}\right)^2,\ \epsilon = \left(\frac{U_0}{L}\right)$$

where L is the wave's length, l is the size of the microstructure. We suppose also that I, C and D verify the following equalities

$$I = \rho l^2 I^*,\ C = l^2 C^*,\ D = l^2 D^*$$

Now we use the slaving principle. It means that φ is determined in terms of U_x using a power expansion: $\varphi = \varphi_0 + \delta\varphi_1 + \delta^2\varphi_2 + ...$ The dimensionless form for equation $(1)_2$ yiels this expression for φ:

$$\text{(2)} \qquad \varphi = \epsilon\frac{A}{B}U_X + \frac{\delta}{B}\left(C^*\varphi_{XX} - \alpha I^*\varphi_{TT} + \frac{D^*}{L}\varphi_X\varphi_{XX}\right)$$

We evaluate φ_0 and φ_1 in terms of U and its partial derivatives obtaining:

$$\varphi_0 = \epsilon\frac{A}{B}U_X \qquad \varphi_1 = \epsilon\frac{A}{B^2}\left(C^*U_{XXX} - \alpha I^*U_{XTT} + \frac{D^*A\epsilon}{BL}U_{XX}U_{XXX}\right)$$

Inserting them into the governing equation $(1)_2$ in its dimensionless form, we get finally the single differential equation for U:

$$U_{TT} = U_{XX} + \frac{\beta\epsilon}{\alpha}\left(U_X^2\right)_X - \frac{A^2}{\alpha B}U_{XX} - \frac{\delta A^2}{\alpha B^2}C^*U_{XXXX} + \\ + \frac{\delta A^2}{\alpha B^2}\left[\alpha I^*U_{XXTT} - \frac{D^*A\epsilon}{BL}\left(U_{XX}U_{XXX}\right)_X\right]$$

To apply the second step in a simple way we suppose $D = 0$ in the previous model. In this case the microstrutured part of the strain energy depends only on φ and φ_x^2, and W is written as

$$W = \frac{1}{2}\alpha u_x^2 + \frac{1}{6}\beta u_x^3 - A\varphi u_x + \frac{1}{2}B\varphi^2 + \frac{1}{2}C\varphi_x^2$$

Let us introduce three positive dimensionless parameters:

- $\epsilon := V << 1$ accounting for the elastic strain;
- $\delta := \dfrac{l^2}{L^2} << 1$ characterizing the ratio between the microstructure size and the wave lenght;
- $\gamma := \dfrac{d}{l}$ characterizing the influence of the dissipation.

We assume the dissipation is weak and we introduce the functions $v = u_x$. Then the governing nonlinear p.d.e. for the macrostrain $v(x, t)$ is:

$$v_{tt} - v_{xx} - \epsilon\alpha_1(v^2)_{xx} - \gamma\alpha_2 v_{xxt} + \delta(\alpha_3 v_{xxxx} - \alpha_4 v_{xxtt}) + \gamma\delta(\alpha_5 v_{xxxxt} + \alpha_6 v_{xttt}) = 0$$

where $\alpha_1, ..., \alpha_6$ are given in [2]. When $\epsilon = O(\delta)$ nonlinearity and dispersion are in balance. If in addition $\gamma = 0$ we have the non-dissipative case governed by the double dispersive equation:

$$v_{tt} - v_{xx} - \epsilon\left[\alpha_1(v^2)_{xx} - \alpha_3 v_{xxxx} + \alpha_4 v_{xxtt}\right] = 0$$

Using the function $v(z) = v(x, t)$ and the boundary conditions $\dfrac{\partial^k v}{\partial z^k} \to 0$ for $|z| \to \infty$, $k = 0, 1, 2, 3$ we obtain the Abel equation:

$$v' = \frac{(V^2 - 1)}{\epsilon\alpha_3 - \epsilon V^2\alpha_4} v v^3 - \frac{\epsilon\alpha_1}{\epsilon\alpha_3 - \epsilon V^2\alpha_4} v^2 v^3$$

and the Weierstrass equation.

$$(v')^2 = \frac{(V^2 - 1)}{\epsilon\alpha_3 - \epsilon V^2\alpha_4} v^2 - \frac{2\epsilon\alpha_1}{\epsilon\alpha_3 - \epsilon V^2\alpha_4} \frac{v^3}{3}$$

The exact bell-shaped travelling solitary wave solution arises as a result of balance between nonlinear and dispersive terms and it is given by:

$$v(z) = \frac{3(V^2 - 1)}{2\epsilon\alpha_1} sech^2\left[2\sqrt{\frac{\epsilon\alpha_3 - \epsilon V^2\alpha_4}{V^2 - 1}}(z - c)\right]$$

4. 2D-case

Now we try to do the same thing for a two-dimensional model. In this case, we suppose that the vectors **r** and **d** are written in this form

$$\mathbf{r} = \mathbf{r}(x, y, t) = u(x, t)\mathbf{i} + v(y, t)\mathbf{j}$$

$$\mathbf{d} = \mathbf{d}(x, y, t) = \varphi(x, t)\mathbf{i} + \chi(y, t)\mathbf{j}$$

We can see that in this case u and φ depend only on the direction **i** and v and χ depend on the direction **j**. We choose the strain energy in terms of $u_x,\ v_y,\ \varphi,\ \chi,\ \varphi_x,\ \chi_y$ as follows:

$$W = \frac{1}{2}Au_x^2 + \frac{1}{2}Bv_y^2 + \frac{1}{2}C\varphi^2 + \frac{1}{2}D\chi^2 + \frac{1}{2}E\varphi_x^2 + \frac{1}{2}F\chi_y^2 + \frac{1}{2}Gu_x^2\varphi + \frac{1}{2}Hv_y^2\chi$$

Then the Euler-Lagrange equations become:

$$\text{(3)} \qquad \begin{cases} \rho u_{tt} = Au_{xx} + Gu_{xx}\varphi + Gu_x\varphi_x \\ \rho v_{tt} = Bv_{yy} + Hv_{yy}\chi + Hv_y\chi_y \\ I\varphi_{tt} = E\varphi_{xx} - C\varphi - \dfrac{1}{2}Gu_x^2 \\ I\chi_{tt} = F\chi_{yy} - D\chi - \dfrac{1}{2}Hv_y^2 \end{cases}$$

To obtain two partial differential equations, each one depending only on one field variable, we couple equation $(3)_1$ to $(3)_3$ and equation $(3)_2$ to $(3)_4$.

As in the one-dimensional case, we introduce the dimensionless variables and parameters

$$U = \frac{u}{U_0},\ V = \frac{v}{V_0},\ X = \frac{x}{L},\ Y = \frac{y}{L},\ T = \frac{c_0 t}{L},\ \delta = \left(\frac{l}{L}\right)^2, \epsilon = \left(\frac{U_0}{L}\right)$$

and we also suppose that I, E and F verify the following equalities:

$$I = \rho l^2 I^*,\ E = l^2 E^*,\ F = l^2 F^*$$

Now we must determine φ in terms of U_x and χ in terms of V_y. We expand them in powers of δ and we use the slaving principle in the same way as in the 1D-case. We get (from eqs. (3)):

$$\begin{cases} U_{TT} = U_{XX} + \dfrac{G}{A}\left(U_{XX}\varphi + U_X\varphi_X\right) \\ \\ \varphi = -\dfrac{G\epsilon^2}{2C}U_X^2 + \dfrac{\delta}{C}(E^*\varphi_{XX} - AI^*\varphi_{TT}) \end{cases}$$

$$\begin{cases} V_{TT} = V_{YY} + \dfrac{H}{B}\left(V_{YY}\chi + V_Y\chi_Y\right) \\ \\ \chi = -\dfrac{H\epsilon^2}{2D}V_Y^2 + \dfrac{\delta}{D}(F^*\chi_{YY} - BI^*\chi_{TT}) \end{cases}$$

We proceed as in the one-dimensional case, and finally we find a couple of partial differential equation depending on the function U and V. In conclusion we have trasformed the starting system of four Euler-Lagrange equations in the functions u, v, φ, χ in this system of two equations in the functions U and V:

$$\begin{cases} U_{TT} = U_{XX} - \dfrac{\epsilon^2G^2}{AC}\left\{\dfrac{1}{2}U_X^2U_{XX} + \dfrac{\delta}{C}U_{XX}\left[E^*\left(U_XU_{XX}\right)_X - AI^*\left(U_XU_{XT}\right)_T\right]\right. \\ \qquad\qquad \left. -U_{XX}^2 + \dfrac{\delta}{C}U_X\left[E^*\left(U_XU_{XX}\right)_{XX} - AI^*\left(U_XU_{XT}\right)_{XT}\right]\right\} \\ \\ V_{TT} = V_{YY} - \dfrac{\epsilon^2H^2}{BD}\left\{\dfrac{1}{2}V_Y^2U_{YY} + \dfrac{\delta}{D}V_{YY}\left[F^*\left(V_YV_{YY}\right)_Y - BI^*\left(V_YV_{YT}\right)_T\right]\right. \\ \qquad\qquad \left. -V_{YY}^2 + \dfrac{\delta}{D}V_Y\left[F^*\left(V_YV_{YY}\right)_{YY} - BI^*\left(V_YV_{YT}\right)_{YT}\right]\right\} \end{cases}$$

Now we consider another two-dimensional model. The vectors **u** and **d** are the same as in the previous case while the strain energy W is slightly different: we add cubic terms for the derivatives of u, v, φ, χ:

$$\begin{aligned} W =& \frac{1}{2}A(u_x^2 + v_y^2) + \frac{1}{2}B(\varphi^2 + \chi^2) + \frac{1}{2}C(\varphi_x^2 + \chi_y^2) \\ &+ \frac{1}{2}D(u_x^2\varphi + v_y^2\chi) + \frac{1}{6}E(u_x^3 + v_y^3) + \frac{1}{6}F(\varphi_x^3 + \chi_y^3) \end{aligned}$$

So, we obtain the Lagrange equations in this forms:

$$\begin{cases} \rho u_{tt} = Au_{xx} + Du_{xx}\varphi + Du_x\varphi_x + Eu_xu_{xx} \\ \\ \rho v_{tt} = Av_{yy} + Dv_{yy}\chi + Dv_y\chi_y + Ev_yv_{yy} \\ \\ I\varphi_{tt} = C\varphi_{xx} + F\varphi_x\varphi_{xx} - B\varphi - \dfrac{1}{2}Du_x^2 \\ \\ I\chi_{tt} = C\chi_{yy} + F\chi_y\chi_{yy} - B\chi - \dfrac{1}{2}Dv_y^2 \end{cases} \tag{4}$$

The procedure is the same as in the previous case, and so, we omit all the passages. We can prove that, from equations $(4)_1$ and $(4)_3$ we obtain the following system

$$\begin{cases} U_{TT} = U_{XX} + \frac{D}{A}\left(U_{XX}\varphi + U_X\varphi_X\right) + \frac{E\epsilon}{A}U_X U_{XX} \\ \varphi = -\frac{D\epsilon^2}{2B}U_X^2 + \frac{\delta}{B}\left(C^*\varphi_{XX} - AI^*\varphi_{TT} + \frac{F^*}{L}\varphi_X\varphi_{XX}\right) \end{cases}$$

and from equation $(4)_2$ and $(4)_4$ the system

$$\begin{cases} V_{TT} = V_{YY} + \frac{D}{A}\left(V_{YY}\chi + V_Y\chi_Y\right) + \frac{E\epsilon}{A}V_Y V_{YY} \\ \chi = -\frac{D\epsilon^2}{2B}V_Y^2 + \frac{\delta}{B}\left(C^*\chi_{YY} - AI^*\chi_{TT} + \frac{F^*}{L}\chi_Y\chi_{YY}\right) \end{cases}$$

Now we write φ and χ in terms of U and V using the slaving principle. Our finally result is the reduction of the starting system (4) to this system:

$$\begin{cases} U_{TT} = U_{XX}\left(1 - \dfrac{3D^2\epsilon^2}{2AB}U_X^2\right) - \dfrac{\delta D^2\epsilon^2}{AB^2}\left\{C^*\left[U_{XX}\left(U_{XT}^2 + (U_{XT}^2)_X\right) + (U_X^2 U_{XTT})_X\right]\right. \\ \qquad -AI^*\left[U_{XX}(U_X + U_{XT})_T + U_X(U_{XX} + U_{XXT})_T\right] \\ \qquad \left. -\dfrac{D\epsilon^2F^*}{BL}\left[U_X U_{XX}(2U_{XX}^3 U_X^3 U_{XXXX}) + U_{XXX}(U_X^3 U_{XX})_X\right]\right\} + \dfrac{\epsilon E}{A}U_X U_{XX} \\ \\ V_{TT} = V_{YY}\left(1 - \dfrac{3D^2\epsilon^2}{2AB}V_Y^2\right) - \dfrac{\delta D^2\epsilon^2}{AB^2}\left\{C^*\left[V_{YY}\left(V_{YT}^2 + (V_{YT}^2)_Y\right) + (V_Y^2 U_{YTT})_Y\right]\right. \\ \qquad -AI^*\left[V_{YY}(V_Y + V_{YT})_T + V_Y(V_{YY} + V_{YYT})_T\right] \\ \qquad \left. -\dfrac{D\epsilon^2F^*}{BL}\left[V_Y V_{YY}(2V_{YY}^3 V_Y^3 V_{YYYY}) + V_{YYY}(V_Y^3 V_{YY})_Y\right]\right\} + \dfrac{\epsilon E}{A}V_Y V_{YY} \end{cases}$$

5. Conclusions

At this stage we have obtained the Abel equation, following the method presented by Samsonov [7], only for a one-dimensional model. The pourpose for future researches is to extend this work also to a two-dimensional model. In particular we want to reduce, if it is possible, the four Euler-Lagrange equations of a two-dimensional model, to a system of two Abel equations. Thereafter, our aim is to obtain a soliton solution.

References

[1] ENGELBRECHT J., BEREZOVSKI A., PASTRONE F. AND BRAUN M., *Waves in microstructured materials and dispersion*, to appear.

[2] PORUBOV A.V. AND PASTRONE F., *Non-linear bell-shaped and kink-spaped strain waves in microstructured solids*, Intl. J. Non-linear Mech. **39** (8) (2004).

[3] PORUBOV A.V., PASTRONE F. AND MAUGIN G.A., *Selection of two-dimensional nonlinear strain waves in icrostructured media* C.R. Acad. Sci., Paris, Ser. I **337** (2004).

[4] ENGELBRECHT J. AND PASTRONE F., *Waves in microstructured solids with nonlinearities in microscale*, Proc. Estonian Acad. Sci. Phys. Math. **52** (12) (2003).

[5] ENGELBRECHT J., CERMELLI P., PASTRONE F., *Wave hierarchy in microstructured solids*, in: "Geometry, Continua and Microstructure" (Ed. Maugin G.A.), Hermann Publ., Paris 1999.

[6] PORUBOV A., *Amplification of nonlinear strain waves in solids*, World Scientific, 2003.

[7] SAMSONOV A.M., *Strain solitons in solids and how to construct them*, Chapman & Hall/CRC, New York 2001.

AMS Subject Classification: 74J30, 74J35.

Alessia CASASSO, Department of Mathematics, University of Turin, Via Carlo Alberto 10, 10123, Turin, ITALY
e-mail: alessia.casasso@unito.it

Rend. Sem. Mat. Univ. Pol. Torino - Vol. 65, 2 (2007)
ISASUT Intensive Seminar

P. Cermelli - T. Armano*

FINE CROSS-SLIP OF A SCREW DISLOCATION IN ANTI-PLANE SHEAR

Abstract. In this work we present the main results of Armano and Cermelli [1] regarding the motion of a screw dislocation in a crystalline solid. It is well known that dislocations can only move along a finite number of crystallographic directions: in two dimensions, the resulting trajectories are piecewise rectilinear paths. However, in special situations such as near an attractor, dislocations are forced to move along curved paths: we characterize this class of motions as fine mixtures of crystallographic motions, using the notion of generalized curves due to L. C. Young, and explicitly compute the parametrized measure associated to a sequence of polygonals.

1. Introduction

We present here the results of Armano and Cermelli [1], and refer to that paper for the proofs of the main theorems and numerical simulations.

We study the motion of a rectilinear screw dislocation in a cylindrical crystalline elastic body, in the framework developed by Cermelli and Gurtin [2]. Peculiar to crystalline materials is the fact that dislocations are restricted to move along special planes, the so-called glide or slip planes.

In elastic materials, a state of stress induces a force on a dislocation, the so-called Peach-Köhler force (cf. [6], [3] and [2]), and the defect moves parallel to the direction on which the projection of this force is maximal (maximum dissipation criterion). Now, the motion of a straight dislocation can be described in terms of the intersection point of the dislocation line with an horizontal plane. The motion of the representative point can be viewed in turn as the solution of a plane dynamical system, obtained by projecting the Peach-Köhler force on the crystallographic directions. Since the number of such directions in a crystal is finite, it follows that the trajectories are piecewise rectilinear paths.

The general properties of this dynamical system have been studied in [2]: we focus here on a special situation, namely the motion near a curve S which is an attractor. The dislocation is attracted by S: when it reaches it, it cannot escape (since it would violate the maximum dissipation criterion), but it cannot move along S either, since it would, in general, violate the crystallographic restriction on the direction of motion. Hence, it seems natural to approximate the motion of the defect on S by a sequence of polygonals, which are piecewise parallel to the crystallographic directions but do not necessarily satisfy the maximum dissipation criterion at all times.

The main result of [1] is the proof that, if such a sequence is a maximizing

*This work was supported by the Italian M.U.R.S.T. research project “Modelli matematici per la scienza dei materiali” (Cofin 2002).

sequence for the dissipation, it converges to a unique smooth motion on S, which we refer to as *fine cross slip*[*].

To study the limits of maximizing sequences we use the notion of generalized curves due to L.C. Young, in their formulation known as parametrized (or Young) measures in the literature on the calculus of variations. Young measures provide a richer characterization of finely oscillating sequences than their weak limits: we compute the Young measure associated to sequences of polygonals maximizing the dissipation, and characterize fine cross slip as a fine mixture of crystallographic rectilinear motions, with weights depending on the direction of the attractor S.

2. Statement of the problem

We shortly summarize in this section the model discussed in [2]. Consider an elastic cylinder $B = \Omega \times \mathbb{R}$, with Ω a domain in $\mathbb{R}^2$. A *screw Volterra dislocation* is a singular displacement field on B which can be constructed by the following ideal procedure [8]: first cut the cylinder B along a vertical half-plane Π, then translate one of the faces along the cut by a constant vertical vector $\boldsymbol{b}$, glue back the faces along Π, and let the cylinder relax to an elastic equilibrium state (Figure 2). The resulting displacement field, measured with respect to the initial configuration, is smooth in $B \setminus \Pi$, but is discontinuous across Π with constant jump $\boldsymbol{b}$. The vertical line $\partial\Pi$ is called the *dislocation line*, and $\boldsymbol{b}$ is the *Burgers vector*. In order to avoid dealing with discontinuous displacement fields, it can be shown that a screw dislocation can be characterized equivalently in terms of a deformation field on $B \setminus \partial\Pi$, singular at $\partial\Pi$. In simple cases, the deformation field generated by a dislocation is independent of the vertical coordinate, and the problem admits a two-dimensional formulation in terms of planar fields on Ω, which are singular at $\boldsymbol{z} = \partial\Pi \cap \Omega$ (cf. [2]).

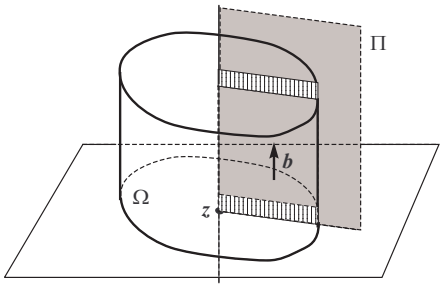

Figure 1: A screw Volterra dislocation in the cylinder $\Omega \times \mathbb{R}$.

Precisely, let Ω be a domain in $\mathbb{R}^2$, with cartesian coordinates (x, y) and associated basis $(\boldsymbol{e}_1, \boldsymbol{e}_2)$, and let $\boldsymbol{x}$ denote a generic point in Ω.

[*]Fine cross slip of screw dislocations has indeed been experimentally observed (cf., e.g., [5] and [4]).

Fix a defect position $\boldsymbol{z} \in \Omega$ and consider the solution $u : \Omega \to \mathbb{R}$ of the Neumann problem

$$\text{(1)} \qquad \begin{cases} \Delta u = 0 & \text{in } \Omega \\ \dfrac{\partial u}{\partial n} = -\boldsymbol{g}_0 \cdot \boldsymbol{n} + \sigma_0 & \text{on } \partial\Omega, \end{cases}$$

with Δ the Laplace operator, $\partial/\partial n$ the normal time-derivative on $\partial\Omega$, $\boldsymbol{n}$ the outward unit normal to $\partial\Omega$ and

$$\text{(2)} \qquad \boldsymbol{g}_0 = \boldsymbol{g}_0(\boldsymbol{x}, \boldsymbol{z}) = \frac{b}{2\pi |\boldsymbol{x} - \boldsymbol{z}|^2}\, \boldsymbol{e}_3 \times (\boldsymbol{x} - \boldsymbol{z}),$$

where b is a real constant, $\boldsymbol{e}_3 = \boldsymbol{e}_1 \times \boldsymbol{e}_2$ is a unit vector in $\mathbb{R}^3$ orthogonal to the plane containing Ω (so that $\boldsymbol{e}_3 \times (\cdot)$ represents a counterclockwise $\pi/2$-rotation in the Ω-plane), and $\sigma_0 = \sigma_0(\boldsymbol{x})$ is an assigned function on $\partial\Omega$. The field u represents the regular part of the displacement due to the dislocation at $\boldsymbol{z}$, while $\boldsymbol{g}_0$ is related to the singular part of the deformation.

For each fixed $\boldsymbol{z} \in \Omega$, the Neumann problem (1) has a unique smooth solution (modulo an additive constant), which we henceforth denote by

$$\text{(3)} \qquad u = u(\boldsymbol{x}, \boldsymbol{z}), \qquad \boldsymbol{x} \in \Omega.$$

Consider now the smooth vector field in Ω

$$\text{(4)} \qquad \boldsymbol{J}(\boldsymbol{x}) = b\, \nabla u(\boldsymbol{x}, \boldsymbol{x}) \times \boldsymbol{e}_3, \qquad \boldsymbol{x} \in \Omega,$$

where $\nabla u(\boldsymbol{x}, \boldsymbol{x}) = \nabla_{\boldsymbol{x}} u(\boldsymbol{x}, \boldsymbol{z})|_{\boldsymbol{z}=\boldsymbol{x}}$ is the gradient of the solution $u(\boldsymbol{x}, \boldsymbol{z})$ of (1), for a dislocation located at $\boldsymbol{z} = \boldsymbol{x}$. The vector field $\boldsymbol{J}(\boldsymbol{x})$ only depends on the domain Ω and the boundary conditions σ_0, and may be identified to the Peach-Köhler force on a dislocation located at $\boldsymbol{x} \in \Omega$.

Let now t denote time and $[0, T]$ be the time interval of interest. In order to study the behavior of a defect under the action of the force (4), consider a dislocation motion

$$\boldsymbol{z} : [0, T] \to \Omega.$$

Introducing the (finite) set of *crystallographic directions*

$$\mathcal{C} = \{\boldsymbol{s}_1, \ldots, \boldsymbol{s}_n\},$$

with $\boldsymbol{s}_i$ fixed unit vectors in $\mathbb{R}^2$, the basic physical idea is that a dislocation can only move parallel to a crystallographic direction $\boldsymbol{s} \in \mathcal{C}$ on which the projection of the force $\boldsymbol{J} \cdot \boldsymbol{s}$ is maximal, provided this is greater than a given threshold F, the so-called Peierls force (Figure 2). Therefore, we write the basic equation governing the motion of a dislocation as

$$\text{(5)} \qquad \dot{\boldsymbol{z}} = \boldsymbol{V}(\boldsymbol{z}), \qquad \boldsymbol{z} \in \Omega,$$

where the superposed dot denotes time-derivative, and where the vector field $\boldsymbol{V}$ is defined by

$$\boldsymbol{V}(\boldsymbol{x}) := \begin{cases} \boldsymbol{0} & \text{if} \quad \boldsymbol{J}(\boldsymbol{x}) \cdot \boldsymbol{s} \leq F \quad \forall \boldsymbol{s} \in \mathcal{C}, \\ M\,(\boldsymbol{J}(\boldsymbol{x}) \cdot \boldsymbol{e}(\boldsymbol{x}) - F)\,\boldsymbol{e}(\boldsymbol{x}) & \text{otherwise,} \end{cases} \tag{6}$$

where $M > 0$ and $F \geq 0$ are given constants, and $\boldsymbol{e}(\boldsymbol{x}) \in \mathcal{C}$ is determined by the *maximum dissipation criterion*, i.e., the requirement that the projection of $\boldsymbol{J}(\boldsymbol{x})$ on $\boldsymbol{e}(\boldsymbol{x})$ be maximal, i.e.,

$$\boldsymbol{J}(\boldsymbol{x}) \cdot \boldsymbol{e}(\boldsymbol{x}) = \max_{\boldsymbol{s} \in \mathcal{C},\ \boldsymbol{J} \cdot \boldsymbol{s} > F} \{\boldsymbol{J}(\boldsymbol{x}) \cdot \boldsymbol{s}\}. \tag{7}$$

It may happen that at some point $\boldsymbol{x}$ the maximization problem (7) admits two solutions: at such points the field $\boldsymbol{e}(\boldsymbol{x})$, and by consequence also $\boldsymbol{V}(\boldsymbol{x})$, is multi-valued. Indeed, $\boldsymbol{J} \cdot \boldsymbol{s}$ can have at most two maxima in $\mathcal{C}$ for $\boldsymbol{J}$ given. Assume in fact that there exist three distinct unit vectors $\boldsymbol{s}_1$, $\boldsymbol{s}_2$, $\boldsymbol{s}_3$ such that $\boldsymbol{J} \cdot \boldsymbol{s}_1 = \boldsymbol{J} \cdot \boldsymbol{s}_2 = \boldsymbol{J} \cdot \boldsymbol{s}_3$; then the endpoints of $\boldsymbol{s}_1$, $\boldsymbol{s}_2$ and $\boldsymbol{s}_3$ belong to the same straight line perpendicular to $\boldsymbol{J}$, which is impossible since the $\boldsymbol{s}_i$ are unit vectors.

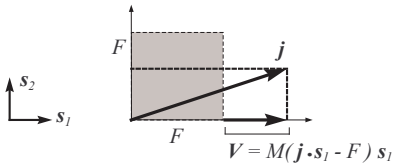

Figure 2: The definition of the vector field $\boldsymbol{V}$.

A detailed analysis of the phase portrait of the dynamical system (5) has been performed in [2], where it is shown that Ω splits into (i) regions where $\boldsymbol{V}(\boldsymbol{x}) = \boldsymbol{0}$, and the dislocation is stationary; (ii) *single slip regions* $R(\boldsymbol{s})$ (open regions in $\mathbb{R}^2$), in which $\boldsymbol{e}(\boldsymbol{x}) = \boldsymbol{s}$ is constant; and (iii) curves S on which $\boldsymbol{e}(\boldsymbol{x})$ is multi-valued. We are interested here in the motion on a so-called *attracting curve* (Figure 3).

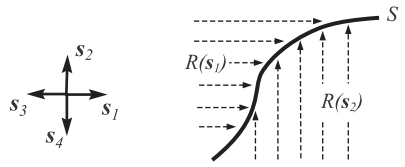

Figure 3: Attracting curve separating two single-slip regions

The motion of a dislocation, solution of (5), can be described as follows: consider, to fix ideas, a dislocation initially at $\boldsymbol{z}_0 \in R(\boldsymbol{s}_1)$: the evolution equation (5) reduces to

$$\dot{\boldsymbol{z}} = V_1(\boldsymbol{z})\boldsymbol{s}_1,$$

with $V_1(\boldsymbol{z}) = M(\boldsymbol{J}(\boldsymbol{z}) \cdot \boldsymbol{s}_1 - F)$. Hence, the dislocation moves along a straight line parallel to $\boldsymbol{s}_1$, until it reaches some point at the boundary of $R(\boldsymbol{s}_1)$. If this point belongs to an attractor, then the solution of (5) cannot be prolonged into the adjacent region, since it would violate the maximum dissipation criterion (Figure 3).

Hence, the problem seems to be ill-posed in the presence of an attractor. In order to remove the ambiguity, it was suggested in [2] that, when the dislocation reaches an attractor S, it continues to move along it according to an evolution equation of the form

$$\dot{\boldsymbol{z}} = \boldsymbol{w}(\boldsymbol{z}), \qquad \text{with} \quad \boldsymbol{w}(\boldsymbol{z}) = V_{12}(\boldsymbol{z})(\alpha_1(\boldsymbol{z})\boldsymbol{s}_1 + \alpha_2(\boldsymbol{z})\boldsymbol{s}_2), \tag{8}$$

where $V_{12}(\boldsymbol{z}) := \boldsymbol{J}(\boldsymbol{z}) \cdot \boldsymbol{s}_1 - F = \boldsymbol{J}(\boldsymbol{z}) \cdot \boldsymbol{s}_2 - F$, and α_1, α_2 are determined by solving

$$\begin{cases} \alpha_1 + \alpha_2 = 1, \\ \alpha_1(\boldsymbol{s}_1 - \boldsymbol{s}_2) \cdot (\nabla \boldsymbol{J})\boldsymbol{s}_1 + \alpha_2(\boldsymbol{s}_1 - \boldsymbol{s}_2) \cdot (\nabla \boldsymbol{J})\boldsymbol{s}_2 = 0. \end{cases} \tag{9}$$

The resulting smooth motion of the dislocation, referred to as *fine cross slip*, is therefore non-crystallographic, since it does not occur along a crystallographic direction $\boldsymbol{s} \in \mathcal{C}$. The purpose of the next section is to show that motion by fine cross slip (8) can be realized as the limit of a sequence of infinitesimal cross slips across the attracting curve S, when this sequence maximizes the dissipation.

Remark. Letting

$$\hat{V}(\boldsymbol{e}, \boldsymbol{J}) := \begin{cases} 0, & \text{if} \quad \boldsymbol{J} \cdot \boldsymbol{e} \leq F, \\ M(\boldsymbol{J} \cdot \boldsymbol{e} - F), & \text{if} \quad \boldsymbol{J} \cdot \boldsymbol{e} > F, \end{cases} \tag{10}$$

we may rewrite condition (7) as the requirement that motion may only occur in those directions $\boldsymbol{e}$ which maximize the *dissipation* $\hat{V}(\boldsymbol{s}, \boldsymbol{J})\,\boldsymbol{J} \cdot \boldsymbol{s}$, i.e.,

$$\hat{V}(\boldsymbol{e}, \boldsymbol{J})\,\boldsymbol{J} \cdot \boldsymbol{e} = \max_{\boldsymbol{s} \in \mathcal{C}} \left[\hat{V}(\boldsymbol{s}, \boldsymbol{J})\,\boldsymbol{J} \cdot \boldsymbol{s} \right], \tag{11}$$

provided that $\hat{V}(\boldsymbol{e}, \boldsymbol{J}) > 0$. The equivalence of (7) and (11) follows from the fact that the function $M(\xi - F)\xi$ is monotonic with respect to ξ for $\xi > F$.

3. Convergence of sequences of admissible polygonals

We study here the motion of a dislocation near an attracting curve, in order to justify (8) rigorously. From now on we regard the vector field $\boldsymbol{J}(\boldsymbol{x})$ in (4) as assigned and smooth in Ω.

Let $\boldsymbol{z} : [0, T] \to \Omega$ be a given motion (not necessarily a solution of (5), (7), and (6)); writing

$$\dot{\boldsymbol{z}}(t) = V(t)\boldsymbol{e}(t), \qquad t \in [0, T], \tag{12}$$

with $V = |\dot{\boldsymbol{z}}|$ and $\boldsymbol{e} = \dot{\boldsymbol{z}}/|\dot{\boldsymbol{z}}|$, we say that $\boldsymbol{z}$ is *admissible* if

(i) $\boldsymbol{z}$ is continuous and piecewise smooth;

(ii) the direction of motion $\boldsymbol{e}(t)$ belongs to the set of crystallographic directions, and the velocity is a function of the projection of the force on that direction[†], i.e.,

$$\boldsymbol{e}(t) \in \mathcal{C} \qquad \text{and} \qquad V(t) = \hat{V}(\boldsymbol{e}(t), \boldsymbol{J}(\boldsymbol{z}(t))), \tag{13}$$

at each time t, with $\hat{V}$ given by (10).

An admissible motion does not necessarily satisfy the maximum dissipation criterion at all times, but its trajectory is a polygonal with edges parallel to the crystallographic directions.

We assume from now on that the set of crystallographic directions is

$$\mathcal{C} = \{\boldsymbol{s}_1, \boldsymbol{s}_2, -\boldsymbol{s}_1, -\boldsymbol{s}_2\}, \tag{14}$$

with $\boldsymbol{s}_1 = \boldsymbol{e}_1$ and $\boldsymbol{s}_2 = \boldsymbol{e}_2$, and consider two adjacent single slip regions $R(\boldsymbol{s}_1)$ and $R(\boldsymbol{s}_2)$, connected open sets in Ω such that[‡] $\overline{R(\boldsymbol{s}_1)} \cap \overline{R(\boldsymbol{s}_2)} \neq \emptyset$ and $\overline{R(\boldsymbol{s}_1)} \cap \partial\Omega = \emptyset$, $\overline{R(\boldsymbol{s}_2)} \cap \partial\Omega = \emptyset$. By definition, in $R(\boldsymbol{s}_1)$ and $R(\boldsymbol{s}_2)$ the dissipation is maximal in the directions $\boldsymbol{s}_1$ and $\boldsymbol{s}_2$ respectively, i.e.,

$$\begin{cases} \boldsymbol{x} \in R(\boldsymbol{s}_1) & \Rightarrow \quad \boldsymbol{s}_1 \cdot \boldsymbol{J}(\boldsymbol{x}) > \boldsymbol{s} \cdot \boldsymbol{J}(\boldsymbol{x}), \qquad \forall \boldsymbol{s} \in \mathcal{C},\ \boldsymbol{s} \neq \boldsymbol{s}_1, \\ \boldsymbol{x} \in R(\boldsymbol{s}_2) & \Rightarrow \quad \boldsymbol{s}_2 \cdot \boldsymbol{J}(\boldsymbol{x}) > \boldsymbol{s} \cdot \boldsymbol{J}(\boldsymbol{x}), \qquad \forall \boldsymbol{s} \in \mathcal{C},\ \boldsymbol{s} \neq \boldsymbol{s}_2. \end{cases} \tag{15}$$

Also, we assume that

$$\boldsymbol{J}(\boldsymbol{x})\cdot\boldsymbol{s}_1 > F \quad \text{and} \quad \boldsymbol{J}(\boldsymbol{x})\cdot\boldsymbol{s}_2 > F, \qquad \boldsymbol{x} \in \overline{R(\boldsymbol{s}_1)} \cup \overline{R(\boldsymbol{s}_2)}.$$

3.1. The definition of attracting curve

Let

$$G(\boldsymbol{x}) := (\boldsymbol{s}_2 - \boldsymbol{s}_1) \cdot \boldsymbol{J}(\boldsymbol{x}), \tag{16}$$

and assume that $\boldsymbol{J}$ is such that $\nabla G \neq 0$ in Ω. By definition,

$$G(\boldsymbol{x}) < 0 \quad \text{for} \quad \boldsymbol{x} \in R(\boldsymbol{s}_1) \qquad \text{and} \qquad G(\boldsymbol{x}) > 0 \quad \text{for} \quad \boldsymbol{x} \in R(\boldsymbol{s}_2),$$

so that, by the smoothness of G and the fact that $\nabla G \neq 0$, the set

$$S = \overline{R(\boldsymbol{s}_1)} \cap \overline{R(\boldsymbol{s}_2)},$$

is a smooth curve on which G vanishes, i.e.,

$$G(\boldsymbol{x}) = 0 \quad \Leftrightarrow \quad \boldsymbol{s}_1 \cdot \boldsymbol{J}(\boldsymbol{x}) = \boldsymbol{s}_2 \cdot \boldsymbol{J}(\boldsymbol{x}) \qquad \boldsymbol{x} \in S. \tag{17}$$

We say that S is an *attracting curve* for $R(\boldsymbol{s}_1)$ and $R(\boldsymbol{s}_2)$ if it satisfies the supplementary conditions

$$\boldsymbol{s}_1 \cdot \nabla G(\boldsymbol{x}) > 0, \qquad \boldsymbol{s}_2 \cdot \nabla G(\boldsymbol{x}) < 0, \qquad \boldsymbol{x} \in S. \tag{18}$$

[†]For $\boldsymbol{z}$ continuous and piecewise smooth, $\dot{\boldsymbol{z}}$ is the right time-derivative at corner points.

[‡]Here $\bar{R}$ denotes the closure of a set $R \subset \Omega$.

Hence, at an attracting curve, $\boldsymbol{s}_1$ points into $R(\boldsymbol{s}_2)$ and $\boldsymbol{s}_2$ points into $R(\boldsymbol{s}_1)$ (Figure 3(c)). We denote by

$$\boldsymbol{\tau} = \boldsymbol{e}_3 \times \frac{\nabla G}{|\nabla G|}$$

the tangent vector to S.

No admissible motion satisfying the maximum dissipation criterion can originate from an attracting curve S. To see this, consider an admissible motion along $\boldsymbol{s}_1$ with initial point on S: by $(18)_1$, G is increasing along $\boldsymbol{s}_1$, and the dislocation moves into the single slip region $R(\boldsymbol{s}_2)$. But in this region the dissipation is maximal in the direction $\boldsymbol{s}_2$, and the maximum dissipation criterion is violated.

Moreover, writing

$$\text{(19)} \qquad \begin{cases} V_1(\boldsymbol{x}) := \hat{V}(\boldsymbol{s}_1, \boldsymbol{J}(\boldsymbol{x})) = M(\boldsymbol{s}_1 \cdot \boldsymbol{J}(\boldsymbol{x}) - F), \\ V_2(\boldsymbol{x}) := \hat{V}(\boldsymbol{s}_2, \boldsymbol{J}(\boldsymbol{x})) = M(\boldsymbol{s}_2 \cdot \boldsymbol{J}(\boldsymbol{x}) - F), \end{cases}$$

for the admissible velocities in the directions $\boldsymbol{s}_1$ and $\boldsymbol{s}_2$ at $\boldsymbol{x} \in \overline{R(\boldsymbol{s}_1)} \cup \overline{R(\boldsymbol{s}_2)}$, (17) implies that $V_1(\boldsymbol{x}) = V_2(\boldsymbol{x})$ at $\boldsymbol{x} \in S$, and we denote by

$$V(\boldsymbol{x}) := V_1(\boldsymbol{x}) = V_2(\boldsymbol{x}) \qquad \boldsymbol{x} \in S,$$

their common value. However, since at S the maximum dissipation criterion admits both $\boldsymbol{s}_1$ and $\boldsymbol{s}_2$ as solutions, the vector field $\boldsymbol{V}$ in (6) is multi-valued, with values

$$V(\boldsymbol{x})\boldsymbol{s}_1 \qquad \text{and} \qquad V(\boldsymbol{x})\boldsymbol{s}_2,$$

at $\boldsymbol{x} \in S$.

3.2. Admissible polygonals

We study here admissible motions which do not necessarily satisfy the maximum dissipation criterion. By definition, an admissible motion $\boldsymbol{z}$ is a time-parametrized polygonal with sides parallel to the crystallographic directions $\boldsymbol{s}_i \in \mathcal{C}$ and piecewise continuous speed given by (10). Restricting to admissible motions occurring in $\overline{R(\boldsymbol{s}_1)} \cup \overline{R(\boldsymbol{s}_2)}$ along the directions $\boldsymbol{s}_1$ and $\boldsymbol{s}_2$ only, we have

$$\text{either} \qquad \dot{\boldsymbol{z}}(t) = V_1(\boldsymbol{z}(t))\boldsymbol{s}_1 \qquad \text{or} \qquad \dot{\boldsymbol{z}}(t) = V_2(\boldsymbol{z}(t))\boldsymbol{s}_2,$$

for $t \in [0, T]$, where V_1 and V_2 are given by (19) and $\dot{\boldsymbol{z}}(t)$ is the right time-derivative at the corner points of the polygonal.

3.3. Sequences of admissible motions

The natural notion of convergence for sequences of admissible motions should account for the fact that the velocity oscillates between the directions $\boldsymbol{s}_1$ and $\boldsymbol{s}_2$, and therefore may only converge in average. Weak-$*$ convergence in $W^{1,\infty}((0, T), \mathbb{R}^2)$ serves

the purpose. We say that a sequence of Lipschitz motions $\{\boldsymbol{z}_k\}$ converges weak-$*$ in $W^{1,\infty}((0,T),\mathbb{R}^2)$ if there exists a motion $\boldsymbol{\xi} \in W^{1,\infty}((0,T),\mathbb{R}^2)$ such that $\boldsymbol{z}_k \to \boldsymbol{\xi}$ strongly in $C([0,T],\mathbb{R}^2)$, and $\dot{\boldsymbol{z}}_k \overset{*}{\rightharpoonup} \dot{\boldsymbol{\xi}}$ in $L^\infty([0,T],\mathbb{R}^2)$, i.e.,

$$\sup_{t\in[0,T]} |\boldsymbol{z}_k(t) - \boldsymbol{\xi}(t)| \to 0,$$

and

$$\int_I (\dot{\boldsymbol{z}}_k(t) - \dot{\boldsymbol{\xi}}(t))\, dt \to 0,$$

for any interval $I \subset [0,T]$, provided $\{\dot{\boldsymbol{z}}_k(t)\}$ is bounded in $L^\infty([0,T],\mathbb{R}^2)$.

The weak limit of a sequence of admissible motions is characterized by the Young measure associated to the sequence of the velocities (cf. Young [9] or, for a more recent approach, [7]). Consider in fact a sequence $\{\boldsymbol{w}_k : (0,T) \to \mathbb{R}^2\}$ converging weak-$*$ to $\boldsymbol{w}_0$ in $L^\infty((0,T),\mathbb{R}^2)$. A Young measure associated with the sequence $\{\boldsymbol{w}_k\}$ is a family of probability measures $\{\nu_t\}_{t\in(0,T)}$ in $\mathbb{R}^2$ which depends measurably on t, i.e., for any $\varphi : \mathbb{R}^2 \to \mathbb{R}$ continuous, the function

$$\bar{\varphi}(t) = \int_{\mathbb{R}^2} \varphi(\boldsymbol{w}) d\nu_t(\boldsymbol{w}) \tag{20}$$

is measurable. The fundamental property of ν_t is that, for any continuous φ, the sequence $\{\varphi(\boldsymbol{w}_k)\}$ converges (modulo a subsequence) weak-$*$ to $\bar{\varphi}$ in $L^\infty((0,T),\mathbb{R}^2)$, i.e.,

$$\int_I \varphi(\boldsymbol{w}_k(t))\, dt \to \int_I \int_{\mathbb{R}^2} \varphi(\boldsymbol{w}) d\nu_t(\boldsymbol{w})\, dt, \tag{21}$$

for any interval $I \subset [0,T]$, provided that $\{\varphi(\boldsymbol{w}_k)\}$ is bounded in $L^\infty([0,T],\mathbb{R})$.

THEOREM 1. *Consider a sequence of admissible polygonals $\boldsymbol{z}_k(t)$ in the directions $\boldsymbol{s}_1$ and $\boldsymbol{s}_2$, converging weak-$*$ in $W^{1,\infty}((0,T),\mathbb{R}^2)$ as $k \to +\infty$ to a Lipschitz motion $\boldsymbol{\xi} \in W^{1,\infty}((0,T),\mathbb{R}^2)$. Then the Young measure associated to the sequence $\{\dot{\boldsymbol{z}}_k\}$ is*

$$\nu_t = \lambda_1(t)\, \delta_{V_1(\boldsymbol{\xi}(t))\boldsymbol{s}_1} + \lambda_2(t)\, \delta_{V_2(\boldsymbol{\xi}(t))\boldsymbol{s}_2}, \qquad t \in (0,T), \tag{22}$$

with $\delta_{V_1(\boldsymbol{\xi}(t))\boldsymbol{s}_1}$ and $\delta_{V_2(\boldsymbol{\xi}(t))\boldsymbol{s}_2}$ Dirac measures localized at $V_1(\boldsymbol{\xi}(t))\boldsymbol{s}_1$ and $V_2(\boldsymbol{\xi}(t))\boldsymbol{s}_2$ respectively, and

$$\lambda_1(t) = \frac{\dot{\boldsymbol{\xi}}(t)\cdot\boldsymbol{s}_1}{V_1(\boldsymbol{\xi}(t))}, \qquad \lambda_2(t) = \frac{\dot{\boldsymbol{\xi}}(t)\cdot\boldsymbol{s}_2}{V_2(\boldsymbol{\xi}(t))}. \tag{23}$$

Notice that, since the velocity of the limit motion is

$$\dot{\boldsymbol{\xi}}(t) = \lambda_1(t)V_1(\boldsymbol{\xi}(t))\boldsymbol{s}_1 + \lambda_2(t)V_2(\boldsymbol{\xi}(t))\boldsymbol{s}_2, \tag{24}$$

it follows that the weak limit of a sequence of admissible motions is not necessarily admissible, but can be represented as a fine mixture of crystallographic motions in the admissible directions $\boldsymbol{s}_1$ and $\boldsymbol{s}_2$.

COROLLARY 1. *Let S be an attracting curve separating two single slip regions $R(\boldsymbol{s}_1)$ and $R(\boldsymbol{s}_2)$: any sequence of admissible polygonals $\boldsymbol{z}_k(t)$ with directions $\boldsymbol{s}_1$ and $\boldsymbol{s}_2$ such that*

$$\operatorname{dist}(\boldsymbol{z}_k(t), S) \to 0, \tag{25}$$

uniformly in $t \in [0, T]$ as $k \to +\infty$, converges weak-$*$ in $W^{1,\infty}((0,T), \mathbb{R}^2)$ (and, in particular, uniformly) to a smooth motion $\boldsymbol{\xi}(t)$ on S with velocity

$$\dot{\boldsymbol{\xi}}(t) = \frac{V(\boldsymbol{\xi}(t))}{\boldsymbol{\tau}(\boldsymbol{\xi}(t)) \cdot (\boldsymbol{s}_1 + \boldsymbol{s}_2)}\, \boldsymbol{\tau}(\boldsymbol{\xi}(t)), \tag{26}$$

with $\boldsymbol{\tau}$ the unit tangent vector to S and $V(\boldsymbol{x}) := V_1(\boldsymbol{x}) = V_2(\boldsymbol{x})$ the speed evaluated at $\boldsymbol{x} \in S$ (cf. (19)). Moreover, the Young measure associated to the sequence $\{\dot{\boldsymbol{z}}_k\}$ is

$$\nu_t = \lambda_1(\boldsymbol{\xi}(t))\, \delta_{V(\boldsymbol{\xi}(t))\boldsymbol{s}_1} + \lambda_2(\boldsymbol{\xi}(t))\, \delta_{V(\boldsymbol{\xi}(t))\boldsymbol{s}_2}, \tag{27}$$

with

$$\lambda_1(\boldsymbol{x}) = \frac{\boldsymbol{\tau}(\boldsymbol{x}) \cdot \boldsymbol{s}_1}{\boldsymbol{\tau}(\boldsymbol{x}) \cdot (\boldsymbol{s}_1 + \boldsymbol{s}_2)}, \qquad \lambda_2(\boldsymbol{x}) = \frac{\boldsymbol{\tau}(\boldsymbol{x}) \cdot \boldsymbol{s}_2}{\boldsymbol{\tau}(\boldsymbol{x}) \cdot (\boldsymbol{s}_1 + \boldsymbol{s}_2)}, \tag{28}$$

for a.e. $\boldsymbol{x} \in S$.

Notice that, even though each admissible motion $\boldsymbol{z}_k(t)$ does not necessarily satisfy the maximum dissipation criterion for all $t \in [0, T]$, the sequence $\boldsymbol{z}_k$ is a maximizing sequence for the dissipation, since the limit motion $\boldsymbol{\xi}$ satisfies the maximum dissipation criterion (recall, though, that the limit motion is not admissible). To see this, let $J(\boldsymbol{x}) := \boldsymbol{J}(\boldsymbol{x}) \cdot \boldsymbol{s}_1 = \boldsymbol{J}(\boldsymbol{x}) \cdot \boldsymbol{s}_2$ and $V(\boldsymbol{x}) := V_1(\boldsymbol{x}) = V_2(\boldsymbol{x})$ for $\boldsymbol{x} \in S$ (cf. (17)): the maximum dissipation (among all admissible motions) at $\boldsymbol{x} \in S$ is (cf. (11) and (15))

$$\max_{\boldsymbol{s} \in \mathcal{C}} \{\hat{V}(\boldsymbol{s}, \boldsymbol{J}(\boldsymbol{x}))\, \boldsymbol{J}(\boldsymbol{x}) \cdot \boldsymbol{s}\} = J(\boldsymbol{x}) V(\boldsymbol{x}), \tag{29}$$

while the dissipation relative to the limit motion $\boldsymbol{\xi}(t)$ is

$$\boldsymbol{J}(\boldsymbol{\xi}(t)) \cdot \dot{\boldsymbol{\xi}}(t) = \frac{V(\boldsymbol{\xi}(t))}{\boldsymbol{\tau}(\boldsymbol{\xi}(t)) \cdot (\boldsymbol{s}_1 + \boldsymbol{s}_2)}\, \boldsymbol{J}(\boldsymbol{\xi}(t)) \cdot \boldsymbol{\tau}(\boldsymbol{\xi}(t)) = V(\boldsymbol{\xi}(t)) J(\boldsymbol{\xi}(t)), \tag{30}$$

since $\boldsymbol{J} = J(\boldsymbol{s}_1 + \boldsymbol{s}_2)$, and these expressions coincide at $\boldsymbol{x} = \boldsymbol{\xi}(t)$.

Also, it is not difficult to prove that (26) coincides with (8). In fact, solving system $(8)_2$ and recalling (16), we obtain

$$\begin{cases} \alpha_1 = \dfrac{(\boldsymbol{s}_2 - \boldsymbol{s}_1) \cdot (\nabla \boldsymbol{J}) \boldsymbol{s}_2}{(\boldsymbol{s}_2 - \boldsymbol{s}_1) \cdot (\nabla \boldsymbol{J}) \boldsymbol{s}_2 - (\boldsymbol{s}_2 - \boldsymbol{s}_1) \cdot (\nabla \boldsymbol{J}) \boldsymbol{s}_1} = \dfrac{\nabla G \cdot \boldsymbol{s}_2}{\nabla G \cdot \boldsymbol{s}_2 - \nabla G \cdot \boldsymbol{s}_1}, \\ \alpha_2 = \dfrac{-(\boldsymbol{s}_2 - \boldsymbol{s}_1) \cdot (\nabla \boldsymbol{J}) \boldsymbol{s}_1}{(\boldsymbol{s}_2 - \boldsymbol{s}_1) \cdot (\nabla \boldsymbol{J}) \boldsymbol{s}_2 - (\boldsymbol{s}_2 - \boldsymbol{s}_1) \cdot (\nabla \boldsymbol{J}) \boldsymbol{s}_1} = -\dfrac{\nabla G \cdot \boldsymbol{s}_1}{\nabla G \cdot \boldsymbol{s}_2 - \nabla G \cdot \boldsymbol{s}_1}, \end{cases}$$

with G given by (16). Now, noting that $\nabla G \cdot \boldsymbol{s}_2 = \nabla G \cdot \boldsymbol{e}_3 \times \boldsymbol{s}_1 = -\boldsymbol{e}_3 \times \nabla G \cdot \boldsymbol{s}_1 = -|\nabla G| \boldsymbol{\tau} \cdot \boldsymbol{s}_1$, and $\nabla G \cdot \boldsymbol{s}_1 = -\nabla G \cdot \boldsymbol{e}_3 \times \boldsymbol{s}_2 = \boldsymbol{e}_3 \times \nabla G \cdot \boldsymbol{s}_2 = |\nabla G| \boldsymbol{\tau} \cdot \boldsymbol{s}_2$, we find

$$\alpha_1 = \frac{\boldsymbol{\tau} \cdot \boldsymbol{s}_1}{\boldsymbol{\tau} \cdot \boldsymbol{s}_1 + \boldsymbol{\tau} \cdot \boldsymbol{s}_2}, \qquad \alpha_2 = \frac{\boldsymbol{\tau} \cdot \boldsymbol{s}_2}{\boldsymbol{\tau} \cdot \boldsymbol{s}_1 + \boldsymbol{\tau} \cdot \boldsymbol{s}_2},$$

which yields (26) recalling that V_{12} coincides with V in our present notation.

3.4. Sequences of admissible polygonals maximizing the dissipation

In this section we show that every sequence of polygonals maximizing the dissipation converges to the smooth motion $\boldsymbol{\xi}$ on S given by (26).

For $\boldsymbol{x} \in \Omega$, let $V_M(\boldsymbol{x})$ and $\boldsymbol{e}_M(\boldsymbol{x})$ denote the speed and direction of motion selected by the maximum dissipation criterion (11) among all admissible velocity fields, i.e. such that

$$V_M(\boldsymbol{x}) \boldsymbol{e}_M(\boldsymbol{x}) \cdot \boldsymbol{J}(\boldsymbol{x}) = \max_{\boldsymbol{s} \in \mathcal{C}} \left\{ \hat{V}(\boldsymbol{s}, \boldsymbol{J}(\boldsymbol{x})) \, \boldsymbol{s} \cdot \boldsymbol{J}(\boldsymbol{x}) \right\}, \tag{31}$$

where $\hat{V}$ is given by (10). Notice that, even though $\boldsymbol{e}_M(\boldsymbol{x})$ is in general multi-valued at S, the maximum dissipation (31) is single valued everywhere. Consider the function $D : \Omega \times \mathbb{R}^2 \to \mathbb{R}$ defined by

$$D(\boldsymbol{x}, \boldsymbol{w}) = \boldsymbol{J}(\boldsymbol{x}) \cdot (V_M(\boldsymbol{x}) \boldsymbol{e}_M(\boldsymbol{x}) - \boldsymbol{w}) \, . \tag{32}$$

For a given motion $\boldsymbol{z} \in W^{1,\infty}((0, T), \mathbb{R}^2)$ the real function $D(\boldsymbol{z}(t), \dot{\boldsymbol{z}}(t))$ belongs to $L^\infty((0, T), \mathbb{R})$, and measures the difference between the maximum possible dissipation and the actual dissipation at each time.

Fix $\boldsymbol{z}_0 \in S$ and consider the set of admissible curves originating from $\boldsymbol{z}_0$:

$$\begin{aligned} \mathcal{A} \quad = \quad & \Big\{ \boldsymbol{z} : [0, T] \to \mathbb{R}^2 \ : \ \boldsymbol{z} \text{ piecewise smooth, } \boldsymbol{z}(0) = \boldsymbol{z}_0 \in S \text{ and} \\ & \text{either} \quad \dot{\boldsymbol{z}}(t) = V_1(\boldsymbol{z}(t)) \boldsymbol{s}_1 \quad \text{or} \quad \dot{\boldsymbol{z}}(t) = V_2(\boldsymbol{z}(t)) \boldsymbol{s}_2, \ t \in [0, T] \Big\} , \end{aligned}$$

where $\dot{\boldsymbol{z}}$ denotes the right time-derivative at corner points of the polygonals.

By definition

$$D(\boldsymbol{z}(t), \dot{\boldsymbol{z}}(t)) \geq 0, \qquad \forall \boldsymbol{z} \in \mathcal{A}, \forall t \in [0, T], \tag{33}$$

although D can be negative for some non admissible motion.

Consider now the functional associated to D,

$$E(\boldsymbol{z}) = \int_0^T D(\boldsymbol{z}(t), \dot{\boldsymbol{z}}(t)) \, dt = \int_0^T \boldsymbol{J}(\boldsymbol{z}(t)) \cdot (V_M(\boldsymbol{z}(t)) \boldsymbol{e}_M(\boldsymbol{z}(t)) - \dot{\boldsymbol{z}}(t)) \, dt, \tag{34}$$

defined for $\boldsymbol{z} \in W^{1,\infty}((0,T),\mathbb{R}^2)$. By the discussion following (18), no admissible motion satisfying the maximum dissipation criterion can originate from S, so that E is strictly positive on $\mathcal{A}$. Indeed, as we shall show in the next section,

$$\inf_{\boldsymbol{z}\in\mathcal{A}} E(\boldsymbol{z}) = 0, \tag{35}$$

and the infimum is not attained on $\mathcal{A}$.

THEOREM 2. *Any sequence of admissible polygonals $\{\boldsymbol{z}_k\} \subset \mathcal{A}$ minimizing E (or, equivalently, maximizing the dissipation), i.e., such that*

$$\lim_{k\to+\infty} E(\boldsymbol{z}_k) = 0, \tag{36}$$

converges weak-$*$ in $W^{1,\infty}((0,T),\mathbb{R}^2)$ to the smooth motion $\boldsymbol{\xi}(t)$ on S, whose velocity is (26).

Theorem 2 is the main result of this paper.

References

[1] ARMANO T. AND CERMELLI P., *Non-crystallographic motion of a dislocation as a fine mixture of rectilinear paths*, SIAM J. Applied Mathematics **64** (2004), 2121–2143.

[2] CERMELLI P. AND GURTIN M.E., *The motion of screw dislocations in materials undergoing anti-plane shear: glide, cross-slip, fine cross-slip*, Arch. Rational Mech. Anal., **148** (1) (1999), 3–52.

[3] ESHELBY J.D., *Energy relations and the energy-momentum tensor in continuum mechanics*, in: "Inelastic behavior of solids" (Eds. Kanninen M., Adler W., Rosenfield A. and Jaffee R.), McGraw-Hill, New York 1970, 77–115.

[4] HIRTH J.P. AND LOTHE J., *Theory of dislocations*, McGraw-Hill, New York 1982.

[5] KUHLMANN-WILSDORF D., *Theory of plastic deformation: properties of low energy dislocation structures*, Mater. Sci. Eng. A **113** (1989), 1–41.

[6] PEACH M. AND KÖHLER J.S., *The forces exerted on dislocations and the stress fields produced by them*, Phys. Rev. **80** (3) (1950), 436–439.

[7] PEDREGAL P., *Parametrized measures and variational principles*, Birkhäuser, Basel 1997.

[8] VOLTERRA V., *Sur l'équilibre del corps élastiques multiplement connexes*, Ann. Ec. Norm. **24** (1907), 401–451.

[9] YOUNG L.C., *Lectures on the calculus of variations and optimal control theory*, Saunders, Philadelphia 1969.

AMS Subject Classification: 74B99, 74H15, 65P99, 74E15.

Paolo CERMELLI and Tiziana ARMANO, Department of Mathematics, University of Turin, Via Carlo Alberto 10, 10123, Turin, ITALY
e-mail: paolo.cermelli@unito.it, tiziana.armano@unito.it

Rend. Sem. Mat. Univ. Pol. Torino - Vol. 65, 2 (2007)
ISASUT Intensive Seminar

G. Indelicato*

INEXTENSIBLE NETWORKS WITH BENDING AND TWISTING EFFECTS

Abstract. Families of inextensible fibers forming a surface are considered. Each fiber supports a twisting couple proportional to the torsion of the fiber. The strain energy density is written in an additive form, such that the contributions due to shearing, twisting and bending effects are taken into account separately. The equilibrium equations, here obtained, are a particular case of the ones obtained by Luo and Steigmann in [1].

1. Introduction

We are interested in the theory of inextensible networks, in particular in the case in which a set of inextensible fibers forms a surface with bending stiffness and in which the twisting fiber effects are taken into account, such that we can model the static behaviour of textile fabrics.

In 1986, Wang and Pipkin [5] formulated a theory of inextensible nets with bending stiffness. The resulting continuum theory is a special form of finite-deformation plate theory in which each fiber has a bending couple proportional to its curvature.

In 2001, a theory of bending and twisting effects in three-dimensional deformation of an inextensible network is presented by Luo and Steigmann [1]. They derive the Euler-Lagrange equations and boundary conditions by using the minimum-energy principle. (A simplified version of these equations represents the equilibrium equations obtained by Wang and Pipkin [5].)

The aim of this work consists of finding the equilibrium equations for a net of inextensible fibers taking into account the twist and the bending of fibers. In section 2, we give the constitutive hypotheses. In section 3, we obtain a set of equations where the effect of the twist of the fibers on the deformation of the sheet is exibited. We assume that each fiber in the fabric supports a twisting couple, since we are looking at some expressions which take into account the twist of fibers we assume that each couple is proportional to the torsion of the fiber. In section 4, we focus on the energy of strain for sets of fibers that undergo shear and twist deformations.

2. Inextensible fibers, constitutive hypotheses

We consider two families of inextensible fibers forming a surface that initially lies in a region B of the (x,y)-plane. We assume that initially the first family of fibers, d_1, stays parallel to the x axis and that the second family of fibers, d_2, stays parallel to the y

*This work was supported by the Italian M.U.R.S.T. research project "Modelli matematici per la scienza dei materiali" (Cofin 2002).

axis. We suppose that fibers are continuously distributed so that every line x=constant or y=constant in B is regarded as a fiber. Each fiber is permanently identified by its initial coordinate, x or y. We suppose that cross-sections of each fiber remain plane, suffer no strain, and are normal to the fiber in every configuration (Bernoulli-Euler hypotheses). We denote the position in the current configuration with $\boldsymbol{r}$(x,y), namely the point of the fibers that initially lies in the position (x,y) moves to the place $\boldsymbol{r}$(x,y) in three-dimensional space.

Let

$$\boldsymbol{d}_1 = \frac{\partial \boldsymbol{r}}{\partial x} = \boldsymbol{r}_{,x} \qquad \boldsymbol{d_2} = \frac{\partial \boldsymbol{r}}{\partial y} = \boldsymbol{r}_{,y}$$

be the tangential vectors to the curve occupied by a fiber y=constant and x=constant, respectively, when the sheet is deformed. We postulate that no part of any fiber can change its length in any admissible deformation so the vectors $\boldsymbol{d}_1$ and $\boldsymbol{d}_2$ are unit tangent vectors [3]. Since x and y are the arc length of the d_1 and d_2 lines, Frenet's formulas allow us to attach to each fiber the normal vector $\boldsymbol{n}$ and the binormal vector $\boldsymbol{b}$, so for the fiber d_1 the triad $\{\boldsymbol{d}_1, \boldsymbol{n}_1, \boldsymbol{b}_1\}$ satisfies:

$$\text{(1)} \qquad \begin{cases} \dfrac{\partial \boldsymbol{d}_1}{\partial x} = k_1 \boldsymbol{n}_1 \\ \dfrac{\partial \boldsymbol{n}_1}{\partial x} = -k_1 \boldsymbol{d}_1 + \tau_1 \boldsymbol{b}_1 \\ \dfrac{\partial \boldsymbol{b}_1}{\partial x} = -\tau_1 \boldsymbol{n}_1 \end{cases}$$

with k_1 the curvature of the d_1 line and τ_1 torsion of the d_1 line. Similarly, for the fiber d_2 we introduce the Frenet triad $\{\boldsymbol{d}_2, \boldsymbol{n}_2, \boldsymbol{b}_2\}$.

The sets of fibers d_1 and d_2 are related through the angle of shear γ, that is defined by the relation

$$\sin\gamma = \boldsymbol{d}_1 \cdot \boldsymbol{d}_2$$

this angle describes the local distortion of the sheet. Moreover, we introduce the normal vector:

$$\boldsymbol{N} = \frac{\boldsymbol{d}_1 \times \boldsymbol{d}_2}{|\boldsymbol{d}_1 \times \boldsymbol{d}_2|}.$$

3. Twisting effects

Wang and Pipkin in [5] assume that each fiber in the fabric supports a bending couple proportional to the curvature of the fiber:

$$\boldsymbol{c}_1 = \Gamma \boldsymbol{d}_1 \times \boldsymbol{d}_{1,x} \qquad \boldsymbol{c}_2 = \Gamma \boldsymbol{d}_2 \times \boldsymbol{d}_{2,y}\,.$$

The stiffness coefficient Γ is the same positive constant for all the fibers. They find the following equations:

$$\text{(2)} \qquad \begin{cases} \boldsymbol{t}_1 = T_1 \boldsymbol{d}_1 + S \boldsymbol{d}_2 - \Gamma \boldsymbol{d}_{1,xx} \\ \boldsymbol{t}_2 = T_2 \boldsymbol{d}_2 + S \boldsymbol{d}_1 - \Gamma \boldsymbol{d}_{2,yy} \\ \boldsymbol{t}_{1,x} + \boldsymbol{t}_{2,y} + \boldsymbol{f} = \boldsymbol{0} \end{cases}$$

with: T_1 and T_2 fiber tensions (reactions to the constraints of fiber inextensibility), S the shearing stress, $\boldsymbol{t}_1$ the force per unit length exerted across a d_2-line x=x_0 by the material on the side x>x_0 on the material on the other side (x≤x_0), $\boldsymbol{t}_2$ the force per unit length exerted across a d_1-line y=y_0 by the material on the side y>y_0 on the material on the other side (y≤y_0).
The equations (2) include the effects of couple-stress vectors that account for bending couples in the deformed sheet.

The aim of our work is to find the equations that express the effect of the twist of the fibers on the deformation of the sheet. We assume that each fiber in the fabric supports a twisting couple, since we are looking at expressions which take into account the twist of fibers we assume that each couple is proportional to the torsion, τ_1 or τ_2, of the fiber. Secondly, chosen a set of fibers, say d_1-lines, we want that the vector associated to the couple is directed like the tangent vector $\boldsymbol{d}_1$, consequently we choose the twisting couples:

$$\boldsymbol{i}_1 = \Lambda \boldsymbol{b}_1 \times \boldsymbol{b}_{1,x} \qquad \boldsymbol{i}_2 = \Lambda \boldsymbol{b}_2 \times \boldsymbol{b}_{2,y} \tag{3}$$

with Λ twisting coefficient. Recalling $(1)_3$ we have: $\boldsymbol{i}_1 = \Lambda\tau_1\boldsymbol{d}_1$ and $\boldsymbol{i}_2 = \Lambda\tau_2\boldsymbol{d}_2$.

Taken a directed arc $d\boldsymbol{r} = \boldsymbol{d}_1 dx + \boldsymbol{d}_2 dy$, whose initial length is ds, the force $\boldsymbol{t}ds$ exerted across it is:

$$\boldsymbol{t}ds = \boldsymbol{t}_1 dy - \boldsymbol{t}_2 dx$$

with $\boldsymbol{t}_1$ and $\boldsymbol{t}_2$ the forces defined before. The couple $\boldsymbol{i}$ per unit initial length across a directed arc is given by:

$$\boldsymbol{i}ds = \boldsymbol{i}_1 dy - \boldsymbol{i}_2 dx.$$

For translational equilibrium we have that, for any part of the sheet, the sum of the external forces and of the forces exerted through the boundary lines is null, so the following equation holds:

$$\oint (\boldsymbol{t}_1 dy - \boldsymbol{t}_2 dx) + \int\int \boldsymbol{f} dx dy = \boldsymbol{0} \tag{4}$$

where the area integral is taken over the considered part, the line integral is taken around its perimeter and $\boldsymbol{f}$ is an externally imposed force per unit of initial area that acts on the surface of the sheet.
Equation (4) holds for any part of the sheet, consequentely, if $\boldsymbol{t}_1$ and $\boldsymbol{t}_2$ are smooth, using the divergence theorem we obtain:

$$\boldsymbol{t}_{1,x} + \boldsymbol{t}_{2,y} + \boldsymbol{f} = \boldsymbol{0}. \tag{5}$$

For rotational equilibrium, we have that the moment of the forces exerted on any part of the sheet plus the twisting couples has to be zero:

$$\oint \boldsymbol{r} \times (\boldsymbol{t}_1 dy - \boldsymbol{t}_2 dx) + \int\int \boldsymbol{r} \times \boldsymbol{f} dx dy + \oint (\boldsymbol{i}_1 dy - \boldsymbol{i}_2 dx) = \boldsymbol{0}. \tag{6}$$

The associated differential form is:

$$(\boldsymbol{r} \times \boldsymbol{t}_1 + \boldsymbol{i}_1),_x + (\boldsymbol{r} \times \boldsymbol{t}_2 + \boldsymbol{i}_2),_y + \boldsymbol{r} \times \boldsymbol{f} = \boldsymbol{0}. \tag{7}$$

If (5) is satisfied, then (7) becomes:

$$\boldsymbol{r},_x \times \boldsymbol{t}_1 + \boldsymbol{r},_y \times \boldsymbol{t}_2 + \boldsymbol{i}_{1,x} + \boldsymbol{i}_{2,y} = \boldsymbol{0}. \tag{8}$$

Recalling that $\boldsymbol{d}_1 = \boldsymbol{r},_x \ \boldsymbol{d}_2 = \boldsymbol{r},_y$, using (1) and (3), we find:

$$\boldsymbol{d}_1 \times \boldsymbol{t}_1 + \Lambda\tau_1 k_1 (\boldsymbol{b}_1 \times \boldsymbol{d}_1) + \Lambda(\tau_1),_x \boldsymbol{d}_1 + \boldsymbol{d}_2 \times \boldsymbol{t}_2 + \Lambda\tau_2 k_2 (\boldsymbol{b}_2 \times \boldsymbol{d}_2) + \Lambda(\tau_2),_y \boldsymbol{d}_2 = \boldsymbol{0}. \tag{9}$$

Starting from equation (9), we obtain:

$$\boldsymbol{d}_1 \times [\boldsymbol{t}_1 - \Lambda\tau_1 k_1 \boldsymbol{b}_1] + \Lambda(\tau_1),_x \boldsymbol{d}_1 = -\boldsymbol{d}_2 \times [\boldsymbol{t}_2 - \Lambda\tau_2 k_2 \boldsymbol{b}_2] - \Lambda(\tau_2),_y \boldsymbol{d}_2.$$

If the torsion remains constant along the fibers, for example in the case of helicoidal fibers, $(\tau_1),_x$ and $(\tau_2),_y$ vanish. The equation above reduces to

$$\boldsymbol{d}_1 \times [\boldsymbol{t}_1 - \Lambda\tau_1 k_1 \boldsymbol{b}_1] = [\boldsymbol{t}_2 - \Lambda\tau_2 k_2 \boldsymbol{b}_2] \times \boldsymbol{d}_2$$

where the first member of the equation is orthogonal to $\boldsymbol{d}_1$ and the second member is orthogonal to $\boldsymbol{d}_2$, and since the two member are equal one to the other they have a common value say $D\boldsymbol{d}_1 \times \boldsymbol{d}_2$. Consequentely

$$\boldsymbol{d}_1 \times [\boldsymbol{t}_1 - \Lambda\tau_1 k_1 \boldsymbol{b}_1] = [\boldsymbol{t}_2 - \Lambda\tau_2 k_2 \boldsymbol{b}_2] \times \boldsymbol{d}_2 = D\boldsymbol{d}_1 \times \boldsymbol{d}_2$$

and

$$\boldsymbol{d}_1 \times [\boldsymbol{t}_1 - \Lambda\tau_1 k_1 \boldsymbol{b}_1 - D\boldsymbol{d}_2] = [\boldsymbol{t}_2 - \Lambda\tau_2 k_2 \boldsymbol{b}_2 - D\boldsymbol{d}_1] \times \boldsymbol{d}_2 = \boldsymbol{0}.$$

Hence, the vector $[\boldsymbol{t}_1 - \Lambda\tau_1 k_1 \boldsymbol{b}_1 - D\boldsymbol{d}_2]$ is parallel to $\boldsymbol{d}_1$, say it has a value $V_1\boldsymbol{d}_1$. Similarly, $[\boldsymbol{t}_2 - \Lambda\tau_2 k_2 \boldsymbol{b}_2 - D\boldsymbol{d}_1]$ is parallel to $\boldsymbol{d}_2$, say it has a value $V_2\boldsymbol{d}_2$. Consequently, we find:

$$\begin{cases} \boldsymbol{t}_1 = D\boldsymbol{d}_2 + \Lambda\tau_1 k_1 \boldsymbol{b}_1 + V_1 \boldsymbol{d}_1 \\ \boldsymbol{t}_2 = D\boldsymbol{d}_1 + \Lambda\tau_2 k_2 \boldsymbol{b}_2 + V_2 \boldsymbol{d}_2 \\ \dfrac{\partial}{\partial x}(\tau_1) = 0 \\ \dfrac{\partial}{\partial y}(\tau_2) = 0 \end{cases} \tag{10}$$

4. Strain energy

In the work of Wang and Pipkin [5] the energy of strain W has an additive form:

$$W = W_0(\boldsymbol{d}_1 \cdot \boldsymbol{d}_2) + \frac{1}{2}\Gamma(\boldsymbol{d}_{1,x} \cdot \boldsymbol{d}_{1,x} + \boldsymbol{d}_{2,y} \cdot \boldsymbol{d}_{2,y}). \tag{11}$$

The energy component W_0 is due to the shearing stress, since this stress component is that which resists to the changes in the angle between the fibers d_1 and d_2, they assume that W_0 is a function of $\boldsymbol{d}_1 \cdot \boldsymbol{d}_2$; the second component of the strain energy is associated to bending, it is a quadratic form in the fiber curvatures. Equation (11) can be written in the following explicit form:

$$W = W_0(\sin\gamma) + \frac{1}{2}\Gamma[(k_1)^2 + (k_2)^2]. \tag{12}$$

In [1], Luo and Steigmann assume the strain energy to be a function of shear, of the curvatures k_1, k_2 of the fibers (they denote them by η) and of the twists β_1, β_2 of the fibers. Applying the minimum-energy principle they derive the Euler-Lagrange equations ([1](5.5)) in the form:

$$\begin{cases} \boldsymbol{F}_1 = -\dfrac{\partial}{\partial x}\left(\dfrac{\partial W}{\partial k_1}\boldsymbol{n}_1\right) + \dfrac{\partial W}{\partial \sin\gamma}\boldsymbol{d}_2 + \dfrac{\partial W}{\partial \beta_1}k_1\boldsymbol{b}_1 + T_1\boldsymbol{d}_1 \\ \boldsymbol{F}_2 = -\dfrac{\partial}{\partial y}\left(\dfrac{\partial W}{\partial k_2}\boldsymbol{n}_2\right) + \dfrac{\partial W}{\partial \sin\gamma}\boldsymbol{d}_1 + \dfrac{\partial W}{\partial \beta_2}k_2\boldsymbol{b}_2 + T_2\boldsymbol{d}_2 \\ \dfrac{\partial}{\partial x}\left(\dfrac{\partial W}{\partial \beta_1}\right) = 0 \\ \dfrac{\partial}{\partial y}\left(\dfrac{\partial W}{\partial \beta_2}\right) = 0 \\ \dfrac{\partial \boldsymbol{F}_1}{\partial x} + \dfrac{\partial \boldsymbol{F}_2}{\partial y} + \boldsymbol{f} = \boldsymbol{0} \end{cases} \tag{13}$$

with $\boldsymbol{F}_1$ and $\boldsymbol{F}_2$ the respective forces on cross sections of $\boldsymbol{d}_1$ and $\boldsymbol{d}_2$ lines. Using as special case (12) in (13), they obtain the equations:

$$\begin{cases} \boldsymbol{F}_1 = T_1\boldsymbol{d}_1 + \dfrac{\mathrm{d}\ W_0}{\mathrm{d}\ \sin\gamma}\boldsymbol{d}_2 - \Gamma\boldsymbol{d}_{1,xx} \\ \boldsymbol{F}_2 = T_2\boldsymbol{d}_2 + \dfrac{\mathrm{d}\ W_0}{\mathrm{d}\ \sin\gamma}\boldsymbol{d}_1 - \Gamma\boldsymbol{d}_{2,yy} \\ \dfrac{\partial \boldsymbol{F}_1}{\partial x} + \dfrac{\partial \boldsymbol{F}_2}{\partial y} + \boldsymbol{f} = \boldsymbol{0} \end{cases} \tag{14}$$

that corresponds to the equations (2) and (5) found by Wang and Pipkin.

We are looking at sets of fibers that undergo twist and shear so it is meaningful to consider the deformation energy W per unit of initial area in the form:

$$W = W_0(\boldsymbol{d}_1 \cdot \boldsymbol{d}_2) + \frac{1}{2}\Lambda(\boldsymbol{b}_{1,x} \cdot \boldsymbol{b}_{1,x} + \boldsymbol{b}_{2,y} \cdot \boldsymbol{b}_{2,y})$$

or equivalently, using Frenet formulas and expressing W_0 through the angle of shear:

$$W = W_0(\sin\gamma) + \frac{1}{2}\Lambda[(\tau_1)^2 + (\tau_2)^2]. \tag{15}$$

We recall formulas (2.12) find by Luo [1], which relate the twists β_1, β_2 of the fibers with the torsions τ_1, τ_2:

$$\beta_1 = \tau_1 + \frac{\partial \theta_1}{\partial x} \qquad \beta_2 = \tau_2 + \frac{\partial \theta_2}{\partial y}. \tag{16}$$

in (16), θ_1 is the angle defined by:

$$\begin{cases} \boldsymbol{a}_2 = \cos\theta_1 \boldsymbol{n}_1 + \sin\theta_1 \boldsymbol{b}_1 \\ \boldsymbol{a}_3 = -\sin\theta_1 \boldsymbol{n}_1 + \cos\theta_1 \boldsymbol{b}_1 \end{cases} \tag{17}$$

where $\{\boldsymbol{d}_1, \boldsymbol{a}_2, \boldsymbol{a}_3\}$ is an orthonormal basis. The angle θ_2 is defined in a similar way.

Differentiating with respect to β_1 and β_2, respectively, equations (16) we have:

$$\frac{\partial \tau_1}{\partial \beta_1} = 1 \qquad \frac{\partial \tau_2}{\partial \beta_2} = 1.$$

By mean of (15), equations (13) read:

$$\begin{cases} \boldsymbol{F}_1 = T_1 \boldsymbol{d}_1 + \dfrac{\mathrm{d}\ W_0}{\mathrm{d}\ \sin\gamma} \boldsymbol{d}_2 + \dfrac{\partial W}{\partial \tau_1} \dfrac{\partial \tau_1}{\partial \beta_1} k_1 \boldsymbol{b}_1 \\ \boldsymbol{F}_2 = T_2 \boldsymbol{d}_2 + \dfrac{\mathrm{d}\ W_0}{\mathrm{d}\ \sin\gamma} \boldsymbol{d}_1 + \dfrac{\partial W}{\partial \tau_2} \dfrac{\partial \tau_2}{\partial \beta_2} k_2 \boldsymbol{b}_2 \\ \dfrac{\partial}{\partial x}\left(\dfrac{\partial W}{\partial \beta_2}\right) = \dfrac{\partial}{\partial x}\left(\dfrac{1}{2}\Lambda 2\tau_1\right) = \Lambda \dfrac{\partial}{\partial x}(\tau_1) = 0 \\ \dfrac{\partial}{\partial y}\left(\dfrac{\partial W}{\partial \beta_2}\right) = \dfrac{\partial}{\partial y}\left(\dfrac{1}{2}\Lambda 2\tau_2\right) = \Lambda \dfrac{\partial}{\partial y}(\tau_2) = 0 \\ \dfrac{\partial \boldsymbol{F}_1}{\partial x} + \dfrac{\partial \boldsymbol{F}_2}{\partial y} + \boldsymbol{f} = \boldsymbol{0} \end{cases} \tag{18}$$

since the torsions τ_1 and τ_2 are constant along the respective fibers, we get the final form:

$$\begin{cases} \boldsymbol{F}_1 = T_1 \boldsymbol{d}_1 + \dfrac{\mathrm{d}\ W_0}{\mathrm{d}\ \sin\gamma} \boldsymbol{d}_2 + \Lambda \tau_1 k_1 \boldsymbol{b}_1 \\ \boldsymbol{F}_2 = T_2 \boldsymbol{d}_2 + \dfrac{\mathrm{d}\ W_0}{\mathrm{d}\ \sin\gamma} \boldsymbol{d}_1 + \Lambda \tau_2 k_2 \boldsymbol{b}_2 \\ \Lambda \dfrac{\partial}{\partial x}(\tau_1) = 0 \\ \Lambda \dfrac{\partial}{\partial y}(\tau_2) = 0 \\ \dfrac{\partial \boldsymbol{F}_1}{\partial x} + \dfrac{\partial \boldsymbol{F}_2}{\partial y} + \boldsymbol{f} = \boldsymbol{0} \end{cases} \tag{19}$$

that could be easily compared with equations (5) and (10).

If also the bending effects are considered, the strain-energy function may be written as:

$$W = W_0(\sin\gamma) + \frac{1}{2}\Lambda[(\tau_1)^2 + (\tau_2)^2] + \frac{1}{2}\Gamma[(k_1)^2 + (k_2)^2] \tag{20}$$

the following equations hold:

$$\begin{cases} \boldsymbol{F}_1 = T_1\boldsymbol{d}_1 + \dfrac{\mathrm{d}\ W_0}{\mathrm{d}\ \sin\gamma}\boldsymbol{d}_2 + \Lambda\tau_1 k_1\boldsymbol{b}_1 - \Gamma\boldsymbol{d}_{1,xx} \\ \boldsymbol{F}_2 = T_2\boldsymbol{d}_2 + \dfrac{\mathrm{d}\ W_0}{\mathrm{d}\ \sin\gamma}\boldsymbol{d}_1 + \Lambda\tau_2 k_2\boldsymbol{b}_2 - \Gamma\boldsymbol{d}_{2,yy} \\ \Lambda\dfrac{\partial}{\partial x}(\tau_1) = 0 \\ \Lambda\dfrac{\partial}{\partial y}(\tau_2) = 0 \\ \dfrac{\partial\boldsymbol{F}_1}{\partial x} + \dfrac{\partial\boldsymbol{F}_2}{\partial y} + \boldsymbol{f} = \boldsymbol{0} \end{cases} \tag{21}$$

or equivalently

$$\begin{cases} \boldsymbol{F}_1 = (T_1 + \Gamma(k_1)^2)\boldsymbol{d}_1 + \dfrac{\mathrm{d}\ W_0}{\mathrm{d}\ \sin\gamma}\boldsymbol{d}_2 + (\Lambda - \Gamma)\tau_1 k_1\boldsymbol{b}_1 - \Gamma k_{1,x}\,\boldsymbol{n}_1 \\ \boldsymbol{F}_2 = (T_2 + \Gamma(k_2)^2)\boldsymbol{d}_2 + \dfrac{\mathrm{d}\ W_0}{\mathrm{d}\ \sin\gamma}\boldsymbol{d}_1 + (\Lambda - \Gamma)\tau_2 k_2\boldsymbol{b}_2 - \Gamma k_{2,y}\,\boldsymbol{n}_2 \\ \Lambda\dfrac{\partial}{\partial x}(\tau_1) = 0 \\ \Lambda\dfrac{\partial}{\partial y}(\tau_2) = 0 \\ \dfrac{\partial\boldsymbol{F}_1}{\partial x} + \dfrac{\partial\boldsymbol{F}_2}{\partial y} + \boldsymbol{f} = \boldsymbol{0}. \end{cases} \tag{22}$$

Equations (22) describe the mechanical behaviour of sets of inextensible fibers forming a surface when shearing, twisting and bending effects are taken into account, such that some elementary modes of the behaviours of woven fabric, where the fibers are the weft and the warp, can be exhibited.

5. Conclusions

An overwiev on the works of Wang and Pipkin [5] and of Luo and Steigmann [1] has been given. A first model that describes a fabric formed by inextensible fibers has been found. In this model, both shear and twist are considered. The balance equations are expressed through the torsions τ_1, τ_2 and the curvatures k_1, k_2 of the d_1, d_2 families of fibers. Strain energy for sets of fibers that undergo shear, twist and bending has been given in a suitable explicit form.

The results presented in this paper represent a first step of my research, whose main purpose is to develop a model for textile fabrics within the framework of Cosserat shell theory, where the shell itself is made of two families of Cosserat rods, namely the weft and the warp of the fabric. This model would encompass more refined phenomena, typical of fabrics, such as wrinkles and krinkles.

References

[1] LUO C. AND STEIGMANN D.J., *Bending and twisting effects in the three-dimentional finite deformations of an inextensible network, Advances in the mechanics of plates and shells*, Kluwer 2001, 213–228.

[2] PIPKIN A.C., *Continuously distributed wrinkles in fabrics*, Arch. Rat. Mech. Anal. **95** (1986), 93–115.

[3] PIPKIN A.C., *Some developments in the theory of inextensible networks*, Quart. Appl. Math. **38** (1980), 343–355.

[4] RIVLIN R.S., *Plane strain of a net formed by inextensible cords*, Arch. Rat. Mech. Anal. **4** (1955), 951–974.

[5] WANG W.B. AND PIPKIN A.C., *Inextensible networks with bending stiffness*, Q. J. Mech. Appl. Math. **39** (1986), 434–459.

AMS Subject Classification: 74K10, 74K25, 74E22.

Giuliana INDELICATO, Università degli studi di Torino, Dipartimento di Matematica, Via Carlo Alberto 10, 10023 Torino, ITALY
e-mail: giuliana.indelicato@unito.it

Rend. Sem. Mat. Univ. Pol. Torino - Vol. 65, 2 (2007)
ISASUT Intensive Seminar

F. Pastrone*

MICROSTRUCTURES AND GRANULAR MEDIA

Abstract. A general model of solids with vectorial microstructures is introduced. The field equationsare the obtained as Euler-Lagrange equations of a suitable energetic functional. The Cosserat model is encompassed in this model and it can be used to study the behaviour of granular media. A first approach to this problem deals with a two dimensional model, since in such a case the field equations have a simpler form, the rotation of the single grain depends on one parameter only, the angle of rotation, but the model is still physically meaningful. In order to obtain constitutive equations rigorously deduced from the principles of Continuum Mechanics, we must take in account both the interaction matrix-grains and grain-grain. As a first step, we deal with linear dissipation, as already done in general for vector microstructures, such that we can also study some simpler problems of wave propagation.

Key words : Microstructures, Cosserat solids, granular media.

1. Introduction

A wide class of phenomena can be described by means of microstructural models of solids and fluids, where the microstructure can be described by vector fields over the body. In principle, there are no restrictions on the number of vector fields, which are unknown variables of the problem, but there are obvious restrictions due to the possible physical meaning of each vector field.

The use of the Cosserat continuum theory to describe the behaviour of granular materials or powders has been proposed in several papers (see, for instance, Grekova [7] and references therein quoted). Basically we refer to [14], but we follow a different approach, in the framework of a general theory of microstructures as developed by Capriz [1], Maugin [8]. In particular we deal with a so-called vector micro- structure, which includes the Cosserat theory. These theory has already been used with some success by Pastrone and others [2, 3, 4, 10, 11, 12] to study wave propagation in one and three-dimensional microstructured solids.

In Section 2, the three dimensional Cosserat model is introduced. A Cosserat microstructure is defined by a triple vector field $\{\mathbf{d}_i\}$, such that $\mathbf{d}_i \cdot \mathbf{d}_j = \delta_{ij}$. The vector fields $\mathbf{d}_i = \mathbf{d}_i(X^h, t)$ are often called "directors", where X^h's are the Lagrangian coordinates of a point $\mathbf{X}$ in a reference configuration of the body which represents the grain, and t is time. The main feature of such a microstructure is its rotation, which is expressed through an angular velocity vector and a "spatial" spin tensor. The basic equations of motion in the three-dimensional case are derived via a variational principle. In fact, we assume the existence of a strain energy function and we take in account the dissipation by means of the expression of the total power expended.

*This work was supported by the Italian M.U.R.S.T. research project "Modelli matematici per la scienza dei materiali" (Cofin 2002).

The case of a plane Cosserat solid is introduced in Section 3, which can be used to model plane granular media. By this way, the model is much more simplified since we restrict our attention to a two-dimensional plane body. The rotation is fullydescribed by a scalar function $\theta = \theta(X^h, t)$ and the field equations reduce to four differential equations. Some interesting identities are derived, such that wecan easily compare our model with

that one introduced by [14] ina general contest and used by [7], but we do not neglect thecoupled-stress. On the other side, we prove that the stress tensor is not symmetric (as natural in such models) and its skew symmetric part is related to the micro body force. Finally, alternative forms of the field equations are provided.

In Section 4, we make a first step toward the introduction of appropriate constitutive equations, taking into account the friction among particles and describing this phenomenological aspect through a dissipation function whose explicit form is suggested by the total power expended in any motion. A simple example, obtained after further simplifications on the dissipation function, is provided, but the problem of a correct constitutive theory for such models is not solved and it will be the main subject of further researches.

2. Vectorial microstructures

The usual approach to microstructure is assumed to be that one introduced by Mindlin [9], where the model is the linear theory of elasticity. We follow his basic ideas for the kinematics, but in the general framework of non linear elasticity, both in the macro and in the micro-structure. We will obtain a model which could be, somehow, encompassed in the model of Capriz, even thought it is not a straightforward procedure.

Let $\mathcal{B}$ be the body, as a manifold embedded in a 3-dimensional affine space, $\mathbf{X}$ a point of this body in its reference configuration C^*, and $\mathbf{x}$ the corresponding point in the actual configuration C. As usual, the displacement is given by the vector function

$$\mathbf{u} \equiv \mathbf{x} - \mathbf{X} \tag{2.1}$$

and, assuming the coordinates X^h of $\mathbf{X}$ as material coordinates, for any motion it will be: $\mathbf{u} = \mathbf{u}(X^h, t)$, since $\mathbf{x} = f(\mathbf{X}, t)$, where f is the deformation function ($f : C^* \to C$).

The macrostructure is a three-dimensional body $\mathcal{B}$, and it can be equivalently be described by a position vector, from some fixed origin $\mathbf{o}$, $\mathbf{r} \equiv \mathbf{x} - \mathbf{o}$, $\mathbf{r} = \mathbf{r}(X^h, t)$ where the X^h's are material coordinates and t is time. Commas denote partial derivatives with respect to X^h and superposed dots denote partial derivatives with respect to time, e.g.:

$$\mathbf{r}_{,h} \equiv \frac{\partial \mathbf{r}}{\partial X^h}, \qquad \dot{\mathbf{r}} \equiv \frac{\partial \mathbf{r}}{\partial t}$$

By microstructure we mean that it is possible to apply a microscope to each point $\mathbf{x} \in C$ and discover a "small world". As shown elsewhere([10]), some features of this "small world" can be captured by a suitable set of vectors $\mathbf{d}_H = \mathbf{d}_H(\mathbf{X}, t)$,

$H = 1, 2, ..., n$, which can be called "directors" and represent the micromotion. Their number depends on the physical aspects we want to describe, In the present case, we can reduce this number to three or less, hence we shall use the same lower case indices as for coordinates: $\mathbf{d}_i = \mathbf{d}_i(\mathbf{X}, t)$, $i = 1, 2, 3$.

The kinetic energy density of the body is defined as a quadratic form in the velocities $\dot{\mathbf{r}}$ and $\dot{\mathbf{d}}_i$:

$$T = \frac{1}{2}[\rho(X^h)\dot{\mathbf{r}} \cdot \dot{\mathbf{r}} + 2\rho^i(X^h)\dot{\mathbf{r}} \cdot \dot{\mathbf{d}}_i + \rho^{ij}\dot{\mathbf{d}}_i \cdot \dot{\mathbf{d}}_j]. \tag{2.2}$$

In Eq. (2.2), ρ is the usual three dimensional mass density, ρ^i and ρ^{ij} are coefficients including density and inertia terms, which must satisfy the conditions:

$$T \geq 0, \quad T = 0 \Leftrightarrow \dot{\mathbf{r}} = \dot{\mathbf{d}}_i \equiv 0.$$

As it is well-known, it is always possible to diagonalize the form making linear transformations on $\mathbf{r}$ and $\mathbf{d}_i$, such that

$$\rho^i = 0, \rho^{ij} = \rho I^{ij};$$

the I^{ij}'s are effective inertia terms of the microstructure.

We assign a strain energy density function

$$\hat{W} = W(\mathbf{r}_{,i}\,; \mathbf{d}_j; \mathbf{d}_{j,h}; X^h) + W_b \tag{2.3}$$

whose existence follows from the assumption that the total power expended P_T is given by $P_{\hat{W}} = \mathrm{d}\hat{W}/\mathrm{d}t$ and the total energy is given by

$$E = \int_{\mathcal{B}} (T - W)\rho \,\mathrm{d}X^1\mathrm{d}X^2\mathrm{d}X^3 - \int_{\mathcal{B}} W_b\rho \,\mathrm{d}X^1\mathrm{d}X^2\mathrm{d}X^3 \tag{2.4}$$

where W_b is the potential of the external body forces, which depends on $\mathbf{r}$ and X^h only. We avoid internal constraints and leave apart the problem of the boundary conditions.

The equations of motion can be derived as the Euler-Lagrange equations of the energy functional $\varepsilon = \int_{t_0}^{t_1} E\,\mathrm{d}t$:

$$\begin{cases} \left(\dfrac{\partial W}{\partial \mathbf{r}_{,i}}\right)_{,i} - \dfrac{\partial W_b}{\partial \mathbf{r}} = \dfrac{\mathrm{d}}{\mathrm{d}t}\dfrac{\partial T}{\partial \dot{\mathbf{r}}} \\ \left(\dfrac{\partial W}{\partial \mathbf{d}_{j,i}}\right)_{,i} - \dfrac{\partial W}{\partial \mathbf{d}_j} = \dfrac{\mathrm{d}}{\mathrm{d}t}\dfrac{\partial T}{\partial \dot{\mathbf{d}}_j} \end{cases} \tag{2.5}$$

Since the microstructure can have a dissipative effect, we introduce dissipation in the field equations Eqs. (2.5). The deformation velocities are given by

$$\dot{\mathbf{r}} = \frac{\partial \mathbf{r}}{\partial t}, \ \dot{\mathbf{r}}_{,i} = \frac{\partial \mathbf{r}_{,i}}{\partial t}, \ \dot{\mathbf{d}}_i = \frac{\partial \mathbf{d}_i}{\partial t}, \ \dot{\mathbf{d}}_{i,j} = \frac{\partial \mathbf{d}_{i,j}}{\partial t}. \tag{2.6}$$

The total power expended is the sum of scalar products as it follows:

$$P_T = \mathbf{b}\cdot\dot{\mathbf{r}} + \sum_i \boldsymbol{\sigma}_i \cdot \dot{\mathbf{r}}_{,i} + \sum_i \boldsymbol{\tau}_i \cdot \dot{\mathbf{d}}_i + \sum_{ij} \boldsymbol{\eta}_{ij} \cdot \dot{\mathbf{d}}_{i,j}\,, \tag{2.7}$$

The quantities $\mathbf{b}$, $\boldsymbol{\sigma}_i$, $\boldsymbol{\tau}_i$, $\boldsymbol{\eta}_{ij}$ are forces, stresses and generalized (or coupled) stresses.

We can split the "conservative" part from the dissipation by means of the decomposition:

$$P_T = P_{\hat{W}} + P_D = \frac{\mathrm{d}\hat{W}}{\mathrm{d}t} + P_D \tag{2.8}$$

where $P_D = \hat{\mathbf{b}}\cdot\dot{\mathbf{r}} + \sum_i \hat{\boldsymbol{\sigma}}_i \cdot \dot{\mathbf{r}}_{,i} + \sum_i \hat{\boldsymbol{\tau}}_i \cdot \dot{\mathbf{d}}_i + \sum_i \hat{\boldsymbol{\eta}}_{ij} \cdot \dot{\mathbf{d}}_{i,j}$, the hat meaning that we deal with the dissipative part of the stresses, or the so-called non-equilibrium stresses. The dissipation implies $P_D > 0$ for any admissible deformation, hence the non-equilibrium stresses cannot be arbitrary, but they must satisfy this inequality.

Finally the stresses can be written in the additive form

$$\begin{cases} \mathbf{b} &= -\dfrac{\partial W_b}{\partial \mathbf{r}} + \hat{\mathbf{b}} \\ \boldsymbol{\sigma}_i &= \dfrac{\partial W}{\partial \mathbf{r}_{,i}} + \hat{\boldsymbol{\sigma}}_i \\ \boldsymbol{\tau}_i &= -\dfrac{\partial W}{\partial \mathbf{d}_i} + \hat{\boldsymbol{\tau}}_i \\ \boldsymbol{\eta}_{ij} &= \dfrac{\partial W}{\partial \mathbf{d}_{i,j}} + \hat{\boldsymbol{\eta}}_{ij} \end{cases} \tag{2.9}$$

and the field equations read

$$\begin{cases} \boldsymbol{\sigma}_{i,i} + \mathbf{b} &= \dfrac{\mathrm{d}}{\mathrm{d}t}\dfrac{\partial T}{\partial \dot{\mathbf{r}}} \\ \boldsymbol{\eta}_{ij,j} + \boldsymbol{\tau}_i &= \dfrac{\mathrm{d}}{\mathrm{d}t}\dfrac{\partial T}{\partial \dot{\mathbf{d}}_i} \end{cases} \tag{2.10}$$

which obviously include (2.5). In many cases the body forces are neglected, hence $\mathbf{b} = \mathbf{0}$ and the microbody force included in $\boldsymbol{\tau}_i$ vanishes as well, but $\boldsymbol{\tau}_i \neq 0$, because the coupling part remains.

3. 3-D Cosserat solids

Let us introduce Cosserat solids as a particular model of vectorial microstructure and obviously it can encompass Cosserat shells and rods as well. In Cosserat models the microstructure is described by a rigid triad $\{\mathbf{d}_i\}$, which is attached to each particle of the body. It means that one must add to our field equations (2.5) the constraint equations:

$$\mathbf{d}_i \cdot \mathbf{d}_j = \delta_{ij}. \tag{3.1}$$

Formally we can apply the Lagrange multipliers method to the energy functional

$$\mathcal{E} = \int_{\mathcal{B}} \left[W + \Lambda^{ij} (\mathbf{d}_i \cdot \mathbf{d}_j - \delta_{ij}) + T \right] \mathrm{d}\mathcal{B} \tag{3.2}$$

and easily derive the equations of motion as a determined set of partial differential equations

$$\begin{cases} \left(\dfrac{\partial W}{\partial \mathbf{r}_{,i}} \right)_{,i} - \dfrac{\partial W_b}{\partial \mathbf{r}} = \dfrac{\mathrm{d}}{\mathrm{d}t} \dfrac{\partial T}{\partial \dot{\mathbf{r}}} \\ \left(\dfrac{\partial W}{\partial \mathbf{d}_{j,i}} \right)_{,i} - \dfrac{\partial W}{\partial \mathbf{d}_j} = \dfrac{\mathrm{d}}{\mathrm{d}t} \dfrac{\partial T}{\partial \dot{\mathbf{d}}_j} - 2\Lambda^{ij} \mathbf{d}_i \\ \mathbf{d}_i \cdot \mathbf{d}_j = \delta_{ij} \end{cases} \tag{3.3}$$

Moreover they contain the constraint reactions (namely, the Lagrange multipliers) while the main interest here is to obtain equations of motion free of reactions, sufficient to determine the motion.

This goal can be attained following an intrinsic approach, by means of the angular velocity $\boldsymbol{\omega}$ such that

$$\dot{\mathbf{d}}_i = \boldsymbol{\omega} \times \mathbf{d}_i \tag{3.4}$$

(since we deal with a rigid microstructure), with

$$\boldsymbol{\omega} = \boldsymbol{\omega}(q^i, \dot{q}^i, t), \;\; q^i = q^i(X^h, t) \tag{3.5}$$

being suitable measures of the rotations in an affine three-dimensional E_3 (i.e., Euler angles), and a "spatial spin" $\Omega \in Lin$ such that

$$\mathbf{d}_{i,h} = \varepsilon^k_{ij} \, \Omega^j_h \mathbf{d}_k \tag{3.6}$$

where ε^h_{ij} is the Levi-Civita symbol, and $\Omega = \Omega(q^i, q^i{}_{,h}, t)$.
Henceforth, we can write

$$\begin{cases} W = W(\mathbf{r}_{,i}, \Omega, x^h) \\ T = T(\dot{\mathbf{r}}, \boldsymbol{\omega}) \end{cases} \tag{3.7}$$

where T is a quadratic form in the variables $\dot{\mathbf{r}}$ and $\dot{q}^i$.
At this point we have to apply the usual variational techniques to the functional

$$\mathcal{E} = \int_{\mathcal{B}} \left[W(\mathbf{r}_i, \Omega, X^h) + T(\dot{\mathbf{r}}, \boldsymbol{\omega}) \right] \mathrm{d}\mathcal{B}. \tag{3.8}$$

The Lagrange equations are $(3.3)_1$ and

$$\partial_i W - \partial_h \partial^h_i W + \partial_i T - \frac{\mathrm{d}}{\mathrm{d}t} \frac{\partial T}{\partial \dot{q}^i} = 0 \tag{3.9}$$

where

$$\partial_i W = \frac{\partial W}{\partial \Omega}\frac{\partial \Omega}{\partial q^i},\ \partial_i T = \frac{\partial T}{\partial \boldsymbol{\omega}}\frac{\partial \boldsymbol{\omega}}{\partial q^i},\ \partial_h \partial_i^h W = \frac{\partial}{\partial X^h}\frac{\partial W}{\partial q^i_{,h}} = \frac{\partial}{\partial X^h}\frac{\partial W}{\partial \Omega}\frac{\partial \Omega}{\partial q^i_{,h}}.$$

If we introduce

$$W_\Omega \equiv \frac{\partial W}{\partial \Omega},\ T_\omega \equiv \frac{\partial T}{\partial \omega}$$

the equations of Cosserat microstructure can be written as

$$\left\{\begin{array}{lcl} \left(\dfrac{\partial W}{\partial \mathbf{r}_{,i}}\right)_{,i} - \dfrac{\partial W_b}{\partial \mathbf{r}} & = & \dfrac{\mathrm{d}}{\mathrm{d}t}\dfrac{\partial T}{\partial \dot{\mathbf{r}}} \\ \left(W_\Omega \dfrac{\partial \Omega}{\partial q^i_{,h}}\right)_{,h} - W_\Omega \dfrac{\partial \Omega}{\partial q^i} & = & \dfrac{\mathrm{d}}{\mathrm{d}t}\left(T_\omega \dfrac{\partial \omega}{\partial \dot{q}^i}\right) - T_\omega \dfrac{\partial \omega}{\partial q^i} \end{array}\right. \tag{3.10}$$

An open problem is to write the (known) explicit expression of $\boldsymbol{\omega}$ in terms of the q^i and $\dot{q}^i$ and the explicit expressions of the spin in terms of the q^i, $q^i{}_{,h}$, hence to write down explicit forms of of the strain energy funtions, such that the field equations become suitable and useful both to obtain analytical results and for applications.

4. 2-D Cosserat solids and plane granular media

If the body is a 2-D solid and its configuration at any time is a domain contained in R^2, we can choose an orthonormal spatial basis $\{\mathbf{e}_h\}$, h = 1,2 and a material basis $\{\mathbf{g}_h\}$, where $\mathbf{g}_h = \mathbf{r}_{,h}$, hence write $\mathbf{r} = x^h(X^k, t)\mathbf{e}_h$; the functions $x^h(X^k, t)$ have the meaning of deformation function components.

The director fields can be reduced to one vector field $\mathbf{d} = \mathbf{d}(X^k, t)$, $\mathbf{d}\cdot\mathbf{d} = 1$, because one director is sufficient to define the orientation of any particle (grain). In the spatial basis it is: $\mathbf{d} = \cos\theta\mathbf{e}_1 + \sin\theta\mathbf{e}_2$, $\theta = \theta(X^k, t)$ being the angle of rotation of the particle with respect to the fixed basis. Physically, we interpret $\mathbf{d}$ as the kinematical characterization of the grain and it is fully determined by the scalar function $\theta(X^k, t)$. If we introduce the unit vector $\boldsymbol{\nu} = -\sin\theta\mathbf{e}_1 + \cos\theta\mathbf{e}_2$, $\boldsymbol{\nu}\cdot\mathbf{d} = 1$, the time and spatial derivatives of the director are given by:

$$\dot{\mathbf{d}} = \boldsymbol{\omega}\times\mathbf{d} = \dot{\theta}\boldsymbol{\nu},\quad \mathbf{d}_{,h} = \boldsymbol{\Omega}_h\times\mathbf{d} = \theta_{,h}\boldsymbol{\nu},$$

where $\boldsymbol{\omega} = 1/2\dot{\mathbf{d}}\times\mathbf{d}$, $\boldsymbol{\Omega}_h = 1/2\mathbf{d}_{,h}\times\mathbf{d}$. The kinetic energy density becomes

$$T = \frac{1}{2}[\rho\dot{\mathbf{r}}\cdot\dot{\mathbf{r}} + 2J\dot{\mathbf{r}}\cdot\dot{\mathbf{d}} + I\dot{\theta}^2] \tag{4.1}$$

where $\rho = \rho(X^h)$ is the density in a reference configuration, $I = I(X^h)$ the inertia term of the grain, J a coupled inertia term that vanishes if we reduce T to a diagonal form, as always possible. The strain energy density becomes

$$W = W(x^h{}_{,k}\,;\theta;\theta_{,k}\,;t) \tag{4.2}$$

while it is convenient to split the potential of the body forces in two parts

$$W_b = W_b^{Macro}(x^h, t) + W_b^{micro}(\theta, t) \tag{4.3}$$

such that the total potential energy density is given by

$$\hat{W} = W + W_b^{Macro} + W_b^{micro}, \tag{4.4}$$

the total energy of the body by

$$E = \int_A (T - \hat{W})\rho \mathrm{d}X^1 \mathrm{d}X^2 \tag{4.5}$$

where A is the domain in $\mathbb{R}^2$ occupied by the reference configuration.

The field equations now read

$$\begin{cases} \left(\dfrac{\partial W}{\partial x^h{}_{,i}}\right)_{,\,i} - \dfrac{\partial W_b^{Macro}}{\partial x^h} & = \dfrac{\mathrm{d}}{\mathrm{d}t}\dfrac{\partial T}{\partial \dot{x}^h} = \rho \ddot{x}^h \\ \left(\dfrac{\partial W}{\partial \theta_{,i}}\right)_{,\,i} - \dfrac{\partial W}{\partial \theta} - \dfrac{\partial W_b^{micro}}{\partial \theta} & = \dfrac{\mathrm{d}}{\mathrm{d}t}\dfrac{\partial T}{\partial \dot{\theta}} = I\ddot{\theta} \end{cases} \tag{4.6}$$

In Eq. (4.6) we used the diagonal form for the kinetic energy

$$T = \frac{1}{2}[\rho \delta_{ij} \dot{x}^i \dot{x}^j + I\dot{\theta}^2] \tag{4.7}$$

The power expended for any motion

$$P = \frac{\partial \hat{W}}{\partial x^h}\dot{x}^h + \frac{\partial \hat{W}}{\partial x^h{}_{,k}}\dot{x}^h{}_{,k} + \frac{\partial \hat{W}}{\partial \theta}\dot{\theta} + \frac{\partial \hat{W}}{\partial \theta_{,h}}\dot{\theta}_{,h} \tag{4.8}$$

suggests us how to introduce the macro and micro stresses

$$\sigma_k^h = \frac{\partial \hat{W}}{\partial x^k{}_{,h}},\ \eta^h = \frac{\partial \hat{W}}{\partial \theta_{,h}},\ \tau = \frac{\partial \hat{W}}{\partial \theta} \tag{4.9}$$

and the macro and micro body forces

$$B_h = \rho \frac{\partial W_b^{Macro}}{\partial x^h},\ b = \rho \frac{\partial W_b^{micro}}{\partial \theta} \tag{4.10}$$

which we refer to intrinsically as $\{\sigma, \boldsymbol{\eta}, \tau, \mathbf{B}, b\}$. Hence the field equations read

$$\begin{cases} \rho \ddot{\mathbf{u}} = \mathrm{Div}\sigma + \rho \mathbf{B} \\ I\ddot{\theta} = \mathrm{Div}\boldsymbol{\eta} - \tau + \rho b \end{cases} \tag{4.11}$$

5. The constitutive equations

The system in Eq. (4.6), or alternatively Eqs. (4.11), must be completed with proper constitutive equations, which allow us to describe the behaviour of some real material. If we want to model the behaviour of granular media, we must take into account the friction among grains, which are described kinematically and dynamically as Cosserat microstructures. One way to describe this kind of friction is to make use of the theory of viscosity or, equally, to introduce some dissipation, that means we assume a dependence of the constitutive functions on the velocity of deformation also. Moreover, from a phenomenological point of view we must consider that the rotation of a single grain makes the other neighbouring grains to rotate, not in the same sense: usually, because of friction, if a grain rotates clockwise, another grain in contact with it rotates counter-clockwise. This problem has been faced by [7], using a different approach.

The form of the total power expended, where we must take into account both the conservative and dissipative parts of the stresses, can suggest the choice of the dissipation function. Hence, we assume again that the stresses are "split" in an additive way, so we can write:

$$P_T = P_{\hat{W}} + P_D = \frac{\mathrm{d}\hat{W}}{\mathrm{d}t} + \sigma_D \cdot \mathrm{L} + \boldsymbol{\eta}_D \cdot \dot{\mathbf{G}} + \tau_D \dot{\theta} \tag{5.1}$$

where L is the gradient of the macro velocity, $\dot{\mathbf{G}}$ the gradient of the micro velocity. In Eq. (5.1) σ_D, $\boldsymbol{\eta}_D$, τ_D are the dissipative parts of stress and forces (or, as said above, the non-equilibrium stresses and forces). They must satisfy the dissipation inequality

$$P_D = \sigma_D \cdot \mathrm{L} + \boldsymbol{\eta}_D \cdot \dot{\mathbf{G}} + \tau_D \dot{\theta} > 0 \tag{5.2}$$

for any admissible motion.

The simplest meaningful assumption we can use on the dissipation is that $\sigma_D \cdot \mathrm{L} + \boldsymbol{\eta}_D \cdot \dot{\mathbf{G}} = 0$ and $\tau_D = D$, such that $P_D = D\dot{\theta}$ and $D = D(X^i, t)$.

Finally, the simpler form of the field equations for a granular plane body, with friction among grains, is given by

$$\begin{cases} \rho \ddot{x}^h = \left(\dfrac{\partial W}{\partial x^h{}_{,i}} \right)_{,\,i} + \rho B^h \\ \\ I\ddot{\theta} = \left(\dfrac{\partial W}{\partial \theta_{,i}} \right)_{,\,i} - \dfrac{\partial W}{\partial \theta} - D\dot{\theta} + \rho b \end{cases} \tag{5.3}$$

Obviously, one can imagine more complicated situations, for instance that the dissipation is given by non linear relations or by a functional in the velocities of deformation, but this model, extremely simple, allows us to claim that it is not necessary to neglect the couple stress, as assumed in [7].

The different equations of motions here obtained allow us to study problems of equilibrium, stability, wave propagation. With regard to wave propagation, some

results have been obtained in [2, 3, 4, 5, 10, 11, 12, 13], mainly in one-dimensional solids with scalar microstructure, with non linearity, dispersion and dissipation. The possibility of propagation of solitary waves has been proved, as well as the possibility of decay and/or amplification of the amplitude.

References

[1] CAPRIZ G., *Continua with microstructure*, Springer Tracts Nat. Phil. **35**, Springer Verlag, Berlin, New York 1989.

[2] CERMELLI P. AND PASTRONE F., *Growth and decay of waves in microstructured solids*, Proc. Estonian Acad. Sci. Phys. Math. **46** (1-2) (1997), 32-40.

[3] CERMELLI P. AND PASTRONE F., *Exchange of energy between the macro- and micro-structure*, in: "Mesomechanics 2000, vol.I" (Ed. Sih G.C.), Tsinghua univ. Press, Beijing 2000, 201–208.

[4] ENGELBRECHT J. AND PASTRONE F., *Waves in microstructured solids with nonlinearities in microscale*, Proc. Estonian Acad. Sci. Phys. Math. **52** (1-2) (2003).

[5] ENGELBRECHT J., CERMELLI P. AND PASTRONE F., *Wave hierarchy in microstructured solids*, in "Geometry, continua and microstructure" (Ed. Maugin G.), Hermann Publ. 1997, 99–111.

[6] ERICKSEN J.L., *Simpler static problems in nonlinear theories of rods*, Int. J. Solids Structures **6** (1970), 371–377.

[7] GREKOVA E.F., *Semi-phenomenological model of dissipative interactions in a polar medium: applications to powders and grains*, in "Proc. of XXIX APM Summer School, Repino, Russia, 21/30 June 2001", (Ed. Ideitsev D.A.), IPME RAS, St. Petersburg 2002, 254–262.

[8] MAUGIN G.A., *Nonlinear wave mechanics in complex material systems*, Proc. Est. Acad. Sci. **52** (1-2) (2003).

[9] MINDLIN R.D. *Microstructure in linear elasticity*, Arch. Rat. Mech. Anal. **1** (1964), 51–78.

[10] PASTRONE F. *Waves in solids with vectorial microstructures*, Proc. Est. Acad. Sci. **52** (1-2) (2003), 21–29.

[11] PASTRONE F. AND PORUBOV A.V. *Influence of microstructures on the evolution of nonlinear strain waves*, in: "International symposium of multiscaling in mechanics", (Eds. Messini, Sih G.C. and Spyropoulos C.P.), National Technical University of Athens Press, Athens 2002, 102–109.

[12] PORUBOV A.V. AND PASTRONE F., *Non-linear bell-shaped and kink-shaped strain waves in microstructured solids*, Int. J. of Non-Linear Mech. **39** (2004), 1289–1299.

[13] PORUBOV A.V., PASTRONE F. AND MAUGIN G.A., *Selection d'ondes de déformation non linéaires à deux dimensions dans des milieux à microstructure*, C. R. Acad. Sc. Paris Ser. I **337** (7) (2004), 513–518.

[14] SUIKER A.S.J., DE BORST R. AND CHANG C.S., *Micro-mechanical modeling of granular material*, Acta Mechanica **149** (2001), 161.

AMS Subject Classification: 74A30, 74B20, 74E20.

Franco PASTRONE, Department of Mathematics, University of Torino, Via C. Alberto 10, 10123 Torino, ITALY
e-mail: franco.pastrone@unito.it

Rend. Sem. Mat. Univ. Pol. Torino - Vol. 65, 2 (2007)
ISASUT Intensive Seminar

A.V. Porubov

ON FORMATION OF THE ROGUE WAVES AND HOLES IN OCEAN

Abstract. Two-dimensional nonlinear models are developed to account for abnormal surface ocean waves generation and propagation. These models are based on the Kadomtsev-Petviashvili equation, the 2D Benjamin-Ono equation and the 2D Gardner equation. Possible mechanisms of the waves formation suggested are the resonant interaction between semi-plane waves or waves with curved fronts or the transverse instability of a plane surface wave.

1. Introduction

This paper intends to consider some models describing sea waves of abnormally high amplitude, or the so-called rogue (or freak) waves [1, 2]. Observations of the rogue waves and various accidents with the ships in ocean caused by their attacks require a development of the theory of the rogue waves and understanding the mechanisms of the rogue waves formation. What is really dangerous that the rogue waves suddenly affect the ships even in the absence of a storm, and the crew cannot see these waves far from the vessel. Despite numerous works done by now [1, 2, 3, 4], many features of the waves remain unclear.

As a rule, rogue waves are considered as elevation free surface waves [2]. However, recently abnormal waves with negative amplitude were observed in the ocean [5, 6]. Certainly these wave are even more dangerous for a vessel than the elevation rogue waves, since their detection is unlikely either by eyes nor by a locator. The amplitude of the rogue wave may exceed 10 meters, hence, more likely, it is nonlinear wave. There is no common point of view what kind of wave is it, long or short [2]. Estimations done on the basis of some observations of both the elevation waves [7] and the deep holes [8] allow us to consider the rogue wave as a long non-linear wave.

In this paper, main attention is paid to the mathematical models. Their detailed physical justification may be found in our recent papers [7, 8]. Among the model equations employed are the Kadomtsev-Petviashvili (KP) equation, the 2D Benjamin-Ono equation and the 2D Gardner equation. The localization of an initial wave is suggested as a possible mechanism of the rogue wave generation. Localization of the wave is accompanied by an increase in its amplitude. In the two-dimensional case, localization may happen both along the direction of the wave propagation (plane localized wave) and in the plane where the wave evolves (2D localized wave). It is found that the former case may be described by exact solitary wave solutions, while the latter case requires a study of the transverse instability and numerical simulations. The conditions are obtained that establish the parameters of the incident waves and/or the ocean stratification required for the rogue wave or hole generation.

2. Long wave modelling of rogue waves

2.1. Kadomtsev-Petviashvili equation

The simplest model implies that the ocean is an inviscid liquid layer of permanent depth H with free deformable surface. Assume the plane $z = 0$ of the Cartesian coordinates coincides with undisturbed free surface of the layer, hence fluid occupies the region $-H < z < \eta$, $\eta(x, y, t)$ is a free surface disturbance. Let us denote velocity components along axes x, y, z by $u(x, y, z, t)$, $v(x, y, z, t)$ and $w(x, y, z, t)$ respectively. Let t is time.

As usual, it is convenient to introduce the velocity potential, $u = \Phi_x$, $v = \Phi_y$ and $w = \Phi_z$. The basic equations and the boundary conditions may be found in [9]. The scales are introduced as follows: L (typical wave size) for x, Y for y, and H for z , $L/\sqrt{gH}$ for t, B for η, and $BL\sqrt{gH}/H$ for Φ. The small parameter of the problem, ε, is chosen according to estimations of the observed elevation rogue waves [7],

$$\varepsilon = B/H = H^2/L^2,$$

The simplified governing equation may be obtained if weak transverse variations are assumed, $L/Y = O(H/L) = O(\sqrt{\varepsilon})$. Introducing the phase variable $\theta = x - t$ and the slow time $\tau = \varepsilon\, t$, one can obtain from the basic equations [7] that the function $\eta(\theta, y, \tau)$ satisfies the equation

$$(2\eta_\tau + 3\eta\eta_\theta + 1/3\ \eta_{\theta\theta\theta})_\theta + \eta_{yy} = 0, \tag{2.1}$$

that is nothing but the Kadomtsev-Petviashvili (KP) equation [10, 11].

2.2. 2D Benjamin-Ono equation

As a rule, freak waves are considered as elevation free surface waves. However, there exist similar waves with deep troughs or surface holes that were observed in various places [5, 6]. It is important that these waves satisfy the relationship $A/H = O(H/L)$, hence, the KP equation is invalid in this case since its applicability requires another ratio between A/H and H/L, $A/H = O(H^2/L^2)$. We consider the model containing semi-unbounded inviscid and incompressible air layer interacting with a finite size layer of inviscid and incompressible water by the normal stresses. The wind in the atmosphere is taken into account in order to check its influence on the 2D localization of the wave on the water surface.

Assume that the width of the water layer is H and it is bounded by the rigid bottom from below. The Cartesian coordinates (x, y, z) are put so as the plane $z = 0$ coincides with undisturbed free surface of the liquid layer. Let $\eta(x, y, t)$ is a disturbance of the water surface. Then the water occupies the region $-H < z < \eta$, while the air occupies $\eta < z < \infty$. Let us denote constant density of the water by ρ, the velocity components along the directions x, y, z by $u(x, y, z, t)$, $v(x, y, z, t)$ and $w(x, y, z, t)$ respectively. Similar notations for the air are ρ', $u'(x, y, z, t)$, $v'(x, y, z, t)$ and $w'(x, y, z, t)$. It is convenient to use in the equations and in the boundary conditions

the potentials Φ, Φ' defined by $u = \Phi_x$, $v = \Phi_y$ and $w = \Phi_z$, $u' = \Phi'_x$, $v' = \Phi'_y$ and $w' = \Phi'_z$. Suppose the wind in the air has the velocity U' directed along the x-axis.

Then the basic equations are written as usual [9] while the boundary conditions are:

$$\Phi_z \;=\; 0 \text{ at } z = -H, \tag{2.2}$$

$$\Phi' \;\to\; 0 \text{ at } z \;\to\; \infty, \tag{2.3}$$

and for $z = \eta$ we get

$$\rho(\Phi_t + 1/2(\Phi_x^2 + \Phi_y^2 + \Phi_z^2) + g\,\eta) = \rho'(\Phi'_t + U'\Phi'_x + 1/2(\Phi_x^{'2} + \Phi_y^{'2} + \Phi_z^{'2}) + g\,\eta), \tag{2.4}$$

$$\eta_t + \Phi_x\eta_x + \Phi_y\eta_y \;=\; \Phi_z. \tag{2.5}$$

$$\eta_t + \Phi'_x\eta_x + \Phi'_y\eta_y \;=\; \Phi'_z. \tag{2.6}$$

The following scales are used: L- for X, Y- for y, H-for z in the water and L - for z in the air, $L/\sqrt{gH}$-for t, A-for η and $AL\sqrt{gH}/H$- for Φ, Φ'. The small parameter ε is introduced as

$$\varepsilon \;=\; A/H \;=\; H/L.$$

It is assumed additionally that $L/Y = \sqrt{\varepsilon}$.

The governing equation is obtained following the well-known procedure [12, 13]. Finally, the phase variable $\theta = x - \sqrt{1-\sigma}\,t$ and the slow time $\tau = \varepsilon\,\sqrt{1-\sigma}\,t$ are introduced, $\sigma \;=\; \rho'/\rho$, and the equation for the function η is obtained,

$$\left(2\eta_\tau + 3\eta\eta_\theta + b\frac{1}{\pi}\int\limits_{-\infty}^{\infty}\frac{\eta_{\theta'\theta'}\,d\theta'}{\theta' - \theta}\right)_\theta + \eta_{yy} \;=\; 0. \tag{2.7}$$

where

$$b \;=\; \sigma\left(1 - \frac{U'}{\sqrt{gH(1-\sigma)}}\right)^2.$$

Equation (2.7) is reduced to the Benjamin-Ono (BO) equation in the one-dimensional case, hence it may be called the two-dimensional generalization of the BO equation or the 2DBO equation.

2.3. 2D Gardner equation

Another model where the ratio $A/H = O(H/L)$ may be realized is the two-layer fluid model. It is known that it may be employed to account for the stratification in the ocean. Let the upper finite width layer has density ρ' and thickness h_0, while the lower one has

density $\rho > \rho'$ and thickness H. Assume that both the interface and the free surface of the upper layer are deformable while an influence of the atmosphere is negligibly small. In the one-dimensional case, long nonlinear waves were considered early in [14]. It was shown there that both surface and internal waves are described by the Korteweg-de Vries (KdV) equations if $A/H = O(H^2/L^2)$. However, the coefficient at the quadratic nonlinear term in the KdV equation may be small itself at certain relationship between widths and densities. In this case the balance between nonlinearity and dispersion required for propagation of localized waves, is realized for $A/H = O(H/L)$, just the ratio observed for the deep holes [8].

Basic equations have the form similar to that used in the previous subsection (we denote now by $'$ variables in the upper liquid layer) with the exception of the wind, now $U' = 0$, and of the boundary conditions to be imposed at the upper free surface $z = h_0 + h(x, y, t)$,

$$\Phi'_t + 1/2(\Phi'^2_x + \Phi'^2_y + \Phi'^2_z) + g\, h = 0,$$

$$h_t + \Phi'_x h_x + \Phi'_y h_y = \Phi'_z. \tag{2.8}$$

Like in the previous subsection, weak transverse variations are considered with $L/Y = \sqrt{\varepsilon}$, where ε is defined in the previous subsection, A- typical amplitude of both the surface and internal waves. Now $\eta(x, y, t)$ is the interface disturbance, other notations are $\sigma = \rho'/\rho$, $m = h_0/H$. The scales are the same as in the previous subsection but for the scale for z in the upper layer now chosen equal to H. Like in the one-dimensional case [14], we obtain that the coefficient at the quadratic nonlinear term is equal to zero for $m = m^*$,

$$m^* = s_+ + s_- + \frac{1}{3}(3 - 3\sigma - \sigma^2),$$

where

$$s_\pm = \Big(\frac{\sigma}{54}[27(1+\sigma) + 2\sigma^2(9 - 18\sigma - 9\sigma^2 - \sigma^3)] \pm \frac{\sigma(1+2\sigma)}{6}\sqrt{\frac{(1-\sigma)(27+5\sigma)}{3}}\Big)^{1/3},$$

Assume that $m = m^* + \varepsilon m_1 + ...$, $v = v^* + \varepsilon v_1 + ...$ In this case, standard asymptotic procedure allows us to reduce basic equations to the governing equation for the free surface disturbance:

$$(h_\tau + a\, h_\theta^2 + c h_\theta^3 + b h_{\theta\theta\theta})_\theta + d h_{yy} = 0, \tag{2.9}$$

where $\theta = x - vt$, $\tau = \varepsilon^2 t$,

$$v^{*2} = \frac{1}{2}(1 + m^* - \sqrt{(1+m^*)^2 - 4(1-\sigma)m^*}),$$

$$a = \frac{3m_1[(2m^*(\sigma-2)+3-5\sigma)v^{*2}+(1-\sigma)(2m^{*2}+3m^*\sigma-1)]}{2v^*[(1+m^*)v^{*2}-2(1-\sigma)m^*](1+m^*-2v^{*2})},$$

$$b = \frac{v^*[(1+m^*)\{1-(1-3\sigma)m^*+m^{*2}\}v^{*2}-(1-\sigma)m^*(1+3m^*\sigma+m^{*2})]}{6[(1+m^*)v^{*2}-2(1-\sigma)m^*]},$$

$$c = \frac{m^*(1-\sigma)(4m^{*2}+m^*-1+4m^*\sigma)-4v^{*2}(m^{*2}(1-\sigma)-m^*(1-2\sigma)+1)}{v^*[(1+m^*)v^{*2}-2(1-\sigma)m^*]},$$

$$d = \frac{v^*}{2},$$

It is easy to check that $b > 0$, c is always negative, while the sign of a is defined by the sign of m_1. Equation (2.9) is nothing but a two-dimensional generalization of the Gardner equation or the 2D Gardner equation.

3. Mechanisms of the rogue waves formation

3.1. Resonant waves interaction

It is known that plane solitary wave solution of the KP equation(2.1),

$$\eta = \frac{4k^2}{3}\cosh^{-2}k(\theta + mZ - \frac{3m^2+2k^2}{6}\tau), \tag{3.1}$$

is stable to transverse disturbances, and exact two-dimensional localized travelling wave solution requires an opposite sign at η_{ZZ} or at $\eta_{\theta\theta\theta\theta}$ [10, 11]. In our case it is unlikely. Hence we cannot anticipate an appearance of 2D localized wave from the single solitary wave. However, the KP equation possesses a two-solitary wave solution [10, 15],

$$\eta = \frac{4}{3}\frac{\partial^2}{\partial\theta^2}\log(F),\ F = 1+\exp(\xi_1)+\exp(\xi_2)+\exp(A_{12}+\xi_1+\xi_2),$$

$$\xi_i = k_i(\theta + m_i Z - \frac{3m_i^2+k_i^2}{6}\tau),\ \exp A_{12} = \frac{(k_1-k_2)^2-(m_1-m_2)^2}{(k_1+k_2)^2-(m_1-m_2)^2} \tag{3.2}$$

It contains a hump in the area of the waves interaction. The hump moves keeping its shape and velocity, and its maximum amplitude may be up to four times higher than the amplitude of each interacting solitary wave. Detailed analysis of this solution and its possible application to the rogue waves description is done in [4]. Now we only mention that this solution describes propagation but not a formation of the localized structure, the last should be presented in the initial condition.

Recently we developed the idea of the use of the waves interaction. However, we consider another solution of the KP equation [7] that does not describe the waves interaction at $t = 0$ in contrast to the exact two-solitary wave solution suggested in [4]. Numerical solution describes a formation of a localized high wave (or a stem) only

when the angle between the incident crested waves lies within a certain interval. Our estimations demonstrate rather fast formation of the stem that may be a reason why the rogue wave appears suddenly for the crew of a vessel. An increase in amplitude is up to four times. Much higher increase is achieved, up to 14 (!) times when the incident waves with curved fronts interact [7]. In the last case, the 2D localized wave is unstable and exists for a short time period. However, fast formation of a high wave *near* the ship gives rise enough time to it to affect the ship before an instability destroys the wave.

The well-known exact solitary wave solution solution $\eta = \eta_0$ of the BO equation may be written as

$$\eta_0 = \frac{4b\sqrt{k}}{3\left(k\xi^2+1\right)}, \tag{3.3}$$

where $\xi = (\theta - 0.5b\sqrt{k}\tau)$. It accounts for a moving elevation plane wave in the two-dimensional case. It is always stable to transverse disturbances for the positive sign of b [8, 13, 16]. One can see that the wind cannot affect the sign of b. The sign of the amplitude is defined by the sign of b, and holes are not described by this solution.

Hence the 2D localization elevation wave may only arise due to the plane waves interaction. This process was studied numerically in [17] where it was found a similarity with the KP case. Again a stem appears due to the waves interaction and its amplitude depends upon the angle between the incident plane waves. However, now the highest amplitude may be eight times larger than the amplitudes of the incident waves. The case of the curved initial waves interaction is not considered by now.

A similar scenario may be realized for the known solitary wave solution $h = h_s$ of the Gardner equation [14]:

$$h_s = \frac{3b\,k^2}{a(B_1\cosh(k\xi)+1)}, \tag{3.4}$$

where

$$B_1 = \sqrt{1+\frac{9bck^2}{2a^2}}, \xi = \theta - bk^2\,\tau.$$

In the two-dimensional case, Eq. (3.4) accounts for the propagation of a plane solitary wave. In contrast to the exact solution of the 2DBO equation now the amplitude may be of either sign. The hump propagation is described for positive values of a, while the wave with a trough propagates for $a < 0$. The solution has an interesting feature for negative c: tendency to the extensive trough shape at $k \to \sqrt{-2a^2/(9b\,c)}$. The amplitude of the wave tends to the limiting value equal to $-2a/3c$. This solution is stable to transverse disturbances [8]. Similar to the KP and 2DBO equations, numerical solution reveals a localization with a great increase in amplitude of the wave as a result of semi-plane or curved incident waves interaction [18]. The results look very similar to those of the KP equation. However, no stem is observed for small negative values of the coefficient at the cubic non-linear term. Possible reason is in the fail of reality of B_1 that happens in the exact solution (3.4) as soon as negative c decreases.

3.2. Transverse instability of plane solitary waves

The Gardner equation (2.9) possesses an extra solution $h = h_p$ that may be employed for explanation of the holes. It appears due to the balance between cubic nonlinearity and dispersion and may be written through the Jacobi elliptic function,

$$h_p = \sqrt{-\frac{2b}{c}}\, k\, \kappa\, \mathrm{sn}(k\xi, \kappa) - \frac{a}{3c} \tag{3.5}$$

where $\xi = \theta - s\tau$, κ, $0 < \kappa < 1$, is the Jacobi function modulus, while the velocity is $s = -bk^2(1+\kappa^2) - a^2/(3c)$. Its minimum is larger that the maximum for negative a. Moreover, the troughs in the solution became extensive as $\kappa \to 1$, and they are separated by the extensive areas of moderate elevation. In the two-dimensional case, these troughs are similar to the shape of the solution (3.4) with the exception of the absence of the limiting amplitude [8].

The transverse instability of the solution (3.5) is studied similar to that of the solitary wave solutions [8]. One can check that the wave (3.5) is always unstable. This may result in an appearance of a periodical train of the waves modulated in the transverse direction, hence the sequence of two-dimensional localized waves. Then another mechanism of the rogue waves and holes formation may be suggested based on the 2D localization due to the transverse instability. It is to be noted the exact solution of the KP equation that may be obtained when the sign at dispersive or transverse η_{yy} term in Eq.(2.1)is negative [19]. This solution describes a transverse modulation of an initial plane solitary wave which is accompanied by an increase in amplitude. However, this increase is not very high, 1.5-2 times. Much more increase may be achieved if a 2D input is used. It was found [20] that growth up to 12 times happens if the input is not so smooth as the 2D Gaussian distribution. The process of the formation of the stable 2D localized wave is fast that may be used to explain sudden appearance of the rogue wave near the ship.

4. Conclusions

The solutions of the model equations considered reflect main features of the abnormally high or deep waves: their fast but rare appearance. The first feature as well as the growth of the amplitude depend upon the shape of the incident waves and the angle between them. The second feature is caused by the strict restrictions required for the existence of the solution, in particular, m should be near the special value m^* for the solution of the Gardner equation. It is found that the conditions yielding 2D localization are governed by physical factors through the signs of the coefficients of the equations. Thus the sign of a separates an appearance of the elevation wave or the hole wave, that is defined by the sign of m_1 or by the ocean stratification. This dependence upon the physical factors is important for a prediction of the rogue waves and holes in the sea.

5. Acknowledgment

The author thanks Professor F. Pastrone for his kind invitation to attend the Intensive Seminar and for his warmest hospitality during the work of the Seminar.

References

[1] OLAGNON M. AND ATHANASSOULIS G.A., *Rogue Waves-2000*, Ifremer, France 2001.

[2] KHARIF C. AND PELINOVSKY E., *Physical mechanisms of the rogue wave phenomenon*, European J. Mechanics B - Fluids, **22** (2003), 603–635.

[3] LAVRENOV I.V., *Wind waves in ocean*, Springer, Berlin 2003.

[4] PETERSON P. ET AL., *Interaction soliton as a possible model for extreme waves in shallow water*, Nonlinear Processes in Geophysics **10** (2003), 503–510.

[5] MONBALIU J., Presentation at MaxWave Project Concluding Symposium, Geneva, 8-12 October, 2003.

[6] MOES H., Presentation at MaxWave Project Concluding Symposium, Geneva, 8-12 October, 2003.

[7] PORUBOV A.V., TSUJI H., LAVRENOV I.V. AND OIKAWA M., *Formation of the rogue wave due to nonlinear two-dimensional waves interaction*, Wave Motion **42** (2005) 202–210 .

[8] LAVRENOV I.V. AND PORUBOV A.V., *Freak wave with deep trough in the sea*, preprint 2005.

[9] WHITHAM G., *Linear and Nonlinear Waves*, John Wiley & Sons, New York 1974.

[10] ABLOWITZ M. AND SEGUR H., *Solitons and inverse scattering transform*, SIAM, Philadelphia 1981.

[11] KADOMTSEV B.B. AND PETVIASHVILI V.I., *The stability of solitary waves in a weakly dispersive media*, Sov. Phys. Dokl. **15** (1970), 539–541.

[12] MATSUNO Y. , *Dynamics of interacting algebraic solitons*, Int. J. Mod. Phys. B. **9** (1995), 1985–2081.

[13] ABLOWITZ M.J. AND SEGUR H., *Long internal waves in fluids of great depth*, Stud. Appl. Math. **62** (1980), 249–262.

[14] KAKUTANI T. AND YAMASAKI N., *Solitary waves on a two-layer fluid*, J. Phys. Soc. Japan, **45** (1978), 674–679.

[15] SATSUMA J., *N-soliton solution of the two-dimensional Korteweg-de Vries equation*, J. Phys. Soc. Japan. **40** (1976), 286–290.

[16] MATSUNO Y., *Transverse instability and collapse of internal algebraic solitary waves in fluids of great depth*, Phys. Let. A. **265** (2000), 358–363.

[17] TSUJI H. AND OIKAWA M., *Oblique interaction of internal solitary waves in a two layer fluid of infinte depth*, Fluid Dyn. Res. **29** (2001), 251–267.

[18] TSUJI H. AND OIKAWA M., *Oblique interaction of solitary waves in an extended Kadomtsev-Petviashvili equation*, in: "Proceeding of the XXXIII international conference advanced problems in mechanics, Saint-Petersburg 2005", 303–310.

[19] PELINOVSKY D.E. AND STEPANYANTS YU. A., *Solitary wave instability in the positive-dispersion media described by the two-dimensional Boussinesq equations*, JETP **79** (1994), 105–112.

[20] PORUBOV A.V., MAUGIN G.A. AND MAREEV V.V., *Localization of two-dimensional nonlinear strain waves in a plate*, Intern. J. Non-Linear Mech. **39** (2004), 1359–1370.

AMS Subject Classification: 76B15, 76B25, 76B70.

Alexey PORUBOV, A.F.Ioffe Physical Technical Institute of the Russian Academy of Sciences,
Polytekhnicheskaya st. 26, 194021, Saint-Petersburg, RUSSIA
e-mail: porubov@math.ioffe.ru

Rend. Sem. Mat. Univ. Pol. Torino - Vol. 65, 2 (2007)
ISASUT Intensive Seminar

T. Soomere

FAST FERRIES AS WAVEMAKERS IN A NATURAL LABORATORY OF ROGUE WAVES

Abstract. The evolution of solitonic waves traveling in slightly different directions is analysed in the framework of the Kadomtsev-Petviashvili equation. Nonlinear interactions of solitonic waves generally lead to phase shifts of the counterparts. If the amplitudes of the interacting solitons, the angle between their crests and the water depth are specifically balanced, interactions result in particularly high wave humps resembling the phenomena occurring during the Mach reflection of solitary waves. Surface elevation up to four times as high as the amplitude of the counterparts may occur, and the slope of the front of the hump may be eight times as large as the maximum slope of the fronts of the interacting waves. Although such a balance occurs seldom, the resulting structure may persist for a long time until the balance is violated. Solitonic waves occur relatively seldom in natural conditions. However, leading waves of wakes from contemporary large high-speed ships sailing in shallow water frequently have solitonic nature. The described interactions are realistic in areas hosting intense fast ferry traffic.

Key words: nonlinear ship waves, high-speed ships, shallow water waves; extreme waves; solitons, soliton interaction

1. Introduction

The concerns related to intense ship traffic are traditionally associated with possible accidents such as ship collisions or grounding, technical and navigation problems caused by severe weather or human errors etc. These concerns are being effectively managed by international shipping and harbor communities with the use of the basic assertion that the risks of water surface transport are localized within a small area around the ship.

The continuing introduction of evermore faster ship services during the last two decades has created new major worries, which are no more located in small areas. For example, the massive growth of exhaust emissions (capable of creating substantial changes in the atmosphere at the height of many hundreds of meters above sea surface, Durkee et al. [1]) may become a part of global troubles and the great increase of the ship-generated noise may adversely affect quality of life in areas adjacent to ship lanes.

The most important issue is the wake generated by large high-speed ships (Guidelines [2], Wood [3]), in particular, specific features of waves excited by strongly powered ships sailing at shallow and moderate depths (up to 100 m). Large-amplitude wake wash propagating shoreward has become an issue of central concern for coastal communities, because it has a significant impact on the safety of people, property and craft (Guidelines [2], Parnell and Kofoed-Hansen [4]). Large wake waves are frequently compact entities which cause violent energy concentration not only in the vicinity of ship lanes but also in remote sea areas (Hamer [5]). It is no more unusual that

holidaymakers are forced to “flee for their lives when enormous waves erupted from a millpond-smooth sea”, or that waves look like “the white cliffs of Dover” (Hamer [5]). There exist several coastal areas which have rough wave conditions but still the contribution of ship waves is significant. For example, ship traffic in Tallinn Bay, the Baltic Sea, is so intense that ship-generated waves form, at least, about 5–8% from the total wave energy and about 18–35% from the wave power in the coastal areas of Tallinn Bay exposed to dominating winds [6,7]. They may be responsible for the erosion of the coastline and the sea bottom [8], and may seriously damage the biological environment.

The most well-known components of a nonlinear ship wake are Korteweg-de Vries (KdV) solitons (Wu [9], Li and Sclavounos [10]). They can be generated either directly by the ship motion or by the long-wave part of classical ship waves. When the latter approaches coastal area, its components frequently become non-dispersive and highly nonlinear shallow water waves that often resemble ensembles of KdV solitons (Soomere et al. [11]). Ship wakes may at times contain some other specific types of disturbances such as monochromatic packets of relatively short waves (Brown et al. [12]), depression areas penetrating into adjacent basins (Forsman [13]), or supercritical bore (Gourlay [14]) that are qualitatively different from the usual Kelvin wake.

In this paper, I give an overview of some aspects of nonlinear interactions of nearly unidirectional KdV solitons. The description of the classical Kelvin ship wave pattern and its changes for increasing ship speeds are sketched first for completeness. Further, I describe recent developments of the analysis of specific features of interactions of (possibly ship-induced) solitonic waves in the framework of the Kadomtsev-Petviashvili equation. Finally, potential modifications of the wave shape and applications of the described results in realistic shallow-water conditions are discussed.

2. Linear wakes

The classical problem of kinematics of ship waves consists in determining the steady pattern of wave crests (more generally, the phase curves) created by a moving ship in the framework of the linear wave theory. The first description of the stationary wave pattern exited by a point source in terms of two sets of waves that move forward and out from the disturbance (diverging waves), and one set of waves that move in the direction of the disturbance (transversal waves) was given by Froude in 1877 [15]. Traditionally, this pattern is called Kelvin wave system, or Kelvin wake (after William Thomson, Lord Kelvin, who constructed the corresponding theory for deep water in 1887 [16]). The work was expanded by Havelock starting from 1908 [17] to resolve some discontinuities in the Kelvin model and to include the effects of water depth.

A quick derivation of the Kelvin wave pattern can be found in [18], §256, or [19] §3.10. The relevant analysis relies on the dispersion relation and needs to apply only three basic ideas: (i) the wave system is stationary, (ii) the constant phase curves are perpendicular to the wave vector, (iii) the local phase velocity (celerity) c_f must be equal to the projection of the ship’s velocity in the direction of the wave vector [20,21]. The first and the third conditions simply mean that the pattern of *wave crests* created by

ship moving steadily with speed V can only be stationary if the wave component traveling under angle θ with respect to the sailing line has the phase velocity $c_f = V\cos\theta$. Since the celerity of surface waves in water of an appreciable depth is smaller than the group velocity c_g, energy of a steady wave system can only exist within a triangular area called Kelvin wedge The half-angle α of the wedge satisfies the geometrical condition $\sin\alpha = 1/(2c_f c_g^{-1} - 1)$ and is defined by $\sin\alpha = 1/3$ in deep water. The basic features of steady wave patterns in deep water therefore do not depend on the sailing speed. If the ship sails in water of finite depth, the ratio of the phase and the group velocity $c_f/c_g = 2/[1 + 2kH\sinh^{-1}(2kH)]$ additionally depends on the water depth H. Yet angle α only depends on the ratio $F_h = V/\sqrt{gH}$ of the ship's speed and the maximum phase velocity of surface waves for the given water depth. This ratio is called depth Froude number. For $F_h < 1$, half angle α can be found from equation $\cos^2\alpha = [8 - 16kH\sinh^{-1}(2kH)] \times [3 - 2kH\sinh^{-1}(2kH)]^{-2}$ [22].

Shallow-water effects become important when wavelength approximately twice exceeds the water depth, equivalently, when $kH < \pi$. The limiting depth Froude number for diverging waves at the edge of the Kelvin edge is $\tilde{F}_{ht} \approx 0.687$. For somewhat longer transverse waves at the sailing line this threshold is $\tilde{F}_{ht} \approx 0.56$ [22]. Therefore, at depth Froude numbers above 0.55–0.7 the ship-generated wave system should response to the water depth.

If the ship's speed $V = \sqrt{gH}$, angle α reaches the maximum value $\alpha = 90°$. Frequently, it is claimed (perhaps after [17,22]) that the transverse and the diverging waves form a single large wave with its crest normal to the sailing line that travels at the same speed as the disturbance at $F_h \to 1$. Such a description is conceptually imprecise, because what exactly happens at these speeds cannot be described by the linear theory. However, it is true that that wave heights increase considerably at $F_h \to 1$ and wave periods increase gradually as the ships speed increases.

The threshold $F_h = 1$ serves as a natural basis of classification of navigational speeds. Operating at speeds resulting $F_h < 1$ is defined as subcritical, at $F_h > 1$ as supercritical and at $F_h = 1$ as critical. There is a relatively wide transcritical speed range $0.84 \lessapprox F_h \lessapprox 1.15$ in realistic conditions, where no clear distinction between sub- and supercritical regimes is possible (Hüsig et al. [23]).

3. Solitonic ship waves

In restricted waters, solitary waves can be generated ahead of the ship bow. John Scott Russell first documented this phenomenon as he watched in 1834 a canal boat pulled by horses stopping suddenly (see his description reprinted, e.g., in [24]). Helm [25] probably first reported that a ship model advancing steadily in towing tank can radiate many solitons subsequently. At certain speeds close to the speed of the maximum wave resistance, the influence of the ship model extended to 4–5 lengths of the model upstream whereas up to 7 wave crests (precursor solitons [9,26]) were detectable. This is a highly intriguing phenomenon, because it is very unusual that a "forcing disturbance moving *steadily* ... in shallow water can generate, *continuously and periodically*, a succession of solitary waves, propagating ahead of the disturbance" (Wu [9], my italics).

This phenomenon is not restricted to ship waves only and may occur in many other areas of research and engineering [9]. It is a generic mechanism of excitation of disturbances in situations where the nonlinear and dispersive effects are specifically balanced, and becomes effective when the group velocity of long waves radiated from the forcing area is close to the velocity of the disturbance. The local wave therefore obtains energy from the source during a relatively long time. In meteorological applications, examples of a single long high wave generated by a moving low pressure disturbance when the disturbance speed is approximately the critical speed were reported long time ago. The resulting wave resembles tsunami wave and is sometimes called "meteorological tsunami" [27].

Solitonic disturbances resembling Korteweg-de Vries (KdV) solitons frequently occur far ahead a ship sailing in confined waters at certain speeds (Neuman et al. [28]). The ship speed is the decisive factor in forming these waves, because for speeds much less than the critical one the linear waves will effectively carry away energy. However, a ship may excite solitary waves starting already from $F_h \geq 0.2$ and such waves can be found in numerical computations for $F_h \geq 0.4$ (Ertekin et al. [29]). They are the largest for the transcritical speeds, and are accompanied by a drastic dropdown of the water surface near the vessel (Forsman [13], Li and Sclavounos [10]). There exists an opinion that these solitons are responsible for some disasters (Hamer [5], Li and Sclavounos [10]). A more probable source of solitonic waves form the long components of diverging waves that become highly cnoidal (Parnell and Kofoed-Hansen [4]) or obtain the shape of KdV solitons (Soomere et al. [11]) in shallow areas.

The theoretical explanation of the phenomenon of generation of precursor solitons was given in (Akylas [30], Cole [31]) for the basically equivalent environments of a moving disturbance and for a flow past a bump. The upstream-propagating solitons can be described by a forced Korteweg-de Vries (fKdV) equation with a singular forcing function. Let $p = p(x+Vt)$ and $b = b(x+Vt)$ represent moving surface pressure patch (the simplest model of the moving ship) and topography whereas the velocity V is nearly critical so that $F_h = 1 + \epsilon\delta$, where $\epsilon = (H/\lambda)^2 \ll 1$ for long waves and $\delta = O(1)$. In the coordinate system moving with the pressure patch or topography, evolution of the water surface $\tilde{\eta}$ is with the accuracy $O(\epsilon^2)$ described by the forced KdV (fKdV) equation [9]:

$$\frac{1}{\sqrt{gH}}\tilde{\eta}_t + \left[(F_h - 1) - \frac{3}{2H}\tilde{\eta}\right]\tilde{\eta}_x - \frac{H^2}{6}\tilde{\eta}_{xxx} = \frac{1}{2}\frac{\partial}{\partial x}\left(\frac{p}{\rho g} + b\right). \tag{3.1}$$

For $F_h = 1$, $p = b = const$ this equation is the classical homogeneous KdV equation. The framework of Eq. (1) intrinsically contains only one spatial dimension. First two-dimensional numerical results showing the existence of waves ahead of the ship were probably presented by Wu and Wu [32]. They used the generalized Boussinesq model of Wu [33] and showed that a solitary wave emerges ahead of the pressure disturbance and propagates upstream when a pressure patch was moving with a near-critical speed $V \approx \sqrt{gH}$ in a two-dimensional tank. Numerical experiments based on the Green-Naghdi fluid sheet equation also demonstrated a series of upstream-propagating soliton-like disturbances ahead of the ship at transcritical speeds ($F_h = 0.9 \ldots 1.2$,

Ertekin et al. [34,35]). Lee et al. [36] established that the forced KdV model and the generalized Boussinesq model give similar predictions of this phenomenon and show a satisfactory agreement with experiments. A comparison between the fully nonlinear model and the two models above was carried out more recently by Casciola and Landrini [37] with the use of the boundary integral approach to simulate the flow.

4. Interaction of solitonic wakes

Analysis of propagation and interactions of KdV solitons (possibly excited by contemporary ships if they sail at transcritical speeds) has an intriguing application not only in the framework of abnormally high waves in shallow coastal areas hosting intense ship traffic but also in the general theory of rogue waves. Namely, it has been suggested by many authors that an appropriate nonlinear mechanism could be responsible for extreme waves [38].

The interaction of unidirectional KdV solitons is today well understood. It does not create any drastic increase in wave amplitudes [24]. However, amplitude amplification may occur under certain conditions when KdV solitons propagating in different directions meet each other [39, 40]. It is known as one of the few mechanisms able to create long-living extremely high wave humps in shallow water [38].

A suitable mathematical model for the description of the interaction of nearly unidirectional KdV solitons is the Kadomtsev-Petviashvili (KP) equation that admits explicit formulae for multi-soliton solutions. A well-known feature of such interactions is that they may lead to spatially localised extreme surface elevations. For interacting waves with equal amplitudes the high humps resemble Mach stem and can be up to four times as high as the incoming waves. Although known for a long time for solitary waves reflecting from a wall [41], this mechanism has been only recently proposed as an explanation of the freak wave phenomenon [42]. The reason is that it may become evident only (i) provided long-crested shallow water waves can be associated with solitons and (ii) provided the KP equation is a valid model for such waves. These conditions are not common for storm waves; however, they may be often satisfied when two or more systems of swell approaching a certain area from different directions. Groups of solitonic waves intersecting at a small angle may also appear if wakes from two ships meet each other in shallow water. Their interaction may be responsible for dangerous waves along shorelines mentioned in [5].

The nondimensional KP equation for surface gravity waves in shallow water reads (Segur and Finkel [43])

$$(\eta_t + 6\eta\eta_x + \eta_{xxx})_x + 3\eta_{yy} = 0. \tag{4.1}$$

The nondimensional (x, y, t, η) and physical variables $(\tilde{x}, \tilde{y}, \tilde{t}, \tilde{\eta})$ are related as follows: $x = \sqrt{\epsilon}(\tilde{x} - \tilde{t}\sqrt{gH})/H$, $y = \epsilon\tilde{y}/H$, $t = \tilde{t}\sqrt{\epsilon^3 gH}/H$, $\eta = 3\tilde{\eta}/(2\epsilon H) + O(\epsilon)$ whereas $\epsilon = |\tilde{\eta}_{\max}|/H \ll 1$. The two-soliton solution to the KP equation can be decomposed into a sum $\eta = s_1 + s_2 + s_{12}$ of two incoming solitons s_1, s_2 and residue s_{12}

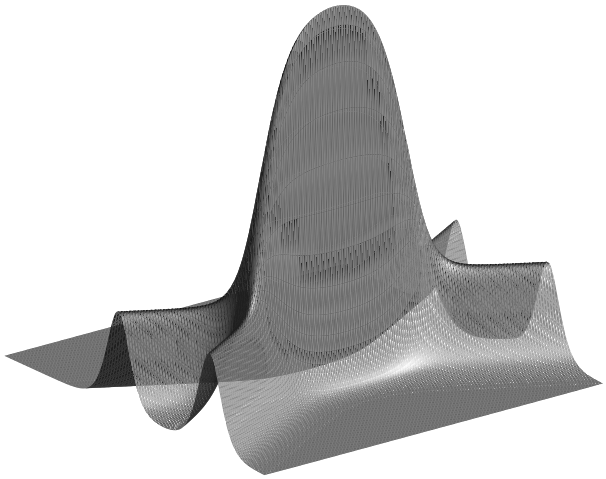

Figure 1: Surface elevation in the vicinity of the interaction area, corresponding to incoming solitons with equal amplitudes $a_1 = a_2$, $l_1 = -l_2 = 1/3$, $k_{res} = \sqrt{1/3}$ and $k = 0.999k_{res}$. Area $0 \le z \le 4a_1$, $|x| \le 30$, $|y| \le 30$, in normalised coordinates is shown.

(Peterson and van Groesen [44]):

$$s_{1,2} = \sqrt{A_{12}}k_{1,2}^2\Theta^{-2}\cosh\left(\varphi_{1,2}x + \ln\sqrt{A_{12}}\right),$$

$$s_{12} = 2\Theta^{-2}\left[(k_1 - k_2)^2 + A_{12}\,(k_1 + k_2)^2\right], \tag{4.2}$$

$$\Theta = \cosh\frac{\varphi_1 - \varphi_2}{2} + \cosh\frac{\varphi_1 + \varphi_2 + \ln A_{12}}{2}.$$

Here $\varphi_i = k_i x + l_i y + \omega_i t$, $\kappa_i = (k_i, l_i)$, $a_{12} = \frac{1}{2}k_{1,2}^2$, $i = 1, 2$, are the wave vectors and amplitudes of the incoming solitons, the frequencies ω_i satisfy the dispersion relation $k_i\omega_i + k_i^4 + 3l_i^2 = 0$ of the linearized KP equation, $A_{12} = [\lambda^2 - (k_1 - k_2)^2]/[\lambda^2 - (k_1 + k_2)^2]$ is the phase shift parameter and $\lambda = l_1k_1^{-1} - l_2k_2^{-1}$. Within restrictions of the KP model, interaction may result in either the positive or the negative phase shift $\Delta = -\ln A_{12}$ of the counterparts. The interaction pattern (Fig. 1) is always symmetric with respect to a particular point called interaction centre, and is stationary in a properly moving coordinate frame.

5. Phase shifts, extreme elevations and slopes, and crest geometry

The phase shifts $\delta_{1,2}$ of the counterparts (Fig. 2) only depend on the amplitudes of the incoming solitons and the angle between their crests. Relations for the phase shifts

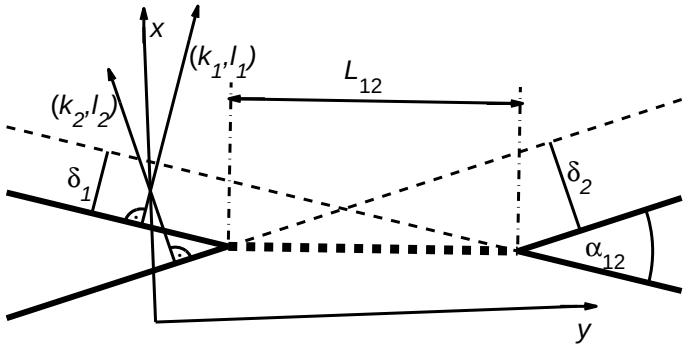

Figure 2: Idealized patterns of crests of incoming solitons (bold lines), their position in the absence of interaction (dashed lines) and the interaction soliton (bold dashed line) corresponding to the negative phase shift case.

$\delta_{1,2} = \ln A_{12}/|\kappa_{1,2}|$ and for the intersection angle $2\tan\frac{1}{2}\tilde{\alpha}_{12} = \lambda$ can be simplified to one transcendental equation with respect to either of the amplitudes of the interacting solitons [44]

$$\delta_1\sqrt{2a_1(1+\lambda^2/4)} = \pm\ln\frac{\delta_2^2\lambda^2 - 2(\delta_2-\delta_1)^2a_1^2}{\delta_2^2\lambda^2 - 2(\delta_2+\delta_1)^2a_1^2}. \tag{5.1}$$

This angle α_{12} and the magnitudes of the phase shifts $\delta_{1,2}$ can be estimated, e.g. from aerial photos. If the sign of the phase shift is known, equation (5.1) uniquely defines the heights of the interacting solitons. The sensitivity of this method and several simplifications of Eq. (5.1) are discussed in Peterson and van Groesen [45].

For the negative phase shift case $A_{12} > 1$ (that is typical in interactions of solitons with comparable amplitudes) an interaction pattern emerges, height of which exceeds that of the sum of the two incoming solitons (e.g., Miles [41], Tsuji and Oikawa [46]). When two waves of arbitrary amplitudes a_1 and a_2 meet, the maximum amplitude M of their superposition can be written as $M = m(a_1 + a_2)$, where the "nonlinear amplification factor" m may depend on both a_1 and a_2 and their intersection angle. The maximum surface elevation for equal amplitude solitons is $a_{\max} = 4a_{1,2}/\left(1 + A_{12}^{-1/2}\right)$ [41,47]. Thus, nonlinear superposition of two equal amplitude solitons may lead to a fourfold amplification of the surface elevation in the resonance case $A_{12} \to \infty$. In a highly idealized case of interactions of five solitons surface elevation may exceed the amplitude of the incoming solitons by more than an order (Peterson [48]).

The extreme water level elevations occur if the solitons intersect under a physical angle $\tilde{\alpha}_{12} = 2\arctan\sqrt{3\tilde{\eta}/h}$ [42]. This angle for two intersecting ship-generated solitary waves in realistic conditions is reasonable. It is about 36° for waves with heights $\tilde{\eta} = 1.8$ m (the maximum ship wave height mentioned in [6]) meeting each other in an area with a depth of 50 m, and about 70° for waves with heights $\tilde{\eta} = 0.8$

m in the coastal zone with a depth of 5 m. Solitons intersecting at the former angle apparently can be described by the KP equation. The latter angle may be too large for this framework.

For unequal amplitude solitons the maximum elevation $a_{\max}$ for finite A_{12} and the amplitude of the resonant soliton a_∞ at $A_{12} = \infty$ are

$$a_{\max} = a_{12} + 2A_{12}^{1/2}\frac{a_1 + a_2}{\left(A_{12}^{1/2} + 1\right)^2}, \qquad a_\infty = \frac{(k_1 + k_2)^2}{2}. \tag{5.2}$$

The expression for a_∞ probably has been first obtained for exact resonance of ion-acoustic solitons in a field-free plasma [49] directly from the resonance conditions assuming that the new structure is a KdV soliton and re-derived from the conditions for stationary points of the explicit two-soliton solution of the KP equation in [50]. A simple derivation of expressions (5.2) based on decomposition (4.2) is given in [51]. It is easy to show that both the incoming solitons and the residue have an extremum at the interaction centre. The nontrivial part of the derivation consists in proving that the global extremum of the composite structure is located at the same point. An elementary proof can be constructed with the use of the fact that every extremum of a 2D surface must correspond to a singularity point of a certain isoline [51].

Certain geometrical features of interaction of long-crested waves in the framework of two-soliton solutions of the KP equation have been analysed in [42,47,51]. In the simplest approximation, the high hump in the framework of soliton interactions may be associated with the area where the interacting waves have a common crest [42]. Its length is proportional to $L_{12} \sim \ln A_{12}$ [42] and therefore is modest unless the interacting solitons are near-resonant. For equal amplitude incoming solitons, the length of the area where the elevation exceeds the sum of amplitudes of the counterparts may considerably exceed the estimates based on the geometry of the wave crests [47]; however, this length also is roughly proportional to $\ln A_{12}$.

The amplification factor $m = 1 + 2k_1k_2/(k_1^2 + k_2^2) \approx 2$ when the amplitudes of the interacting solitons differ insignificantly and is close to 1 when the incoming solitons have fairly different amplitudes. Therefore, for largely different amplitudes of the interacting solitons the amplitude amplification remains modest. However, the spatial extent of the influence of nonlinear interaction of solitons with considerably different amplitudes is roughly as large as if the amplitudes were equal. The interaction mostly leads to bending of the crests of both the counterparts (Fig. 3). This effect may lead to hits by high waves arriving from an unexpected direction.

The process of formation of the high wave hump has been recently studied in [52] based on numerical simulation of collision of truncated (semi-infinite) structures with sech^2 profile, height of which varies along the crest. Since the initial profiles of the interacting waves are effectively two-dimensional, transversal energy flow along the crests supposedly occurs, and the results are not directly comparable with the ones presented above. However, an extremely high wave hump, the height of which considerably exceeds the sum of the heights of the counterparts, is formed quite fast in a certain interaction region. Evolution and interactions of solitary waves localized in

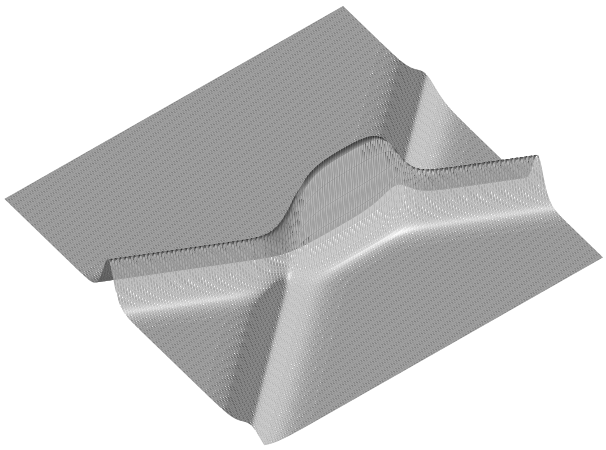

Figure 3: Surface elevation in the vicinity of the interaction area, for $k_2 = 1/3$, $l_1 = -l_2 = 0.2$, $k_{res} = 0.6$ and $k_1 = 0.9999k_{res}$ in normalised coordinates (x, y). Area $|x| \leq 60$, $|y| \leq 90$ is shown.

one half-plane have been studied numerically by Tsuji and Oikawa [53] also in the framework of the modified KP (mKP) equation in which the quadratic term of the KP equation is replaced by cubic term $6\eta^2\eta_x$. As different from the classical KP equation, the mKP equation admits both positive and negative solitary wave solutions. Interaction of positive solitary waves results either in structures containing very high and narrow wave hump or in transforming the incoming waves into a sequence of much smaller waves.

Plots of two-soliton solutions in Peterson et al. [42], Peterson and van Groesen [44], Haragus-Courcelle and Pego [54] suggest that the near-resonant high hump is particularly narrow and its front is very steep. This feature can be recognized also in experiments with the Mach reflection of supercritical ship wakes in narrow channels (Chen et al. [55]) where the highest part of the wave hump generally is narrower than the incoming solitons. The area of extreme elevations is very narrow indeed whereas the front of the resulting structure may be very steep. The maximum slope of the front of the two-soliton solution may be eight times as large as the slope of the incoming solitons, giving the relevant maximum "nonlinear slope amplification factor" equal to 4 [47]. For unequal amplitude solitons, the amplification of the slope of the front of the interaction pattern is proportional to the amplitude amplification [56].

The extraordinary steepness of the front of the near-resonant hump, although intriguing, is not totally unexpected, because the resonant KdV soliton is higher and therefore narrower than the incoming solitons. This feature may be a manifestation of the new physics, which seems to be necessary to correctly describe factually measured rogue waves [57].

6. Soliton interactions in realistic conditions

The above has shown that the extension of the particularly high hump in nonlinear interaction of KdV solitons normally is modest, and has a considerable length only when the heights of the incoming waves, their intersection angle and the local water depth are specifically balanced. Consequently, the fraction of sea surface occupied by extreme elevations is apparently small as compared with the area of a wave storm or area covered by ship wakes.

However, an important difference should be underlined between high waves possibly excited by the described mechanism and those arising owing to focusing of transient and directionally spread waves. In the latter case a number waves with different frequencies and propagation directions are focused at one point at a specific time instant to produce a time-varying transient wave group that normally does not propagate far from the focussing area [38]. A wave hump from nonlinear interaction, theoretically, has unlimited life-time and may cross large sea areas in favourable conditions [38]. Thus, one should account for the expected life-time of nonlinear wave humps (additionally to the sea area covered by extreme elevation at a certain time instant) when estimating the probability of occurrence of abnormally high waves. One could speculate that such high and steep wave hump might easily break before it reaches its theoretically maximum height, or after if propagates into an area where the conditions for existing of the two-soliton solution are not satisfied [42]. The possibility of breaking of the high and nonlinear wave hump makes a hit by a near-resonant structure exceptionally dangerous.

Acknowledgements

This work was supported by the Estonian Science Foundation (Grant 5762). The study was partially carried out when the author was visiting the Institute of Coastal Research, GKSS Forschungszentrum. The financial support of the Alexander von Humboldt Foundation, which makes this visit possible, is gratefully acknowledged.

References

[1] DURKEE P.A., CHARTIER R.E., BROWN A., TREHUBENKO E.J., ROGERSON S.D., SKUPNIEWICZ C. AND NIELSEN K.E., *Composite ship track characteristics*, J. Atmos. Sci. **57** (2000), 2542–2553.

[2] *Guidelines for managing wake wash from high-speed vessels*, Report of the Working Group 41 of the Maritime Navigation Commission, International Navigation Association (PIANC), Brussels 2003.

[3] WOOD W.A., *High speed ferry issues for operators and designers*, Mar. Technol. SNAME News **37** (2000), 230–237.

[4] PARNELL K.E. AND KOFOED-HANSEN H., *Wakes from large high-speed ferries in confined coastal waters: management approaches with examples from New Zealand and Denmark*, Coastal Manage **29** (2001), 217–237.

[5] HAMER M., *Solitary killers*, New Scientist **163** (2201) (1999), 18–19.

[6] SOOMERE T. AND RANNAT K., *An experimental study of wind waves and ship wakes in Tallinn Bay*, Proc. Estonian Acad. Sci. Eng. **9** (2003), 157–184.

[7] SOOMERE T., *Fast ferry traffic as a qualitatively new forcing factor of environmental processes in non-tidal sea areas: a case study in Tallinn Bay, Baltic Sea*, Env. Fluid Mech. **5** (2005), 293–323.

[8] SOOMERE T. AND KASK J., *A specific impact of waves of fast ferries on sediment transport processes of Tallinn Bay*, Proc. Estonian Acad. Sci. Biol. Ecol. **52** (2003), 319–331.

[9] WU T.Y., *Generation of upstream advancing solitons by moving disturbances*, J. Fluid Mech. **184** (1987), 75–99.

[10] LI Y. AND SCLAVOUNOS P.D., *Three-dimensional nonlinear solitary waves in shallow water generated by an advancing disturbance*, J. Fluid Mech. **470** (2002), 383–410.

[11] SOOMERE T., PÕDER R., RANNAT K. AND KASK A., *Profiles of waves from high-speed ferries in the coastal area*, Proc. Estonian Acad. Sci. Eng. **11** (2005), 245–260.

[12] BROWN E.D., BUCHSBAUM S.B., HALL R.E., PENHUNE J.P., SCHMITT K.F., WATSON K.M. AND WYATT D.C., *Observations of a nonlinear solitary wave packet in the Kelvin wake of a ship*, J. Fluid Mech. **204** (1989), 263–293.

[13] FORSMAN B., *From bow to beach*, SSPA Highlights **3** (2001), 4–5.

[14] GOURLAY T.P., *The supercritical bore produced by a high-speed ship in a channel*, J. Fluid Mech. **434** (2001), 399–409.

[15] FROUDE W., *Experiments upon the effect produced on the wave-making resistance of ships by length of parallel middle body*, Trans. Inst. Naval Architects **18** (1877), 77–87.

[16] THOMSON W. (LORD KELVIN), *On ship waves*, Trans. Inst. Mech. Eng. (1887), 409–433.

[17] HAVELOCK T.H., *The propagation of groups of waves in dispersive media, with application to waves on water produced by a travelling distance*, Proc. R. Soc. London Ser. A **81** (1908), 398–430.

[18] LAMB H., *Hydrodynamics*, Cambridge University Press, Cambridge 1997.

[19] LIGHTHILL J., *Waves in Fluids*, Cambridge University Press, Cambridge 1978.

[20] YIH C.-S. AND ZHU S., *Patterns of ship waves*, Q. Appl. Math. **47** (1989), 17–33.

[21] YIH C.-S. AND ZHU S., *Patterns of ship waves II. Gravity-capillary waves*, Q. Appl. Math. **47** (1989), 35–44.

[22] SORENSEN R.M., *Ship-generated waves*, Adv. Hydrosci. **9** (1973), 49–83.

[23] HÜSIG A., LINKE T. AND ZIMMERMANN C., *Effects from supercritical ship operation on inland canals*, J. Waterw. Port Coast. Ocean Eng. — ASCE **126** (2000), 130–135.

[24] DRAZIN P.G. AND JOHNSON R.S., *Solitons: an introduction*, Cambridge Texts in Applied Mathematics, Cambridge University Press, Cambridge 1989.

[25] HELM K., *Tiefen- und Breiteneinflüsse von Kanälen auf den Schiffswiderstand*, in: "Hydromechanische Probleme des Schiffsantriebs, Teil II, Veröffentlichung der Vorträge, die anlässlich des 25-jährigen Bestehens der Hamburgischen Shiffbau-Versuchungsanstalt an 14. Juni 1939 gehalten wurden, Kempf G. (Herausgeber)", Verlag von R. Oldenbourg, München und Berlin 1940, 144–171 (in German).

[26] WU D.M. AND WU T.Y., *Precursor solitons generated by three-dimensional disturbances moving in a channel*, in "IUTAM Symposium on Non-linear Water Waves, August 25–28, 1987", Tokyo 1987.

[27] RABINOVICH A.B. AND MONSERRAT S., *Generation of meteorological tsunamis (large amplitude seiches) near the Balearic and Kuril Islands*, Natural Hazards **18** (1998), 27–55.

[28] NEUMAN D.G., TAPIO E., HAGGARD D., LAWS K.E. AND BLAND R.W., *Observation of long waves generated by ferries*, Can. J. Remote Sens. **27** (2001), 361–370.

[29] ERTEKIN R.C., WEBSTER W.C., AND WEHAUSEN J.V., *Waves caused by a moving disturbance in a shallow channel of finite width*, J. Fluid Mech. **169** (1986), 275–292.

[30] AKYLAS T., *On the excitation of long nonlinear water waves by a moving pressure distribution*, J. Fluid Mech. **141** (1984), 455–466.

[31] COLE S.J., *Transient waves produced by flow past a bump*, Wave Motion **7** (1985), 579–587.

[32] WU D.M. AND WU T.Y., *Three dimensional nonlinear long waves due to moving surface pressure*, in "Proc. 14th Symp. Naval Hydrodyn. Ann Arbor, Michigan", National Academy Press, Washington 1982, 103–129.

[33] WU T.Y., *Long waves in ocean and coastal waters*, J. Eng. Mech. Div. ASCE **107** (1981), 501–522.

[34] ERTEKIN R.C., WEBSTER W.C. AND WEHAUSEN J.V., *Waves caused by a moving disturbance in a shallow channel of finite width*, J. Fluid Mech. **169** (1986), 275–292.

[35] ERTEKIN R.C., WEBSTER W.C. AND WEHAUSEN J.V., *Ship-generated solitons*, in "Proc. 15th Symp. Naval Hydrodyn., Hamburg, Germany", The National Academy Press, Washington 1984, 347–364.

[36] LEE S.J., YATES G.T. AND WU T.Y., *Experiments and analyses of upstream-advancing solitary waves generated by moving disturbances*, J. Fluid Mech. **199** (1989), 569–593.

[37] CASCIOLA C.M. AND LANDRINI M., *Nonlinear long waves generated by a moving pressure disturbance*, J. Fluid Mech. **325** (1996), 399–418.

[38] KHARIF C. AND PELINOVSKY E., *Physical mechanisms of the rogue wave phenomenon*, Eur. J. Mech. B Fluids **22** (2003), 603–634.

[39] HAMMACK J., MCCALLISTER D., SCHEFFNER N. AND SEGUR H., *Two-dimensional periodic waves in shallow water. Part 2. Asymmetric waves*, J. Fluid Mech. **285** (1995), 95–122.

[40] HAMMACK J., SCHEFFNER N. AND SEGUR H., *Two-dimensional periodic waves in shallow water*, J. Fluid Mech. **209** (1989), 567–589.

[41] MILES J.W., *Resonantly interacting solitary waves*, J. Fluid. Mech. **79** (1977), 171–179.

[42] PETERSON P., SOOMERE T., ENGELBRECHT J. AND VAN GROESEN E., *Soliton interaction as a possible model for extreme waves in shallow water*, Nonlinear Process. Geophys. **10** (2003), 503–510.

[43] SEGUR H. AND FINKEL A., *An analytical model of periodic waves in shallow water*, Stud. Appl. Math. **73** (1985), 183–220.

[44] PETERSON P. AND VAN GROESEN E., *A direct and inverse problem for wave crests modelled by interactions of two solitons*, Physica D **141** (2000), 316–332.

[45] PETERSON P. AND VAN GROESEN E., *Sensitivity of the inverse wave crest problem*, Wave Motion **34** (2001), 391–399.

[46] TSUJI H. AND OIKAWA M., *Oblique interaction of internal solitary waves in a two-layer fluid of infinite depth*, Fluid Dyn. Res. **29** (2001), 251–267.

[47] SOOMERE T. AND ENGELBRECHT J., *Extreme elevations and slopes of interacting solitons in shallow water*, Wave Motion **41** (2005), 179–192.

[48] PETERSON P., *Multi-soliton Interactions and the Inverse Problem of Wave Crests*, Ph.D. Thesis, Tallinn Technical University, Tallinn 2001.

[49] GABL E.F. AND LONNGREN K.E., *On the oblique collision of unequal amplitude ion-acoustic solitons in a field-free plasma*, Phys. Lett. A **100** (1984), 153–155.

[50] DUAN W.-S., SHI Y.-R. AND HONG X.-R., *Theoretical study of resonance of the Kadomtsev-Petviashili equation*, Phys. Lett. A **323** (2004), 89–94.

[51] SOOMERE T., *Interaction of Kadomtsev-Petviashvili solitons with unequal amplitudes*, Phys. Lett. A **332** (2004), 74–81.

[52] PORUBOV A.V., TSUJI H., LAVRENOV, I.V. AND OIKAWA M., *Formation of the rogue wave due to non-linear two-dimensional waves interaction*, Wave Motion **42** (2005), 202–210.

[53] TSUJI H. AND OIKAWA M., *Two-dimensional interaction of solitary waves in a modified Kadomtsev Petviashvili equation*, J. Phys. Soc. Japan. **73** (2004), 3034–3043.

[54] HARAGUS-COURCELLE M. AND PEGO R.L., *Spatial wave dynamics of steady oblique wave interactions*, Physica D **145** (2000), 207–232.

[55] CHEN X.-N., SHARMA S.D. AND STUNTZ N., *Zero wave resistance for ships moving in shallow channels at supercritical speeds. Part 2. Improved theory and model experiment*, J. Fluid Mech. **478** (2003), 111–124.

[56] SOOMERE T. AND ENGELBRECHT J., *Extreme elevations and slopes of interacting Kadomtsev-Petviashvili solitons in shallow water*, in: "Proc. of a workshop organized by IFREMER and held in Brest, France, 20-22 October 2004" IFREMER Actes de Colloques **39**, Brest 2005, 92–101.

[57] WALKER D.A.G., TAYLOR P.H. AND TAYLOR R.E., *The shape of large surface waves on the open sea and the Draupner New Year wave*, Applied Ocean Research **26** (2004), 73–83.

AMS Subject Classification: 76B25, 76B15, 76B20, 35Q51, 35Q53.

Tarmo SOOMERE, Centre for Non-linear Studies, Tallinn University of Technology, Akadeemia tee 21, 12618 Tallinn, ESTONIA
e-mail: soomere@cs.ioc.ee

Special issues and Conference Proceedings published in Rendiconti

Stochastic Problems in Mechanics	(1982)
Linear Partial and Pseudo-differential Operators	(1983)
Differential Geometry on Homogeneous Spaces	(1983)
Special Functions: Theory and Computation	(1985)
Algebraic Varieties of Small Dimension	(1986)
Linear and Nonlinear Mathematical Control Theory	(1987)
Logic and Computer Sciences: New Trends and Applications	(1987)
Nonlinear Hyperbolic Equations in Applied Sciences	(1988)
Partial Differential Equations and Geometry	(1989)
Some Topics in Nonlinear PDE's	(1989)
Mathematical Theory of Dynamical Systems and ODE, I-II	(1990)
Commutative Algebra and Algebraic Geometry, I-III	(1990-1991)
Numerical Methods in Applied Science and Industry	(1991)
Singularities in Curved Space-Times	(1992)
Differential Geometry	(1992)
Numerical Methods in Astrophysics and Cosmology	(1993)
Partial Differential Equations, I-II	(1993–1994)
Problems in Algebraic Learning, I-II	(1994)
Number Theory, I-II	(1995)
Geometrical Structures for Physical Theories, I-II	(1996)
Jacobian Conjecture and Dynamical Systems	(1997)
Control Theory and its Applications	(1998)
Geometry, Continua and Microstructures, I-II	(2000)
Partial Differential Operators	(2000)
Liaison and Related Topics	(2001)
Turin Fortnight Lectures on Nonlinear Analysis	(2002)
Microlocal Analysis and Related Topics	(2003)
Splines, Radial Basis Functions and Applications	(2003)
Polynomial Interpolation and Projective Embeddings - Lecture Notes of the School	(2004)
Polynomial Interpolation and Projective Embeddings - Proceedings of the Workshop of the School	(2005)
Control Theory and Stabilization, I-II	(2005-2006)
Syzygy 2005	(2006)
Subalpine Rhapsody in Dynamics	(2007)
ISASUT Intensive Seminar on Non Linear Waves, Generalized Continua and Complex Structures	(2007)

Rendiconti del Seminario Matematico
dell'Università e del Politecnico di Torino

Volume 65, N. 2 (2007)

ISASUT Intensive Seminar on Non Linear Waves,
Generalized Continua and Complex Structures

CONTENTS

ISSN 0373-1243

UNIVERSITÀ DEGLI STUDI DI TORINO
DIPARTIMENTO DI MATEMATICA